Università del Piemonte Orientale

Department of Health Sciences

Ph.D. Program in Medical Sciences and Biotechnology

XXXIII cycle

Extra coagulative roles of FVIII in endothelial cell functionality

Supervisor: Prof. Antonia Follenzi

Coordinator: Prof. Marisa Gariglio

PhD candidate: Alessia Cucci

SSD: BIO/17

Student declaration

I declare that the PhD thesis titled “Extra coagulative roles of FVIII in endothelial cell functionality” represent my own work and that it has not been submitted, in whole or in part, in any previous application for a degree.

I generated and analyzed the data herein reported. The following experiments have been conducted in collaboration:

- RNAseq data analysis were performed in the laboratory of Prof. Salvatore Oliviero in collaboration with Dr. Ivan Molineris and Dr. Francesca Anselmi (Epigenetics Lab, Dept. of Life Science and System Biology, Università di Torino)

- Animal procedures were performed by Dr. Cristina Olgasi, Dr. Chiara Borsotti and Dr. Ester Borroni (Histology Lab, Dept. of Health Sciences, Università del Piemonte Orientale)

This PhD thesis is intended as confidential since the work, or part of it, is not submitted for publication yet.

Some of the results that I reported and discussed in this PhD thesis were previously published or currently under revision, as indicated in the text.

The work done in my PhD program is not exclusive of this thesis, but I contributed to the following publications:

“Efficient and safe correction of hemophilia A by lentiviral vector-transduced BOECs in an implantable device” [under revision] C. Olgasi*, C. Borsotti*, S. Merlin*, T. Bergmann, P. Bittorf, A. Badi Adewoye, N. Wragg, K. Patterson, A. Calabria, F. Benedicenti, **A. Cucci**, A. Borchiellini, B. Pollio, E. Montini, D. Mazzuca, M. Zierau, A. Stolzing, P.Toleikis, J. Braspenning, A. Follenzi.

“iPSC-Derived Liver Organoids: A Journey from Drug Screening, to Disease Modeling, Arriving to Regenerative Medicine” Int. J. Mol. Sci. 2020. C. Olgasi*, **A. Cucci***, A. Follenzi

“Deciphering the Ets-1/2-mediated transcriptional regulation of F8 gene identifies a minimal F8 promoter for hemophilia A gene therapy” Haematologica. 2020. “R. Famà*, E. Borroni*, S. Merlin, C. Airoldi, S. Pignani, **A. Cucci**, D. Corà, V. Bruscaggin, S. Scardellato, S. Faletti, G. Pelicci, M. Pinotti, G. E. Walker, A. Follenzi.

“Patient-Specific iPSC-Derived Endothelial Cells Provide Long-Term Phenotypic Correction of Hemophilia A”. Stem Cell Reports 2018. C. Olgasi*, M. Talmon*, S. Merlin, **A. Cucci**, Y. Richaud-Patin, G. Ranaldo, D. Colangelo, F. Di Scipio, G.N. Berta, C. Borsotti, F. Valeri, F. Faraldi, M. Prat, M.Messina, P. Schinco, A. Lombardo, A. Raya, A. Follenzi.

TABLE OF CONTENTS

Abstract

Hemophilia A (HA) is a recessive X-linked bleeding disorder that occurs in 1:5000 male live births and is due to the lack or reduced activity of coagulation factor VIII (FVIII).

Based on its residual activity, three degrees of HA severity can be recognized, and spontaneous bleeding episodes can occur more frequently in severe HA patients. These bleedings primarily consist of hemarthroses and spontaneous intracranial hemorrhage that occur without a clear cause. Currently, there is no definitive cure, and the therapeutic treatment involves the frequent administration of FVIII in the form of recombinant or plasma-derived protein to avoid bleeding episodes. However, standard therapies are ineffective in preventing recurrent joint and intracranial bleedings. It is well established that FVIII is mainly secreted by endothelial cells (ECs), but little is known about the genetic and proteomic profiles between healthy and HA ECs. Therefore, we aimed to explore the extra-coagulative role of FVIII in endothelial stability and identify significant differences in HA and healthy ECs.

In *in vitro* experiments we demonstrated a reduced functionality of two HA ECs models [iPSCs-derived-ECs (iECs) and blood outgrowth endothelial cells (BOECs)] compared to healthy ones in terms of tubule formation, migration, and permeability. The transduction of HA ECs with a LV carrying the B deleted-domain (BDD) form of coagulation FVIII under the control of an endothelial promoter, VE-cadherin (LV-VEC.FVIII) partially restored the impaired capabilities of these cells. Based on *in vitro* results, we investigated if the impaired endothelial functionality could also occur *in vivo* demonstrating an increased vascular permeability in a mouse model of HA compared to wild type.

Transcriptomic analysis on healthy, HA and LV-VEC.FVIII HA ECs allowed us to identify gene expression changes between healthy and HA ECs. The genes downregulated in HA ECs are implicated in ECM organization, focal adhesion, and angiogenesis pathways supporting the differences observed in endothelial functionality of HA versus healthy cells.

By *in vitro* experiments, we demonstrated that recombinant FVIII treatment increased the ability of HA ECs to form tubule network and to migrate. Conversely, we detected an enhancement on vessel density and diameter of newly formed vessels in *in vivo* experiments reinforcing the hypothesized role of FVIII in maintaining ECs stability and functionality.

In conclusion, information from the possible extra-coagulative role of FVIII can be crucial to understand the key molecular targets missing in HA patients at the cellular level impairing EC functionality. This information can lead to new therapeutic approaches resulting in a safer and more efficient treatment of HA.

Sommario

L'emofilia A (HA) è una malattia recessiva legata al cromosoma X che si presenta con una incidenza di 1:5000 nati vivi. Il fenotipo emorragico tipico dei pazienti emofilici è causato da un'assente o ridotta attività del fattore FVIII della coagulazione (FVIII). In base all'attività residua del FVIII si possono distinguere tre forme di HA. I pazienti affetti dalla forma grave sono soggetti a frequenti emorragie che possono presentarsi come emartrosi o emorragie intracraniche spontanee. Ad oggi non esiste una cura definitiva e il regime terapeutico prevede il trattamento con FVIII ricombinante o emoderivato. Tuttavia, la terapia convenzionale non è in grado di prevenire del tutto gli eventi emorragici. È noto che il FVIII è principalmente prodotto dalle cellule endoteliali (CE), ma non è stata mai investigata la differenza nel profilo trascrittomico tra le CE emofiliche e sane. Pertanto, lo scopo di questa tesi è quello di studiare i possibili ruoli extra-coagulativi del FVIII nel mantenimento della stabilità endoteliale e identificare le differenze rilevanti tra CE emofiliche e sane. Mediante studi *in vitro* condotti su due modelli endoteliali (CE derivate da iPSC e CE circolanti del sangue) abbiamo dimostrato che le CE emofiliche presentano una ridotta funzionalità endoteliale, rispetto a quelle sane, in termini di capacità di formare tubuli, di migrare e nella permeabilità. La trasduzione delle CE HA, con un vettore lentivirale che esprime il FVIII la privo del dominio B sotto il controllo del promotore endoteliale Ve-caderina (LV-VEC.FVIII), ha permesso il parziale recupero delle capacità funzionali di queste cellule. Inoltre, abbiamo dimostrato in un modello murino emofilico, un aumento della permeabilità vascolare rispetto ai corrispettivi topi "wild type". L'analisi del profilo trascrittomico di cellule sane, HA e HA trasdotte ci ha permesso di identificare variazioni di espressione genica tra le cellule sane e HA. I geni "downregolati" nelle CE HA sono implicati nell'organizzazione della matrice extracellulare, nelle adesioni focali e meccanismi coinvolti nell'angiogenesi. Per avvalorare il ruolo extra-coagulativo del FVIII, le cellule HA sono state trattate in coltura con il FVIII ricombinante (rFVIII), dimostrando un aumento della capacità di formare i tubuli e di migrare. Allo stesso modo, dati ottenuti dai topi iniettati con una matrice extracellulare di natura organica arricchita di rFVIII hanno rinforzato l'ipotesi che il FVIII abbia un ruolo nella stabilità e funzionalità endoteliale.

In conclusione, lo studio sulle funzioni extra coagulative del FVIII potrebbe diventare fondamentale per identificare i bersagli molecolari mancanti nelle cellule HA responsabili della disfunzione endoteliale. Questi dati potrebbero essere cruciali per identificare nuovi approcci terapeutici volti a migliorare lo stile di vita dei pazienti emofilici.

Introduction

1. Hemophilia A and coagulation factor VIII

Hemophilia includes a group of inherited hemorrhagic disorders that alter the body's normal hemostasis. There are two forms of hemophilia, the first is hemophilia A (HA) resulting from the deficiency or insufficiency of functional coagulation factor VIII (FVIII) in the blood and the second is hemophilia B when a functional FIX is mutated. HA is the most common coagulopathy occurring in 1:5000 male live births (Iorio et al., 2019).

FVIII gene (*F8*) is located on the X chromosome and when mutated, causes the X-linked disease of HA which may be inherited or arise from spontaneous mutations in carrier mothers. The reduction or lack of plasma FVIII causes prolonged and excessive bleeding, either spontaneously or secondary to mild trauma, of clinical severity proportional to the degree of FVIII reduction. Based on the residual FVIII activity, three forms of HA can be distinguished: severe form, characterized by levels of FVIII below 1%, moderate form, in which FVIII levels range from 1 to 5%, and mild form showing 5 to 40% of FVIII activity (Bolton-Maggs and Pasi, 2003).

F8 is located on the long arm of the X chromosome (Xq28) and exhibit a peculiar structure: it extends for 186 kb with 24 short exons (69-262 bp) and 2 long exons, exon 14 (3106 bp) and exon 26 (958 bp). The resulting mRNA is around 9 kb and the coding sequence is 7053 bp long. *F8* introns have a long span ranging from 14 to 32 kb, but intron 22 is the largest with 32 kb of extension. Several mutations in *F8* have been described causing HA.

The most frequent mutation, affecting almost 50% of patients with the severe form, is the inversion of the first 22 exons of *F8* caused by intrachromosomal recombination between the intron 22 (int22h1) with two homologous sequences that span 500 kb from the gene (int22h3 and int22h3) (White et al., 2001). Other mutations causing the severe form are small deletions or insertions, missense and non-sense mutations that taken together occur in 45% of severe HA patients. Less frequent mutations are large deletions, splice site mutations and intron 1 inversion (Oldenburg and Pavlova, 2006). In contrast, missense mutations are mainly associated with moderate and mild form (Graw et al., 2005).

To date, 3756 unique *F8* variants are listed in the CDC Hemophilia A Mutation Project (CHAMP) (Payne et al. 2020) (**Table 1**).

Variant Type	No. of Variants	% of Variants
Missense	1745	46,5%
Nonsense	416	11,1%
Frameshift	908	24,2%
Splice site change	320	8,5%
Large Structural Change	210	5,6%
Small Structural Change	86	2,3%
Synonymous	39	1,0%
Promoter	14	0,4%
3'UTR	13	0,3%
5'UTR	5	0,1%
Total	3756	

Table 1. Frequency of F8 Variant. F8 mutation listed in CHAMP database representing worldwide HA patients. https://www.cdc.gov/ncbddd/hemophilia/champs.html

Alongside the molecular diagnostic, the analysis of *F8* mutations is useful to further characterize the gene defect and the risk of inhibitor development, one of the major concerns of HA current treatment that reduce the residual activity of FVIII, making the treatment ineffective (Franchini and Mannucci, 2014). It was reported that patients with severe HA and mutations predicting a null allele developed inhibitors more frequently (22% to 67%) than patients with missense mutations (5%) (Margaglione et al., 2008).

F8 encodes for a mature protein of 2332 amino acids (263 KDa) containing 19 amino acids (aa) signal oligopeptide at the N-terminal (Vehar et al., 1984). A singularity of *F8* is the presence of two additional genes known as *F8A* and *F8B* genes in its intron 22 (IVS22), but so far, *F8A* and *F8B* functions are not known (Rossetti et al., 2011). FVIII is synthesized as an inactive single chain and it is organized in 6 domains: A1, A2, B, A3, C1, C2 (**Fig. 1**). In the blood, after cleavage by furin protease, this protein is divided into two chains: a heavy chain of 200 kDa (A1-A2-B) and a light chain of 80 kDa (A3-C1-C2).

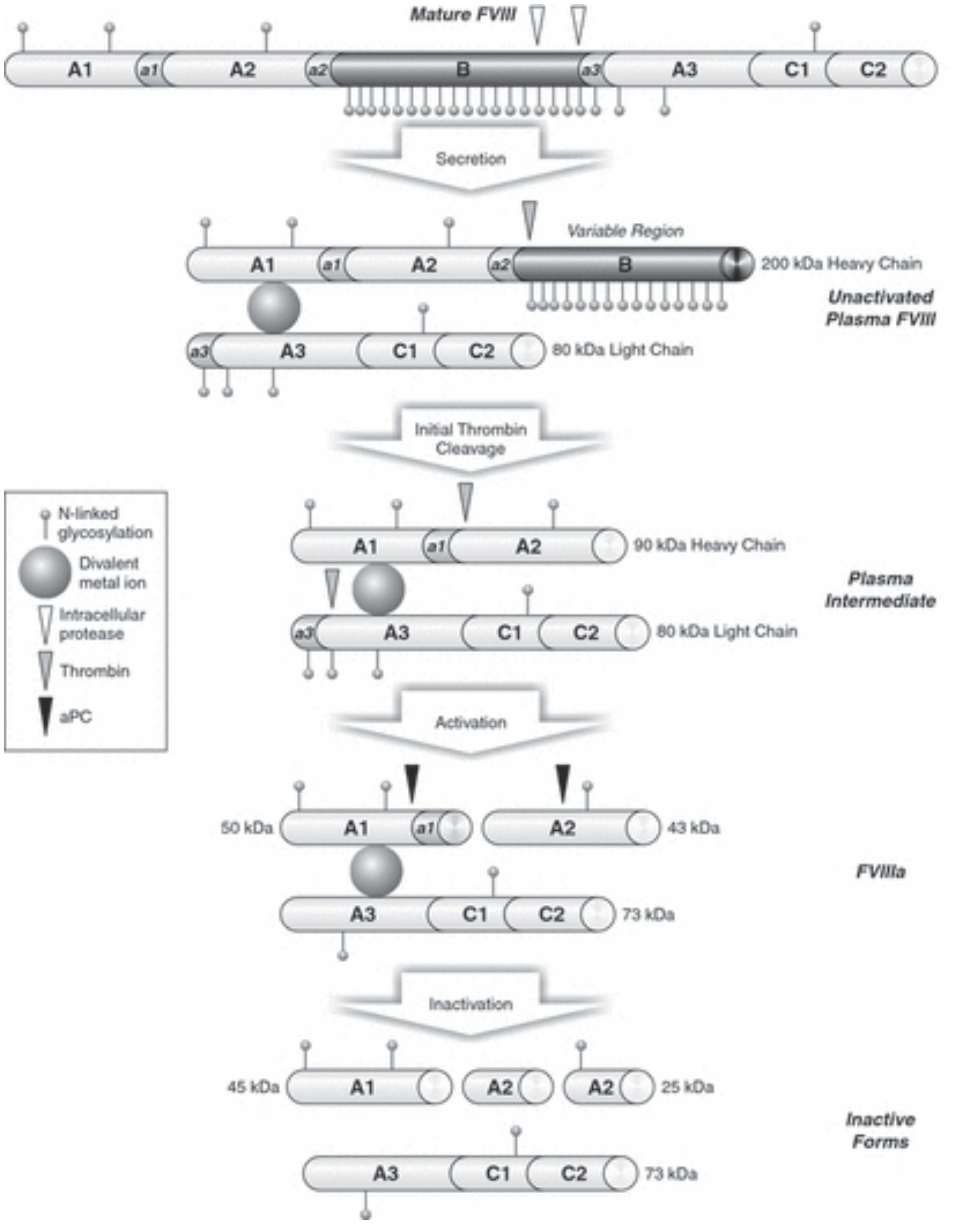

Figure 1: Domain structure and processing of FVIII. VIII is synthesized as an inactive single chain organized in 6 domain structure: A1-A2-B-A3-C1-C2. a1, a2 and a3 are acidic amino acid rich regions between the major structural domains and contain sulfated tyrosine residues. After cleavage at the C-terminal region of B domain, FVIII consists in a heterodimer formed by the heavy chain and the light chain linked by a divalent metal ion between the A1 and A3 domains. aPC, activated protein C; FVIII, factor VIII; FVIIIa, activated factor VIII (Pipe 2009)

Three acidic subdomains, identified as a1–a3 – A1(a1)–A2(a2)–B–(a3)A3–C1–C2, localize at the boundaries of A domains and play a fundamental role in the interaction between FVIII and other proteins.These regions contain the thrombin binding sites (Arg372, Arg740, Arg1689) crucial for FVIII activation (Fang et al., 2007). Mutations in these subdomains reduce the level of FVIII activation by thrombin (Donath, 1996; Kjalke et al., 1995).

The B-domain encoded by a single long exon is partially removed from the mature protein. The B-domain contains 25 potential N-glycosylation sites, 16–19 of which are occupied and

exhibit a significant level of microheterogeneity. Ser743 in the N-terminal region of B domain is connected with Glu1638 in the C-terminal of B domain forming a SQ specific site comprising 14 aa (SFSQNPPVLKRHQR) situated between domains A2 and A3. The presence of this site allows intracellular cleavage of the 170 kDa single chain and formation of the 80–90 kDa active complex. It is correlated with the presence of aa in positions –1 and –4 (relative to the Glu1649 site) in SQ enabling proteolytic cleavage by furin protease. FVIII is inactive or minimally active as a cofactor in blood coagulation process. Its activation as a cofactor occurs only after proteolytic cleavage in the SQ site (Ngo et al., 2008; Thompson, 2003). The function of the B-domain, comprising 40% of FVIII mass, is not fully understood. This domain does not affect FVIII activity in the process of blood coagulation. B-domain-deleted natural or recombinant FVIII (rFVIII) heterodimers show comparable or even higher activity. The central B-domain is the largest of all the domains and is highly glycosylated (Berntorp, 1997; Pittman et al., 1993).

In vivo, coagulation FVIII activation is induced by FXa and involves the introduction of proteolytic breakdowns at several points. Activation results from cleavage of the heavy chain in: Arg372 (A1 — A2 domain linkage) and Arg740 (A2 — B domain linkage) aa sites and cleavage of the light chain in amino acid site Arg1689 (B— A3 domain linkage). The active form of coagulation FVIII, FVIIIa is a trimer consisting of A1 (aa 1–372) and A2 (aa 373–740) noncovalently bound, and domains A3 — C1–C2 (aa 1690–2332). The B-domain does not comprise the FVIIIa form. The function of FVIIIa in the coagulation cascade is to accelerate FX activation in the presence of FIXa, phospholipids and calcium ions (Bhopale and Nanda, 2003; Eaton et al., 1986; Fay, 2004) (**Fig. 2**).

Following thrombin-induced FVIII activation, FVIIIa binds to the phospholipid surface (PS) and starts to impact on FIXa, in a complex that activates factor X (FX) which, converging in the common pathway of the coagulation cascade, allows to the conversion of fibrinogen to fibrin and the consequent clot formation. The active form of FVIII, indeed, accelerates FX activation about 10^5 times (Eaton et al., 1986). In physiological conditions, circulating FVIII is present in the blood plasma at a concentration of 0.1–0.2 μg/ml (Adamson, 1994). FVIII n plasma is complexed with a chaperone, the von Willebrand factor (VWF), which is 50-folds in excess compared to the FVIII.

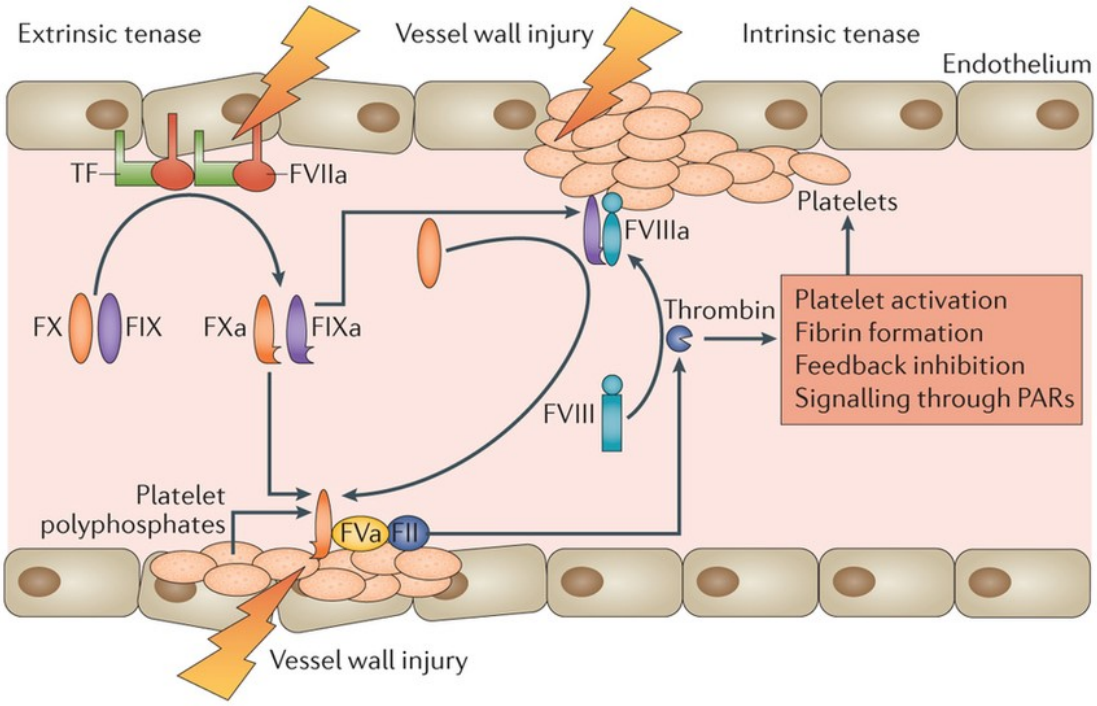

Figure 2. Initiation, amplification, and propagation of coagulation. Upon vessel wall injury and/or activation of endothelial cells, tissue factor (TF) is exposed to blood and binds to FVII or FVIIa, promoting FVII activation or enhancing its catalytic activity. The TF–FVIIa (extrinsic tenase) complex activates small amounts of FIX and FX. FXa associates with FVa to form the prothrombinase complex, which cleaves FII to generate a small amount of thrombin. This initiation phase is followed by the amplification phase, in which thrombin activates cell-surface bound FV and FVIII and platelet-bound FXI. FIXa binds to FVIIIa on negatively charged surfaces, activating FX (intrinsic tenase), and initiating a burst of thrombin generation—the propagation phase. a, activated; F, factor; (Madhusudhan 2015)

VWF, which is secreted by vascular endothelial cells, stabilizes FVIII in the blood stream and increase the half-life of FVIII by reducing the clearance and avoiding the inactivation by activated protein C (APC) (Nogami et al., 2002). Furthermore, VWF prevents the nonspecific binding of FVIII to the membranes of vascular endothelial cells and platelets. *In vitro* experiments demonstrated how VWF helps the association of FVIII chains and the preservation of procoagulant activity in the conditioned medium of cells producing FVIII (Wise et al., 1991). Inactivation of FVIIIa can occur spontaneously or be induced by two specific inactivators: APC and FXa. APC cleaves FVIIIa at positions R562 and R336, disrupting the region of interaction between FVIII and FIX and destabilizing the interaction between the A1 and A2 domains (Cramer and Gale, 2011). FXa promotes the inactivation of FVIIIa more rapidly *in vivo* than APC and the mechanism involves the cleavage at positions R336 and K36, resulting in the destabilization of A1 domain and the unbound of A2 domain (Nogami et al., 2003).

2. Current treatment and beyond

To date, for HA there is not a definitive cure, and the therapeutic practice consists in a replacement therapy of rFVIII delivered by intravenous injections, as needed to treat acute hemorrhages, or according to prophylactic regimens to prevent bleeds (Collins et al., 2009). The primary aim of regular long-term prophylaxis is to avoid frequent joint bleeds, prevent chronic arthropathy and reduce mortality. Despite the great outcomes achieved with replacement therapy, some unmet medical needs need to be addressed, such as the reduction of the intravenous injection frequency, and the increase of the short half-life of native FVIII (8–12 h). Moreover, long-term follow up data from large cohorts of patients treated over decades with regular prophylaxis showed that minimal concentrations of FVIII are sufficient to prevent bleedings even though the development of joint damage was not completely abolished but only delayed in time (Srivastava et al., 2020). New generation of standard rFVIII was obtained by refinements of the recombinant protein by optimizing relevant post-translational modifications like glycosylation that can improve the stability of the mature FVIII protein (Lissitchkov et al., 2017) or the introduction of a covalent link between the FVIII heavy and light chains that preserves the FVIII molecule from premature degradation and confers a higher binding affinity for VWF (Mahlangu et al., 2016). These modifications have been shown to provide effective prophylaxis with two or less injections per week in approximately 30% of patients (Lentz et al., 2018; Mahlangu et al., 2016; Saxena et al., 2016). Over the years new bioengineered molecules were developed with at least 1:4 times extended plasma half-life (EPHL) (Mahlangu et al., 2018) and improved pharmacokinetics properties given by the fusion of rFVIII with the Fc portion of immunoglobulin (Mahlangu et al., 2014) or with the conjugation of polyethylene glycol (PEGylation) (Konkle et al., 2015). However, EPHL products are still regulated by the interaction with vWF (approximately 15 h half-life), thus limiting half-life extension of FVIII with techniques available today (Graf, 2018). The introduction of EPHL has provided further improved prophylaxis effectiveness in bleeding control, prevention and better adherence to the treatment and the reduction of the weekly number of injections to a once-per-week dosage (Giangrande et al., 2017; Reding et al., 2017). The replacement therapy, even if improved the patient's quality of life, does not represent a definitive cure and several issues are still to be solved. Intravenous route of administration is a substantial burden especially for young or infant patients and possible complications, such as infection or thrombosis, could occur. Nevertheless, the main complication is the development of neutralizing antibodies (inhibitors) to FVIII that is common in 20-40% of patients with the severe form.

This worsens the clinical aspect making the treatment ineffective, reducing the residual activity of the endogenous FVIII and exposing patients to an increased risk of morbidity and mortality (Van Den Berg et al., 2019; Dimichele, 2002). Therefore, alongside clotting factors concentrates advancements, another class of drugs called non-replacement therapy is emerging to overcome the difficulties of intravenous delivery and to improve the effectiveness of therapies in all patients, regardless of the presence or absence of inhibitors (Oldenburg et al., 2017; Pasi et al., 2017; Shapiro et al., 2018). New non-replacement agents do not contain FVIII protein, thus the therapy does not cause a specific immune response against FVIII and is not neutralized by pre-existing inhibitory anti-FVIII. A key feature of these new non-replacement therapies, besides a subcutaneous method of delivery and similar effectiveness in patients both with and without inhibitors, is a substantially longer duration of action that leads to a more stable steady state hemostatic effect. The first one to be approved for prophylaxis in patients with and without inhibitors, is a humanized bispecific monoclonal antibody (emicizumab) that bridges activated FIX and FX, mimicking the co-factorial function of activated FVIII (Kitazawa et al., 2012). Emicizumab can be administered once every 7, 14, or 28 days, with comparable efficacy across different ages and bodyweights (Oldenburg et al., 2017; Pipe et al., 2019b). Other compounds that have been developed are hemostatic rebalancing agents, but efficacy and safety are currently under investigation (Zhao et al., 2021). These agents target the natural inhibitors of the coagulation cascade: antithrombin, tissue factor pathway inhibitor (TFPI), and activated protein C (Cardinal et al., 2018; Gu et al., 2017; Sehgal et al., 2015). Nevertheless, pharmacokinetic and pharmacodynamic studies carried out on patients treated with emicizumab, antithrombin and anti-TFPI antibodies, showed that the level of hemostatic correction is comparable to that of patients with mild hemophilia (as measured by thrombin generation assays). Bleeding events can still occur after trauma requiring the use of additional hemostatic agents, according to the patients' inhibitor status (Ebbert et al., 2020; Santagostino et al., 2019; Zimowski et al., 2019). Finally, the non-replacement therapy is not based on a recombinant FVIII protein and due to the possible biological roles for FVIII beyond its procoagulant function, the long-term bone and joint health can be affected (Lenting et al., 2017; Samuelson Bannow et al., 2019).Altogether, treatment optimization has been the main objective over the last decade for HA patient's healthcare, but several concerns remain. Thus, further therapeutic approaches are still required, and cell and gene therapy strategies have been developed with the aim of finding a definitive cure for HA.

3. Gene therapy for hemophilia A

Gene and cell therapy could represent an optimal therapeutic approach for monogenic disease. Gene therapy is a form of molecular medicine that have been developed since the 1980s and it is still evolving: the main purpose is to introduce genetic material into the target cells, tissues or organs in a safe and efficient way, with the goal to obtain a therapeutic effect, or to slow down the patient disease progression. The challenge of gene therapy is to develop one or more systems capable of achieving an efficient gene transfer in selected tissues without causing pathological consequences to the patient. The genetic material should be delivered by a vector capable of overcoming the biological barriers between cells and surrounding environment, efficiently target the suitable cell type for the pathology and allow a regulated long-lasting gene expression without life-threatening side effects for the patient. Gene therapy can be applied: i) *in vivo*, by direct injection of a vector expressing the gene of interest, either systemically or directly into the damaged tissue; ii) *ex vivo*, using vectors to genetically manipulate the patient's autologous cells and then transplant the corrected cells back into the patient himself (Verma and Weitzman, 2005).

Vectors for gene therapy are commonly divided in viral and non-viral, the choice of which may depend on the specific application (**Fig.3**).

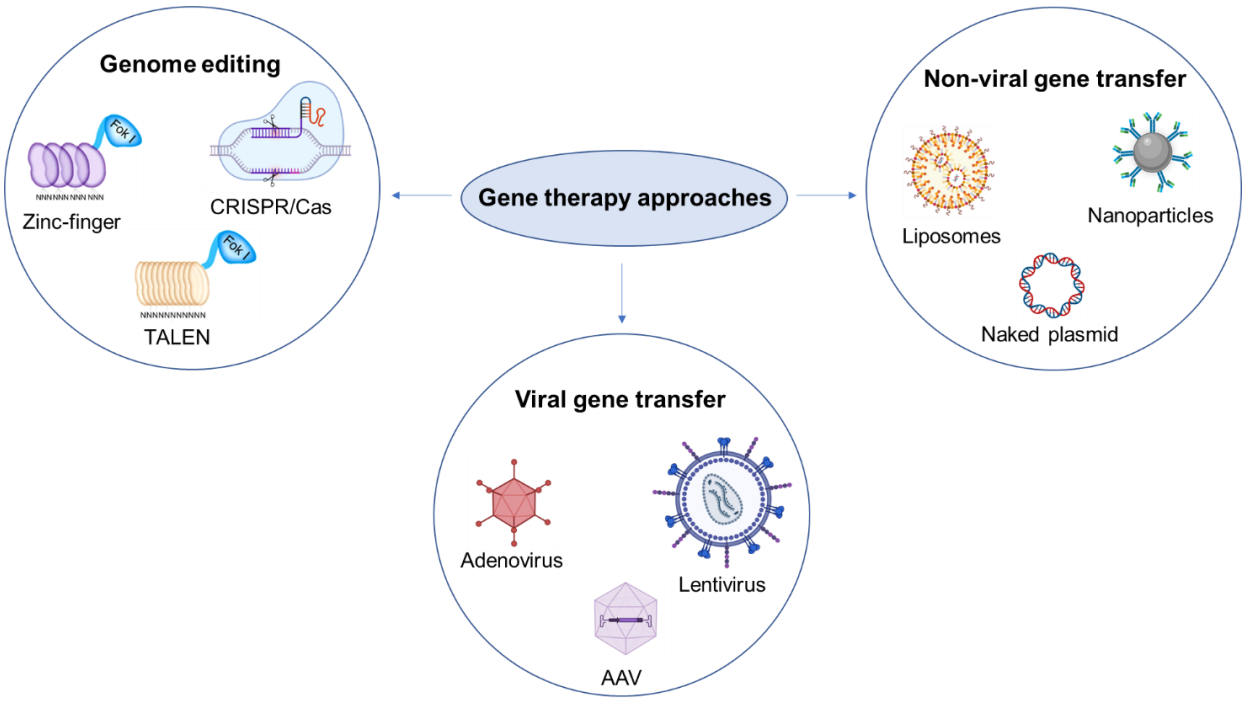

Figure 3. Gene therapy approaches. Schematic illustration of gene therapy approaches showing viral, non-viral and genome editing methods.

Many viral and non-viral vectors can be used as potential delivery vehicles for gene therapy. Examples of non-viral gene delivery are naked/plasmid DNA, lipofection and nanoparticles. To date, viral vectors are the most used in clinics because of the efficiency and safety of the gene transfer. Vectors derived from an extensive engineering of several classes of virus satisfy the biosafety requirement and carry the gene of interest. Viral-based delivery systems simply exploit the natural ability of viruses to deliver genes into the host cell genome, excluding their replication and pathogenic assets. This can be achieved by spatially separating viral cis-acting sequences and trans-acting regulatory genes into different plasmids during vector production. Additional safety measures aimed to prevent homologous recombination between common sequences that could reconstitute the parental viral genome (Verma and Weitzman, 2005). Several viral vectors have been designed and includes integrating and non-integrating vectors, with either DNA or RNA genome. The adenoviral associated vectors (AAVs) have been reported as the non-integrating vectors largely used in the clinics whereas among the integrating vectors retroviral and lentiviral vectors (LV) are the most frequently used.

Hemophilia A represents an ideal target for gene therapy since restoring FVIII from severe to moderate levels is sufficient to ameliorate the bleeding phenotypes of patients with a general improvement of quality of life. The goal of gene therapy for HA is to develop gene therapy products as single-dose treatments that may provide long-term expression of the deficient FVIII coagulation factor at steady-state levels and a sustained duration of action. This would liberate patients from the need for regular intravenous infusions. Thus, both AAV and LV gene therapy strategies for HA have been conducted over the years to accomplish a safe transgene expression without the development of inhibitors.

3.1 AAV-based gene therapy strategies for hemophilia A

AAVs are small, non-enveloped icosahedral viruses (25 nm) that belong to the Parvovirus family. It has been described that they can rarely integrate into the host genome, mostly at sites of actively transcribed genes or double strand breaks (Deyle and Russell, 2009). AAVs are capable of infecting both mitotic and post-mitotic cells but as they are episomal they are more suitable for gene replacement therapy in non-dividing cell therapies. Potential limitations associated to the use of AAV are represented by the widespread pre-existing immunity against the most common serotypes (Mingozzi and High, 2013) and by a limited capacity in terms of transgene size as it can contain small DNA inserts up to a maximum of 4.5kb (Grieger and Samulski, 2012).

However, the immune responses to AAVs remain a major obstacle, especially for *in vivo* applications. Indeed, it has been demonstrated that patients that exhibited cellular and humoral immunity toward vector antigens lose the transgene expression. Therefore, testing for innate immunity is becoming more widespread and is used as an exclusion criterion for clinical trial eligibility (Mingozzi and High, 2013; Rabinowitz et al., 2019).

Advances in hemophilia gene therapy was first achieved in a clinical trial for hemophilia B (Nathwani et al., 2011) using AAV8 capsid protein to deliver FIX into patients (Nathwani et al., 2014) increasing the quality of patients' life and encouraging new efforts to improve this approach as an alternative approach to replacement therapy. Despite the relevant results obtained for hemophilia B, gene therapy for HA progress slower due to several factors. The smaller size of the FIX coding sequence (1.4 kb) compared with the FVIII coding sequence (7 kb) has allowed researchers to more easily identify suitable vectors to transfer the FIX cDNA into potential target cells, making the overall progress of gene therapy more rapid for hemophilia B. Moreover, using a comparable vector delivery, transduced cells express 100-fold less FVIII level than FIX (Lynch et al., 1993). Finally, FVIII is naturally 5-6-fold more immunogenic than FIX, making the transgene mediated immune response a big concern. Nevertheless, the AAV-FIX clinical trials by Nathwani et al. have detected an anti-AAV capsid immune response at high vector doses (Nathwani et al., 2014). This limit is very challenging for FVIII gene therapy because the necessary dose to achieve therapeutic levels of FVIII are higher than for FIX (High, 2012). To overcome some of these issues, FVIII molecule has been extensively modified by deleting the B-domain, that is not relevant in clotting function, and by codon optimization of the sequence. These modifications allowed the size reduction of FVIII cDNA closing the gap with the small capacity of the AAV cassette. Despite sustained FVIII levels have been reached using AAV vectors in HA animal models (Finn et al., 2010; McIntosh et al., 2013; Nguyen et al., 2019), the doses needed to reach therapeutic correction were significantly higher than the maximum doses of AAV-FIX administered to patients in clinical trials.

Over the years, several approaches for HA gene therapy using different AAV capsid were attempted, and recent clinical trials are listed in **Table 2**.

Type of vector	Transgene	N° of patients	FVIII activity %	Trial status	Sponsor	References
rAAV5 (NCT03370913)	BDD-FVIII	134	13-20	Active, not recruiting	Biomarin	Rosen 2020; Pasi 2020; Rangarajan 2017
rAAVhu37 (NCT03588299)	BDD-FVIII	30	5-17	Recruiting	Bayer	Pipe 2019
AAV8 (NCT04676048)	BDD-FVIII	12	NR	Not yet recruiting	ASC Therapeutics	N/A
rAAV2/6 (NCT04370054)	BDD-FVIII	63	7-169	Recruiting	Pfizer	Leavitt 2020; Konkle 2019
rAAV-LK03 (NCT03003533)	BDD-FVIII	30	13-30	Recruiting	Spark Therapeutics	Ran 2020; High 2018
rAAV2/8 (NCT03001830)	FVIII-V3	18	6-76	Recruiting	UCL	Nathwani 2018

Table 2. Recent Clinical Trials for Hemophilia A Gene Therapy. All recent clinical trials for hemophilia A rely on systemic administration of AAV vector. Data were collected from clinicaltrials.gov as of April 2021. (High et al., 2018; Konkle et al., 2019; Leavitt, 2020; Nathwani et al., 2018; Pasi et al., 2020; Pipe et al., 2019a; Ran et al., 2020; Rangarajan et al., 2017; Rosen et al., 2020)

A crucial point for these studies will be achieved in longer follow-ups to show if FVIII concentrations will be stabilized or if the decline will be progressive with the complete loss of expression. To date, young patients are still excluded because of many practical restrictions and safety concerns. Of relevance, the episomal state of the transgene after AAV transduction cannot ensure stable transgene expression in a growing liver because of the dilution effect from cellular division. Since AAV are common non-pathogenic viruses that infect humans beginning in childhood, pre-existing antibodies are frequently present in the general population. Furthermore, patients with inhibitors are now excluded from this therapeutic approach. Therefore, lentiviral vectors (LVs) could represent a viable approach able to overcome some AAV limitations in gene therapy for HA.

3.2 Lentiviral vector-based gene therapy strategies for hemophilia A

Lentiviruses are single-stranded viruses of the Retroviridae family, characterized by the ability to retrotranscribe their RNA genome into a cDNA copy, which is then stably integrated into the host cell genome. The integration ability of these viruses has rendered these vectors the preferable choice in gene therapy when aiming at permanent gene transfer even if they tend to integrate more randomly into the genome (Biffi et al., 2011). LVs dispose of an active transport mechanism of translocation of the genomic material into the nucleus regardless of the cell cycle status. Thus, they can transduce both non-dividing and dividing cells guaranteeing stable and persistent transgene expression *in vitro* and *in vivo*, opening the

possibility for the treatment of a broad range of genetic disorders. The lack of viral proteins and the accommodation of expression cassettes of up to 10 Kb are additional advantages. Human immunodeficiency virus type 1 (HIV-1)-based vectors are the most extensively studied and used LV so far (Naldini, 2019). To build safe vectors, the lentivirus genome was modified over the years by segregating the cis-acting sequences and trans-acting genes in different plasmid constructs. Based on the evolution of the packaging constructs used for vector production LVs are classified into “generations”. Third-generation vectors are the most advanced version utilized to produce LV, with enhanced safety achieved by splitting sequences and genes necessary for viral production into four different plasmids. Moreover, the use of cell- and tissue-specific internal promoters selectively targets the vector expression to the desired tissue allowing prolonged gene expression. Ubiquitous promoters allow a strong transgene expression, even though they happen to be inactivated over the time impairing the sustained transgene expression. Hepatocyte-specific promoters have been widely used to obtain prolonged expression in the liver and mitigated immune responses (Follenzi et al., 2004). Inducible promoters are also a valid option, as they provide an additional regulatory element that can be induced under specific conditions in selected tissues (Vigna et al., 2005). Moreover, another degree of cell targeting is represented by the post-transcriptional regulation based on micro RNAs (miRNAs). For gene transfer purpose, the insertion of complementary sequences to a specific miRNA (miRNA target sequence, mirT) to the 3' of the expression cassette, offers the possibility to reduce selectively the transgene synthesis in the cell types in which that selected miRNA is expressed (Brown et al., 2006).

However, innate or adaptive immune response can occur against the transgene once is expressed by antigen presenting cells (Annoni et al., 2007). Therefore, the use of cell specific promoter to de-targeted transgene expression in antigen presenting cells allowed the sustained expression of therapeutic gene in the selected cells, by reducing immune response.

Despite no clinical trial is ongoing with other viral vectors except for AAVs, LVs were employed for the treatment of HA in preclinical models allowing stable multi-year transgene expression in the liver of mice and dogs (VandenDriessche et al., 1999; Xu et al., 2005).

Transplantation of LV-transduced hematopoietic stem cells (HSCs) in conditioned recipient mice resulted in a successful phenotypic correction of HA mice and, in addition, in immunological tolerance induction to the transgene. One of the attractive features of LV-transduction of HSCs is that by using megakaryocytic specific promoters, FVIII expression

can be directed to platelets resulting in hemostatic correction, as it was demonstrated in mouse, rats and dog models of HA (Du et al., 2013; Shi et al., 2007, 2020). After vascular damage, FVIII was released with platelets degranulation only in the site of injury, providing a locally inducible treatment to maintain hemostasis for HA. Notably, phenotypic correction was achieved also in HA mice presenting high-titer inhibitory (Kuether et al., 2012). This strategy could be an innovative treatment for HA patients with pre-existing inhibitors. However, preconditioning of bone marrow is not without risky side effects and risk/benefits ratio need to be carefully assessed for this type of gene therapy for HA. A similar approach was explored by direct intraosseous delivery of LV in HA mice in which bone marrow cells and HSCs were transduced *in situ* bypassing the conditioning treatment (Wang et al., 2015). Liver, and especially, hepatocytes have been considered the perfect target for HA gene therapy due to their limited transgene mediated immune response. However, FVIII inhibitors development is still a current drawback for the success of HA gene therapy, thus, additional suitable cell types were evaluated.

The specifically targeted FVIII expression in organs or cell types with immuno-tolerant properties could overcome inhibitor development. Liver sinusoidal endothelia cells (LSECs) represent an optimal candidate since their ability to induce tolerance against antigen presented by themselves (Knolle and Wohlleber, 2016). Besides FVIII production in specific cell type, immune response can be reduced by narrowing transgene expression in APCs. This was obtained by using the microRNA target sites miRT142-3p that provided a sustained FVIII expression in mice without antibodies formation (Matsui et al., 2011).

FVIII is largely secreted by ECs, particularly by LSECs, and to a lesser extent by hematopoietic cells in both humans and mice (Follenzi et al., 2008; Fomin et al., 2013; Shahani et al., 2014; Zanolini et al., 2015). To increase the target specificity of FVIII expression, in the study of our group, miRTs were included (i.e., miRT142.3p, miRT-126, and miRT-122) to silence expression in hematopoietic cells, endothelial cells, and hepatocytes, respectively. FVIII expression was thereby restricted to endothelial or myeloid cells using LVs containing endothelial-specific (LV.VEC) or myeloid-specific (LV.CD11b) promoters. Remarkably, transcriptional targeting for ECs by using VEC promoter in presence/absence of miRT122-142 allowed long-term therapeutic levels of FVIII expression in HA mice and induced the production of regulatory T cells (Tregs) that inhibited the immune response (Merlin et al., 2017).

Recently, our group targeted FVIII expression in naturally FVIII-producing cells by generating a LV containing the BDD-FVIII transgene under the control of the *F8* promoter

(pF8). Tail vein injection of this LV in HA mice resulted in sustained production of therapeutic levels of FVIII that were higher compared to the ones obtained by targeting specifically ECs with VEC promoter. pF8 demonstrated to be active in an organ-dependent manner allowing transgene expression in hepatic endothelial cells as well as in splenic hematopoietic cells. Moreover, no inhibitors were observed, and stable tolerance was reached via a mechanism involving Treg induction, even following FVIII challenges (Merlin et al., 2019).

The idea of pF8-driven transgene expression to correct the bleeding phenotype in HA was pursued in another work of our group. Firstly, from an *in silico* analysis of pF8 sequence, it was predicted the role of the most represented endothelial-specific transcription factor binding sites (TFBSs) that may have a role on *F8* transcriptional regulation. Identifying the transcription factors (TF) required for maximal promoter activity in ECs, may offer an important step forward in the development of gene therapeutic approaches for HA. *In vitro* luciferase assays demonstrated the central role of Ets family of TFs in the modulation of pF8 activity. According to the position of Ets1/2 TFBSs, the length of the native pF8 sequence was reduced gradually until the minimal portion of pF8 required to efficiently drive FVIII expression *in vivo* was found. FVIII gene transfer in HA mice, indeed, confirmed the power of the length-reduced promoters to drive long-term and stable FVIII expression without inhibitors development. It should be noted that therapeutic levels of FVIII activity were detectable in all treated mice at similar levels to those observed in mice delivered with the native pF8 (Famà et al., 2020). Besides comprehending the underlying mechanism of *F8* transcription, such optimization of the minimal pF8 size opens the possibility to explore new perspectives with respect to the current obstacles associated with the achievement of an efficient FVIII gene delivery.

4. Cell and gene therapy: endothelial cells as optimal cell source

Despite its advantages, “pure” gene therapy approaches face some challenges in HA treatment. A combined approach of gene and cell therapy deserves further consideration to determine if an effective and safe cell-based treatment can be developed. Cell therapy consists in the infusion or transplantation of cells in a patient from external sources to achieve the treatment of a specific disease. For genetic disease, cell therapy approaches also called *ex vivo* gene therapy, involve the gene transfer of the correcting gene into the cells to be transplanted representing an alternative strategy to pure gene therapy.

This approach is most frequently applied to hematopoietic stem cells, which is becoming a powerful and versatile strategy to treat a growing number of human diseases. Albeit great outcomes of cell therapy were achieved, some concern about immune rejection of donor cells remain. To overcome potential immune response of transplanted allogeneic cells, technologies such as hydrogels encapsulation and medical devices were developed. Implantable devices, for example, can provide a vascularized encapsulated environment for therapeutic cells to produce and release missing proteins into the bloodstream while providing immune protection (NCT03513939).

To design a cell-based therapy approach it is fundamental to identify the best cell sources to treat the disease. Expression of FVIII, the missing factor in HA, is tissue-specific and although FVIII mRNA is detected in several human and mouse organs such as liver, spleen, lymph nodes, kidney (Hollestelle et al., 2001; Wion et al., 1985) and hematopoietic cells (Follenzi et al., 2012; Zanolini et al., 2015), transplantation studies in HA animal models and patients demonstrated that liver is the primary source of FVIII (Bontempo et al., 1987) and among liver cells, liver sinusoidal endothelial cells (LSECs) are the main sources of FVIII.

In 2005, it was demonstrated that the presence of ECs in several liver-cell combinations was essential for the correction of clotting dysfunction of transplanted HA mice (Kumaran et al., 2005). Afterward, Follenzi et al. transplanted purified mature LSECs into the portal vein of HA mice and demonstrated the engraftment in the liver and the therapeutic correction of HA reaching above 10% FVIII activity of normal plasma levels (Follenzi et al., 2008). Additionally, successful transplantation of human LSECs isolated from adult liver in HA mice was also reported (Filali et al., 2013; Fomin et al., 2013; Zanolini et al., 2015). Therefore, LSECs were recognized as the main source of FVIII in the liver, bringing them to the forefront in the design of alternative therapeutic approach for HA, such as gene and cell therapy. In the context of cellular therapy for HA, potential sources of transplantable cells could be represented by LSECs or immature endothelial progenitors. However, cell therapy with adult

LSECs is limited by access to living donor tissue or cadaverous livers. Thus, other stem cell and progenitor populations were evaluated for their potential for *in vivo* FVIII production either by acting as carrier cells for ectopic FVIII expression or differentiation into LSECs after transplantation. Even though LSECs and stem cells derived from various adult and fetal sources may play a great role in the therapy of HA, there are potential limitations that may hinder their clinical utility such as: i) lack of availability of a suitable donor tissue; ii) low yield of LSECs from liver homogenates, iii) limited expansion potential of stem cells or LSECs due to loss of functional or proliferative capacity in vitro. The extent of these potential limitations is not fully known and requires further studies. Nonetheless, to provide good quality and an appropriate number of cells to treat HA, investigation into alternative LSECs sources is prudent.

In addition to LSECs, other cell sources competent for FVIII production can be identified in bone marrow-derived stem cells, blood-outgrowth endothelial cells (BOECs), endothelial progenitor cells derived from the differentiation of induced pluripotent stem cells (iPSCs) and embryonic stem cells (ESCs). (**Fig. 4)**

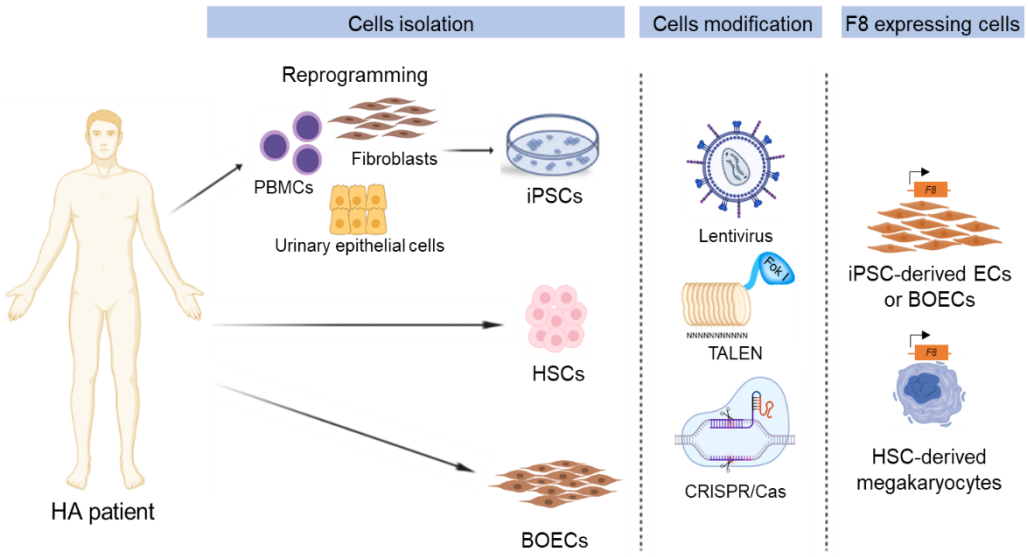

Figure 4. Gene and cell therapy for hemophilia A. Schematic representation of *ex vivo* gene therapy approaches to genetically correct HA patient's cells. PBMCs, fibroblasts or urinary epithelial cells can be reprogrammed into iPSCs. Alternatively, primary cells such as HSCs or BOECs can be used for subsequent F8 gene correction using lentiviral vector or gene-editing techniques to obtain differentiated cells expressing the functional form of FVIII. HA, hemophilia A; PBMC, peripheral blood mononuclear cells; iPSCs, induced pluripotent stem cells; HSCs, hematopoietic stem cells; BOEC, blood outgrowth endothelial cells; TALEN Transcription activator-like effector nucleases; CRISPR/Cas; clustered regularly interspaced short palindromic repeat

4.1 iPSC-derived endothelial cells

In 2006 a major scientific milestone was achieved when iPSCs were discovered (Takahashi et al., 2006). The finding of generating embryonic-like stem cell starting from somatic cells has revolutionized the fields of disease modelling, drug discovery and cell therapy development. In contrast to human ESCs, human iPSCs are easier to obtain and do not generate ethical controversy. Since then, due to their extensive potential for self-renewal, growth, and pluripotency, the establishment of iPSC allowed the generation of differentiated cells belonging to all three primary germ layers and, thus, including endothelial cells (ECs). Since FVIII is primarily expressed and post-translationally modified in ECs, iPSC differentiation approach ensures a consistent and potentially unlimited source of ECs for *in vitro* studies and regenerative medicine.

ECs are cells of mesoderm origin that line the inner layers of the blood and lymphatic vessels. Alongside the vessel barrier role, ECs are actively involved in the immune response, inflammation, and transportation processes (Bierhansl et al., 2017).

According to their function and location, ECs can be morphologically characterized as continuous, fenestrated, or sinusoidal (Aird, 2012). For example, liver sinusoids display a discontinuous endothelium that allow the exchange of solutes and macromolecules, while the endothelium of large vessels display tight junctions that serve as a barrier (Dela Paz and D'Amore, 2009). Subtypes of ECs can be distinguished also by their origin whether it be arterial, venous, or lymphatic, with their size determining whether they are macrovascular or microvascular ECs. Despite subtypes of ECs can be identified by unique markers, some common markers are shared among all ECs, such as CD31, vWF, CD144, and VEGFR2 (Ribatti et al., 2020).

Primary ECs can be isolated from endothelial biopsies, but they are difficult to retrieve and have a limited proliferation potential (Hewett, 2016). For this purpose, iPSCs are an attractive source for generating ECs, especially if the potential to generate patient-specific cells is considered, thus reducing the risk of immune rejection by offering an autologous source of cells in the perspective of transplantation.

Several methods have been developed to differentiate iPSCs into ECs, but general vessel specificity of iPSCs-derived ECs is difficult to obtain and, therefore, more specific protocols were investigated (Zhang et al., 2014). Despite many ECs differentiation protocols are now available, only one group has achieved the differentiation of iPSC into LSECs. Koui et al. obtained LSEC progenitors by exhibiting a mature endothelial morphology and expressing specific markers, such as FLK1, F8, STAB2, and LYVE1 (Koui et al., 2017). Recently, the

same protocol for LSEC differentiation was confirmed by Danoy et al., who further characterized the generated cells with additional specific markers, including CD144 and STAB1, and a new set of genes overlapping the gene expression profile of primary human LSECs (Danoy et al., 2020).

The use of cell therapy in the treatment of HA in the past few year consisted mainly in the transplantation of healthy cells to repair or replace the coagulation factor deficiency (Follenzi et al., 2012; Kumaran et al., 2005; Ohashi et al., 2005; Zanolini et al., 2015). These procedures were led mainly with adult stem cells and, more recently, with progenitor cells partially differentiated from iPSCs, but the mechanisms by which transplanted cells engraft, proliferate and function remain unknown. Xu and colleagues (Xu et al., 2009), evaluated the therapeutic application of iPSCs using iPSC-derived endothelial cells for treatment of a preclinical mouse model of HA. Following transplantation of these cells into the HA mice liver, the levels of plasma FVIII in treated mice increased to 8%-12% and HA mice survived. Moreover, they examined the liver distribution of GFP-labeled transplanted cells and demonstrated that these cells appeared to reconstitute structurally the sinusoidal endothelial compartment in the liver.

Several studies aimed to develop HA iPSCs models. Jia et al. established human HA models using hepatocytes-like cells differentiated from integration-free-iPSCs, but obtained cells failed to secrete FVIII (Jia et al., 2014). Subsequently, other strategies were investigated to generate a FVIII-deficient model cell line avoiding the use hemophilic patient samples.

At the beginning of the genome-editing era, an HA model cell line was developed using a transcription activator-like effector nuclease (TALEN) pair to invert a chromosomal segment that spans the portion of the FVIII gene in human healthy iPSCs (Park et al., 2014). This study demonstrated that TALEN could be used not only to model HA, but also to correct genetic defects. Other genetic engineering tools such as PiggyBac transposon were used to recapitulate (Matsui et al., 2014) or to revert (Neumeyer et al., 2019) FVIII mutations in HA-iPSC patients, that after differentiation in ECs were able to restore FVIII levels in a mouse model of HA. After the discovery of an “easy-to-use” gene editing platform, as clusters of the regulatory interspaced palindromic repeats (CRISPR)-Cas9 system, several works have been published since then (Park et al., 2015, 2019; Sung et al., 2020).

Our group published in 2018 a preclinical study in which iPSCs were obtained from 4 HA severe patients, besides healthy donors. Our approach took advantage of peripheral blood sampling as the safest and easiest procedure for hemophilic patients, if compared with skin biopsies. Among the cells of peripheral blood, we identified CD34+ cells as the optimal cell

source for reprogramming, by obtaining *bona fide* iPSCs after 20 days. The differentiation protocol into ECs was improved by adding a mesoderm transition step driven by the presence of BMP4, before definitive endothelial differentiation. The resulting cells were able to form functional and stable microvascular ECs that manifest an endothelial gene expression pattern specific for blood endothelial cells. Moreover, in contrast to HA-ECs, healthy-ECs were able to long-term secrete FVIII. For HA cell therapy HA-iPSCs were corrected by gene transfer using a LV carrying the functional BDD-FVIII under the control of the endothelial-specific VEC (cadherin 5) promoter. The use of VEC promoter limited the FVIII expression only in the iPSC-derived differentiated cells that were effectively ECs. HA-ECs, indeed, were able to express and secrete FVIII after genetic correction, demonstrating the transcriptional activation of the endothelial-specific promoter *in vitro* and *in vivo*. Upon injection through the portal vein into a conditioned mouse model of HA, the FVIII-expressing HA-iPSC-derived ECs were able to engraft and repopulate the liver parenchyma by forming new vessel network. Of greater importance, the transplantation rescued the hemophilic phenotype of the mice by restoring therapeutic levels of FVIII activity up to 12 weeks (**Fig. 5**) (Olgasi et al., 2018).

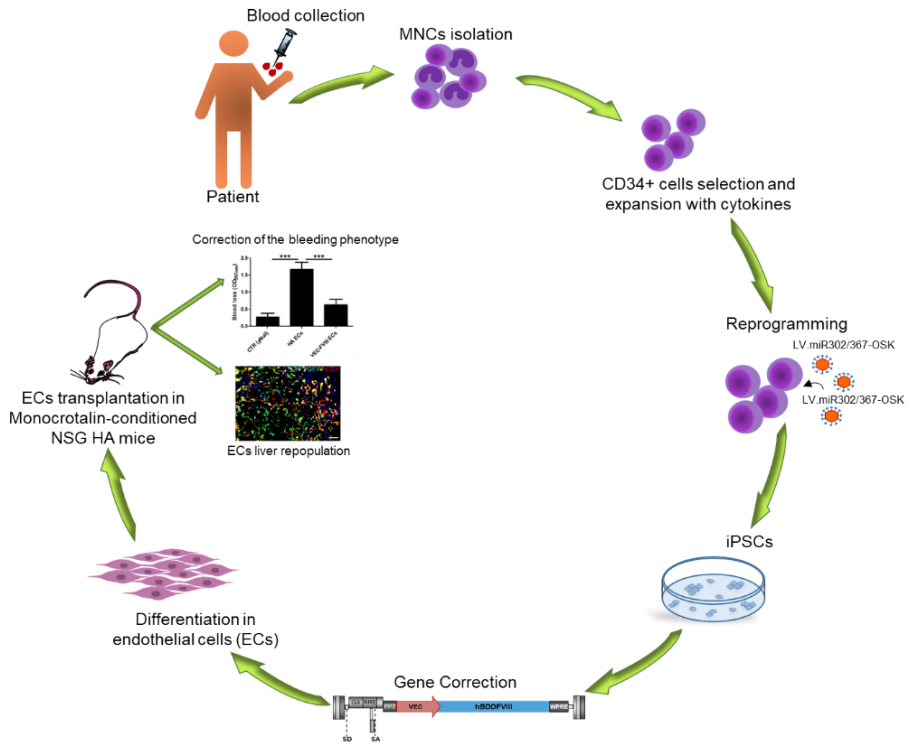

Figure 5. Patient-specific iPSC-derived endothelial cells provide long-term phenotypic correction of hemophilia A. Upon blood collection of HA patients, CD34+ cells were isolated from MNC and reprogrammed with a LV carrying miRNAs 302/367 cluster and OSK. Obtained bona fide HA-iPSCs were gene corrected by using a LV carrying the BDD-FVIII under the control of VEC promoter and differentiated in ECs. Transplantation of HA-iPSC-derived-ECs in monocrotaline-conditioned NGS HA mice engrafted and repopulated liver vessel network and most importantly corrected long-term the bleeding phenotype of HA mice (Olgasi 2018). MNC, mononuclear cells; OSK; OCT4 SOX2 KLF4; iPSC, induced pluripotent stem cells.

These studies provide the proof of concept for the potential to develop cell therapy strategies based on iPSCs technology correcting the bleeding phenotype of the disease. Indeed, the possibility to differentiate patient-derived iPSCs into ECs and correct them by gene transfer could represent an unlimited source of transplantable FVIII producing cells to treat HA.

4.2 Blood outgrowth endothelial cells (BOECs)

BOECs are a sub-population of human endothelial cells, found within the peripheral blood. The first group to report the presence of circulating cells which could differentiate into cells with the phenotypic characteristics of vascular endothelium was described by Lin et al. (Lin 2000). The concept of endothelial cells that could be isolated from blood is not new, but the origin of those cells was controversial until Hebbel shed light to the miscalling of these cells, identifying the subset of blood ECs as depicted in **Fig. 6** (Hebbel, 2017).

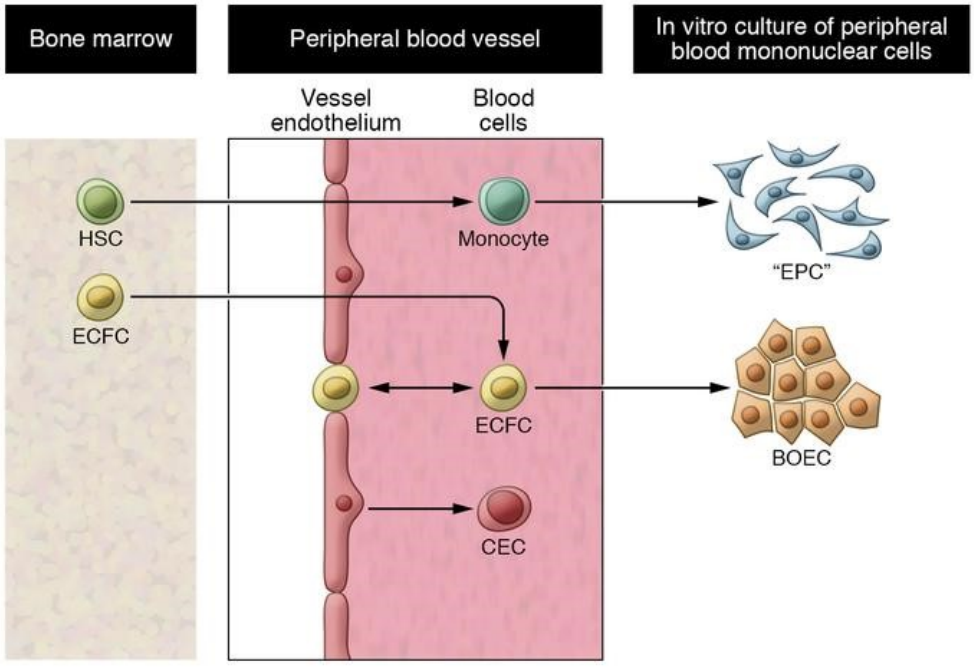

Figure 6. Blood endothelial cell types, origins, and culture. Circulating endothelial cells (CEC) are detached from the vessel wall endothelium as the result of injury and/or disease. Blood outgrowth endothelial cells (BOEC) have all the characteristics of mature endothelial cells. They seem to be progeny of endothelial colony–forming cells (ECFC), a marrow-derived progenitor that resides both in blood and within in situ endothelium. The other relevant cell appearing from appropriate culture of blood mononuclear cells was labeled “EPC” (intended for endothelial progenitor cells). These were later shown to be of hematopoietic stem cell (HSC) origin. (Hebbel 2017)

Circulating endothelial cells (CECs) are the result of vessel wall endothelium detachment due to injuries or pathological conditions. CEC have a very limited proliferative ability but may be useful for reporting the status of the endothelium (Solovey et al., 1997). In contrast, cultures of peripheral blood mononuclear cells produce an outgrowth of cells that can be divided in endothelial or non-endothelial classes, depending on specific culture method. The cells formerly referred as endothelial progenitor cells (EPCs) (Asahara et al., 1997) are of hematopoietic origin, characterized by limited growth potential and inability to produce mature endothelial cells (Medina et al., 2010; Yoder et al., 2007), even though in certain conditions could provide nutritive support for endothelial cell expansion. Conversely, BOECs, are fully differentiated endothelial cells in every aspect: morphology, phenotype, organelle content, response to stimuli, observable behaviors, and gene expression pattern. The origin of BOECs, that are obtained by *in vitro* culture, is to be intended from a progeny of circulating, marrow-derived, transplantable cells that are supposed endothelial progenitor cells also called endothelial colony–forming cells (ECFCs) (Lin et al., 2000). Supposedly, ECFCs reside in the vessel wall endothelium at higher numbers than found circulating in blood, even though they can be found in the early stage of the same cultures from which BOEC ultimately emerge (Yoder et al., 2007).

Despite their still debated origin, BOECs have attracted significant attention due to the potential for translational studies, gene therapy and vascular regeneration, especially when cells are required from a specific donor such as in autologous cell therapy.

BOECs find their applications in bioengineering when they have been used in the advance of bioartificial vascular networks, valve coatings, and nano matrix materials for wound healing. In cell biology, BOEC cultures allow the study of the effect of a specific protein on endothelial biology and as a matter of fact they have been injected as bait and later recaptured to identify the roles of specific signaling molecules during vasculogenesis (Rohban et al., 2013).

BOECs also have been used for experimental gene therapy. For example, autologous BOECs have been successfully used for gene therapy in animal models of HA (Lin et al., 2002; Matsui et al., 2007; Ozelo et al., 2014).

The first experiment reported by Lin et al. demonstrated the feasibility of using BOECs as a delivery system for the administration of FVIII. After expansion, BOECs were transfected with a nonviral plasmid vector carrying the BDD form of FVIII and then tail-vein injected in NOD/SCID mice. Results of the study indicate that BOECs expanded *in vivo* after administration and sustained therapeutic levels of FVIII up to 5 months. Moreover, it was

revealed that BOECs accumulated only in bone marrow and spleen and that these cells retained endothelial phenotype and transgene expression (Lin et al., 2002).

BOECs isolated from canine and murine blood were transduced with a LV containing the canine BDD-FVIII (cFVIII) transgene and then subcutaneously implanted in Matrigel plugs in immunodeficient and immunocompetent mice. In both mouse models, therapeutic levels of cFVIII persisted up to 27 weeks after implantation. Loss of cFVIII expression was then observed due to a gradual loss of BOEC viability (Matsui et al., 2007).

cFVIII-transduced BOECs have also been grown into monolayer sheets and then transplanted subcutaneously resulting in a partial correction of the bleeding phenotype in HA mice (Tatsumi et al., 2013).

Subsequently, cFVIII-overexpressing autologous BOECs were implanted in the omentum of a canine model of HA. These implanted cells formed new vessels in the omentum thereby secreting into circulation therapeutic levels of cFVIII up to 1 year after the transplantation (Ozelo et al., 2014).

To improve transplanted cells engraftment, Gao et al. proposed a co-transplantation study. Cord blood isolated BOECs were transduced with a LV carrying the BDD-FVIII and were intramuscularly injected in combination with placenta-derived mesenchymal stromal cells (PMSCs) in neonatal and adult immunodeficient mice. Longer engraftment was achieved in the co-transplanted mice in which the engrafted BOECs expressed FVIII, maintained endothelial phenotype, and generated functional vasculature. Overall, when co-transplantation of BOECs and PMSCs was proven in HA mice, a significantly attenuation of the bleeding symptoms of the mice was observed (Gao et al., 2019).

Our group successfully isolated BOECs from healthy donors and HA patients with no differences in terms of number of colonies achieved. After *in vitro* expansion both BOECs from healthy donors and HA patients showed the classical endothelial cobblestone-like morphology and the conventional endothelial markers such as CD31, KDR, Tie-2, VEC, VWF, while the hematopoietic phenotype was excluded due to CD34 and CD45 absence. For FVIII correction, isolated cells were transduced with a LV carrying the BDD form of FVIII driven by the VE-cadherin promoter (LV-VEC.hBDD-FVIII). The ability to secrete FVIII was first evaluated *in vitro*, and subsequently upon BOECs injection in association with microcarrier beads in NSG-HA mice. Transduced healthy and HA BOECs were able to partially restore FVIII activity, which reached 10% at 4 weeks post injection and persisted above 5% for up to 10 weeks. Moreover, BOECs were subjected to large-scale expansion under GMP-compliant conditions without any changes in terms of morphology, functionality,

and ability to secrete FVIII. As a proof-of-concept study, BOECs were encapsulated into an implantable, scalable, pre-vascularized device already in phase III clinical trial for type I diabetes. The device, called Cell Pouch™, when implanted in HA mice, allowed survival of BOECs and subsequent FVIII secretion that was able to reach therapeutic level of plasma FVIII up to 13 weeks (Olgasi et al. under revision; manuscript attached in the appendix). Further investigation will be needed to assess the long-term survival of the encapsulated BOECs. Cell Pouch™ is currently used in a clinical trial for diabetes type I in which insulin producing Islets of Langerhans are encapsulated in the device (NCT03513939). The Cell Pouch™ is designed as a scaffold made of non-degradable polymers, formed into small cylindrical chambers which, when placed in the subcutaneous site, becomes incorporated with tissue and microvessels. After the tissue incorporation, the plugs are removed, leaving fully formed tissue chambers with central void spaces for the transplantation of therapeutic cells, including islets. The scalable design of Cell Pouch™ allow several re-implantation of therapeutic cells on demand.

To date, our study was the first therapeutic approach that combines the GMP production of autologous human BOECs with the use of a safe *ex-vivo* approach based on an implantable pre-vascularized device.

Finally, despite BOECs cannot be successfully isolated from peripheral blood from all individuals due to low number of circulating ECFC in the blood, ECFC/BOECs represent a powerful tool to study molecular endothelial dysfunction in disease, giving access to ECs from patients and healthy controls in a non-invasive way. On the other hand, the number of preclinical studies involving BOECs are growing, with the potential to be applied in clinical studies.

5. Clinical manifestations of hemophilic patients: is it only a bleeding disorder?

HA is a disabling condition associated with chronic pain, joint impairment, and reduced quality of life starting at an early age. General bleeding is considered the hallmark of HA occurring in any body district, but the most affected sites are joints and muscles. The extent of clinical manifestations of HA patients depends on the severity of the FVIII deficiency.
The onset of the disease occurs at early age in severe HA patients, meanwhile bleeding occurs only in response to injury/trauma or surgery in patients with mild and moderate HA (Franchini et al., 2010). The major manifestations include abnormal bleeding in association with surgical procedures, excessive bruising, or hematomas with activities considered normal for age. In the absence of an informative family history, moderate and particularly mild HA may go undetected up to prepuberal age. Patients with severe HA commonly experience spontaneous bleeding episodes, therefore, the disease can be fatal in early infancy without treatment (Hay et al., 2021).
The factors that initiate hemorrhage are not known, and the onset of hemorrhage often is a random event, occurring either spontaneously or after minimal injury. Approximately 80 percent of hemorrhage occurs into joints, at the level of knees, elbows, and ankles (Gooding et al., 2021). However, other pathological conditions seem to be correlated with FVIII deficiency, as cartilage degeneration, bone remodeling, renal and cardiovascular diseases and intracranial hemorrhages.

5.1 Hemarthroses development

Due to recurrent joint bleeding, one of the main and common long-term complications in the management of the hemophilic patients is the development of hemophilic arthropathy (Lobet et al., 2014; Luck et al.; Simpson and Valentino, 2012).
Spontaneous hemarthroses are quite characteristic of severe HA as to be considered a diagnostic factor. Even if the vascular proliferation is not usually a feature of the normal joint, inflammatory conditions, such as recurrent bleeding, stimulates angiogenesis leading to reorganization of articular blood vessels and hypertrophic synovia (Knobe and Berntorp, 2011; Valentino, 2010).
Primary prophylaxis, which is initiated prior to or immediately following the first hemarthrosis, is used to prevent joint destruction or to halt its progression. In the absence of primary prophylaxis patients will develop a first hemarthrosis, typically manifesting between the ages

of 1 and 5 years (Lobet et al., 2014). Repeated hemarthrosis is responsible for arthropathy in adulthood and, if left untreated, severe HA patients may present more than 30 hemarthroses/year (Stephensen et al., 2009).

The pathological mechanism underlying the development of hemophilic arthropathy is not yet fully understood. The mechanism is multifactorial, involving cartilage degradation and inflammation of the synovial membrane due to the toxic effects related to blood effusions (Acharya et al., 2011). Vascular development and angiogenesis are an essential component of blood-induced joint disease. Just as angiogenesis is required for tumor growth, it also appears to be necessary for synovial expansion. Synovial joints are susceptible to spontaneous bleeds because the synovium is well-vascularized. In case of repeated extravasations or ongoing bleeding, the amount of blood exceeds the synovial removal capacity. Neovascularization causes the synovial membrane to thicken and develop friable fronds and villous projections. A network of capillaries forms under the hypertrophied synovium in response to joint irritation and increase blood flow to remove blood breakdown products. Iron, one of the hemoglobin degradation products of red blood cells, accumulates in the tissue as well as hemosiderin deposits, which trigger synovial inflammation (Calcaterra et al., 2020).

It was demonstrated that high levels of inflammatory cytokines are present in hemosideritic synovium than in normal tissue (Roosendaal and Lafeber, 2003). Moreover, in a murine HA model it was observed the activation of nuclear factor kappa B (NF-kB)-associated signaling pathways when joint bleeding was induced (Sen et al., 2013). Pro-inflammatory cytokines like interleukin (IL)-1, IL-6, interferon-gamma (IFN gamma) and tumor necrosis factor-alpha (TNFa) were found upregulated as observed in other manifestations such as cartilage degeneration in osteoarthritis and rheumatoid arthritis (Schuerwegh et al., 2003). The presence of iron transforms the thin synovial membrane into a hypertrophic and hyperplasic membrane characterized by the proliferation and the persistence of inflammatory cells. The inflammation site requires higher level of oxygen stimulating the release of growth factors like VEGF, that in turn promotes neoangiogenesis, both locally and systemically (Acharya et al., 2011). Chronic inflammation triggers the release of tissue-destructive enzymes and cytokines that contribute to progressive joint damage (DUNN, 2011) (**Fig. 7**).

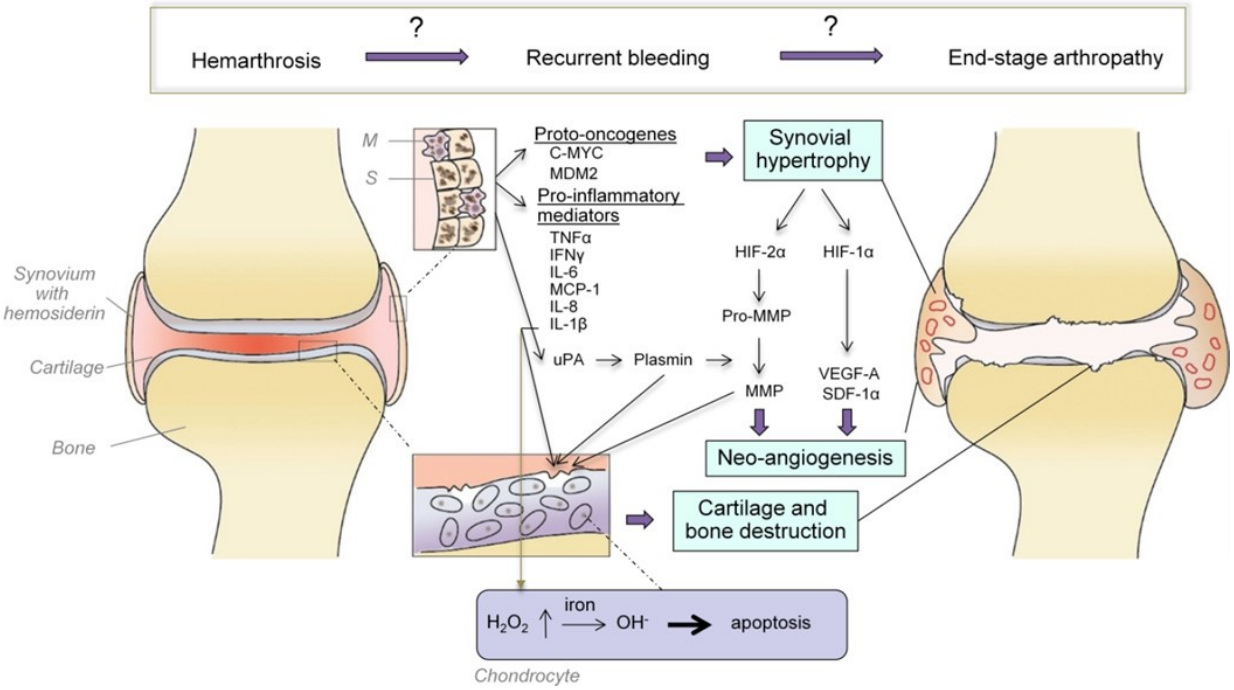

Figure 7. Pathobiology of hemophilic arthropathy. Erythrocytes in the joint space are processed by synoviocytes (S) and tissue macrophages (M), that store iron released from erythrocytes as hemosiderin. The expression of the oncoproteins C-MYC and MDM2 in response to iron results in synovial hypertrophy. Synovial hypertrophy creates a hypoxic environment causing arise in hypoxia-inducible factor (HIF)-1α and HIF-2α, which induce increased expression of the pro-angiogenic mediators vascular endothelial growth factor-A (VEGF-A) and stromal-cell derived factor1α (SDF-1α), as well as pro-matrixmetalloproteinases (pro-MMP). VEGF-A stimulates synovial neoangiogenesis and plasmin-mediated conversion to MMPs results in glycosaminoglycan release from the cartilage matrix, and cartilage and subchondral bone destruction. Synoviocytes and tissue macrophages also release pro-inflammatory mediators, such as tumor necrosis factor alpha (TNF-α), interferon-γ, interleukin (IL)-1β, IL-6, and monocyte chemoattractant protein-1(MCP-1) fueling these processes. Secreted IL-1β induces increased production of hydrogen peroxide (H2O2) in the chondrocytes, which upon reaction with iron (Fe2þ) forms cytotoxic hydroxylradicals (OH-) and prompts chondrocyte apoptosis. Neoangiogenesis and vascular remodeling are assumed to maintain a vicious cycle of re-bleeding that results in progressive hemophilic arthropathy, characterized by synovial hypertrophy, cartilage and bone destruction, and joint deformities (Wyseure 2016).

As a result of hemarthroses escalated in synovitis, target joints become more susceptible to mechanical damage and because of the vascular remodeling, more vulnerable to further bleeding (Bhat et al., 2015). A target joint is clinically defined as a joint in which 3 or more spontaneous bleeds occur within a consecutive 6-month period. About 25% of patients with severe hemophilia will experience recurrent bleeding and develop single or multiple target joints that are often painful and affect their quality of life (Klamroth et al., 2011). Over the years, periodic hemarthroses lead to chronic synovitis and ultimately the synovium becomes fibrotic. Clinical deformity of the joints can be difficult to treat and if canonic treatment options are not successful, surgery may be required to replace the damaged joint (Lobet et al., 2014).

5.2 Cartilage degeneration and bone remodeling

Cartilage consists of chondrocytes and matrix, mainly containing collagen type II and proteoglycan (aggrecan) which are required for the tensile strength and resilience of the cartilage tissue. As a result of joint bleeding, cartilage degeneration occurs both from synovial dependent and independent mechanisms. At first, hemophilic synovitis leads to the transformation of the cartilage in an invasive and destructive layer, called pannus, that is placed over the cartilage surface (Hoots, 2006). Characteristic of the pannus tissue is the presence of proliferative fibroblast-like mesenchymal cells, macrophage infiltration and other inflammatory cells that drive the degradation of the cartilage matrix by releasing collagenolytic enzymes, synovial derived pro-inflammatory cytokines, plasmin, and matrix metalloproteinases (MMPs) (Nieuwenhuizen et al., 2013). Secondly, the presence of blood exerts a direct harmful effect on cartilage. Exposure of blood on chondrocytes inhibits their ability to produce proteoglycans and other extracellular matrix proteins, by unbalancing the matrix turnover. Moreover, oxidative stress induced by pro-inflammatory cytokines lead to chondrocyte apoptosis, facilitating the tissue destruction (Hooiveld et al., 2003).

In parallel with synovitis and cartilage degeneration, also the underlying bone of target joint becomes impaired. Bone remodeling results from an unbalanced equilibrium of bone resorption and bone formation leading to a reduction of bone mineral density (BMD) and osteoporosis (Katsarou et al., 2010; Kovacs, 2008). A decreased BMD has been observed both in children and adult with HA (Barnes et al., 2004; Paschou et al., 2014). As a consequence, the risk of bone fracture is higher compared with the general population, especially for HA patients affected by the severe form (Gay et al., 2015). The reason behind this fracture risk is not completely understood but it could be addressed to impaired joints or to decreased BMD. Certainly, the sedentary lifestyle and hemarthroses contribute to poor bone health.

Apart from the association of hemophilia and BMD, animal models have provided evidence for a specific role of FVIII in bone remodeling. Bone remodeling is controlled by bone formation and resorption, primarily induced by osteoblasts and osteoclasts, respectively.

The mechanism behind hemarthrosis bone turnover is supposed to result from changes in the RANK-L//RANK/OPG pathway that result in the stimulation of osteoclastogenesis and in an enhanced disruption of bone tissue (Shahi et al., 2017). In HA patients presenting severe arthropathy, the synovial tissue shows an increased expression of RANK and RANK-L with a stimulation of the osteoclastic differentiation and thus bone resorption (Baud'huin et al., 2009).

5.3 Cardiovascular disease

The link between hemophilia and cardiovascular disease (CVD) has been investigated in several studies. Technically, because of the bleeding phenotype of HA patients, a reduced risk of thrombotic events might be expected. A systematic review including almost 15000 HA patients found no significant reduction in arterial thrombosis-related mortality compared to the general population (Kamphuisen and Ten Cate, 2014). Despite the role of FVIII is not clear in the formation of atherosclerotic plaques, thrombin generation is likely to play a key role. Conversely, in terms of acute thrombosis, a risk factor for venous thromboembolism has been described in presence of supraphysiological FVIII levels (Simioni et al., 2021). However, the regular infusion of FVIII on CVD risk in HA has not been investigated (Samuelson Bannow et al., 2019).

Another contributing factor for the risk of CVD is represented by hypertension. Age and body mass index are major risk factor in HA patients as well as in the general population. Yet, an increased prevalence of hypertension has been reported, especially in patients with moderate and severe HA compared with those with mild HA (Von Drygalski et al., 2013). Because of the bleeding events, also the kidney undergoes to neoangiogenesis, thus contributing to the hypertension observed in HA patients (Renna et al., 2013). As mentioned above, severity of hypertension is correlated to the enhanced risk of ICH that is 20-50-fold more common in hemophilic patients (Barnes et al., 2016).

Another threatening factor for HA patients with hypertension is the increased risk of fracture. A link between osteoporosis and hypertension has been reported (Ilić et al., 2013). In a rat model of hypertension, bone structure was impaired and osteoclastogenic markers were upregulated.

However, the causal relationship among hemophilia, osteoporosis, and hypertension has not been studied. Meanwhile, both blood pressure and osteoclastogenesis markers should be considered for further studies (Wang and Bai, 2021).

5.4 Unstable endothelial functionality

Recently, it was demonstrated an attenuated microvascular endothelial functionality in hemophilic patients and altered collagen levels in the plasma of HA patients, suggesting a dysfunction in endothelial cells (Kjeld et al., 2018).

Based on the correlation between hemophilia and arthropathy development, several groups investigated if there was a correlation between serum collagen levels and the annual

bleeding rate (Kjeld et al., 2018; Manon-Jensen et al., 2016). The extracellular matrix (ECM) remodeling is necessary for the maintenance of healthy tissues and an altered formation and degradation of ECM proteins can be associated to several pathologies (Xu and Shi, 2014). Recent studies demonstrated a correlation between an altered ECM and the development of hemophilic arthropathy. Amongst the ECM proteins, collagens are the most abundant. Moreover, it has been shown in hemophilic patients that high levels of collagen XVIII correlates to higher annual bleeding rates (Kjeld et al., 2018). The ECM dysfunction in ECs could result in their enhanced permeability and tight junctions where integrins may be involved in vascular function and permeability (Lampugnani et al., 2018; Sheppard, 2002). However, whether FVIII replacement therapy will impact neoangiogenesis is not known.

5.5 Intracranial hemorrhage

Despite the FVIII deficiency, newborns affected by the severe form of HA could live their first few months without any symptoms of the disease. However, approximately 3 to 5 percent of such patients develop intracranial hemorrhage (ICH) in the perinatal period due to trauma as the major precipitating factor (Zanon and Pasca, 2019). During ICH episodes, seizures commonly occur, letting long-term complications such as psychomotor retardation and cerebral palsy (Balami and Buchan, 2012).

It appears obvious that ICHs represent the most serious event that can occur in HA patients resulting in high rates of mortality and disability (Ljung, 2008; Zanon et al., 2012). Mortality caused by ICH, indeed, is around 20% (Stieltjes et al., 2005) and is higher in younger children (Senapati et al., 2016). The manifestation of ICH is often spontaneous, and it mainly occurs in children (up to 2yrs) and in patients that do not adhere to the prophylaxis regimen (Chalmers et al., 2018). Although the cause of the development of spontaneous ICH is still unknown (Kulkarni et al., 2017), a correlation between the severe form of hemophilia and ICH in children has been described, emphasizing the importance of prophylaxis in reducing the risk of ICH development (Andersson et al., 2017; Bladen et al., 2016).

In adult HA patients the major risk factor for ICH is hypertension as well as cardiovascular diseases (Von Drygalski et al., 2013). Indeed, it has been demonstrated a higher risk of developing hypertension and cardiovascular diseases in hemophilic patients compared to healthy subjects, but also in this case the mechanisms are not yet fully understood.

Aim of the thesis

Hemophilia A (HA) is an inherited bleeding disorder caused by genetic defects in coagulation FVIII. Based on its residual activity, there are several degrees of severity and spontaneous bleeding episodes can occur more frequently in severe HA patients. These bleedings primarily consist of hemarthroses and spontaneous intracranial hemorrhage that occur without a clear cause. Moreover, it has been described an impairment in vessel stability in HA patients but the correlation with the absence or low activity of FVIII has never been explored. Endothelium fragility has never been a focus in HA and to date, very little is known regarding the differences in the genetic profile between healthy and hemophilic endothelial cells (ECs). Such information may be crucial to understand if key molecular targets are missing in HA cell patients impairing EC functionality.

The main goals of this PhD thesis are: i) to understand the involvement of FVIII in EC functionality *in vitro* and *in vivo*; ii) to investigate if restoring FVIII in HA cells using recombinant FVIII protein or by LV transduction carrying FVIII transgene result in an improvement of EC functionality; iii) to evaluate the differences in transcriptomic profile of healthy, HA and FVIII corrected HA ECs to define the genes involved in endothelial cell physiology.

Therefore, the overall goal is to investigate the potential extra-coagulative roles of FVIII and elucidate the molecular mechanisms in which it is involved.

Understanding the role of FVIII in EC stability can help to shape the development of new therapeutic approaches resulting in a more efficient treatment of HA.

Materials and methods

Cell culture

iPSC-derived ECs (iECs) were differentiated as previously published (Olgasi et al., 2018) from one healthy donor and two severe HA patients. Obtained HA-iECs were transduced with a LV carrying the B domain deleted (BDD) form of F8 under the control of the endothelial VE-cadherin (VEC) promoter (LV-VEC.FVIII). iECs were cultured on 0.1% gelatin and maintained in KnockOut DMEM (Gibco) enriched with 10% fetal bovine serum (American origin – Euroclone), 1% glutamine (Gibco®, Life Technologies), 1% non-essential amminoacids (Gibco®, Life Technologies), 0.1% B-mercapthoethanol (Gibco®, Life Technologies), 50 ng/ml of VEGF (Cell Guidance System). BOECs were isolated from two healthy donors and three severe HA patients. Isolated HA-BOECs were LV-VEC.FVIII transduced as described for iECs. BOECs were maintained on CellCoat Collagen Type 1-coated Tissue Culture Flasks (Greiner Bio-One) at a 10^4 cells/cm^2 in MCDB 131 medium (Gibco®, Life Technologies) containing proprietary supplements.

BOECs LV transduction

Healthy, HA and LV-VEC.FVIII BOECs were plated at the 10^4 cells/cm^2 density and after 6-8 hours transduced with a lentiviral vector carrying the green fluorescent protein under the control of VE-cadherin promoter (LV-VEC.GFP) using a Multiplicity of Infection (MOI) of 20. After 14-16 hours incubation, fresh medium was added to the cells and 72 hours later half of the cells were harvested for FACS analysis using, while the other half was further cultured.

Flow cytometry analysis

Healthy, HA and LV-VEC.FVIII HA BOECs transduced with LV-VEC.GFP were analyzed by to assess the GFP positivity. For each sample, 1.5×10^5 live events were acquired on the Attune NxT Acoustic Focusing Cytometer (ThermoFisher Scientific, Waltham, MA, USA). Data were analyzed by FCS Express 6 (DeNovo Software, Glendale, CA, USA).

In vitro tubulogenic assay

Matrigel Matrix (Corning) was thawed overnight on ice. Twenty-four-well tissue culture plates were coated with 300 µl Matrigel per well and allowed to solidify at 37°C for 30 minutes. $5*10^4$ healthy, HA, LV-VEC.FVIII HA BOECs or $3*10^5$ iECs, were resuspended in culture medium and placed on top of the Matrigel. For FVIII stimulation, HA BOECs were

resuspended in serum free medium containing 1U/ml of one of the two recombinant form of FVIII (rBDD-FVIII or rFL-FVIII). Plates were incubated at 37°C, 5% CO_2 and observed after 16 hours of incubation. Images were acquired under inverted microscope Leica ICC50. ImageJ Angiogenesis software was used for the quantification of number of nodes, junctions, branches, and total length.

In vitro migration assay

Healthy, HA or LV-VEC.FVIII HA BOECs or iECs were plated into the upper compartment of the 8-µm pore size transwell chamber (Corning Incorporated, Corning, NY) at a density of 10^5 in serum free medium (MCDB131) while the lower compartment of the chamber was filled with complete medium. For FVIII stimulation, HA BOECs were resuspended in serum-free medium containing 1U/ml of one of the two recombinant form of FVIII (rBDD-FVIII or rFL-FVIII) and then placed in the upper chamber. After 24 hours, medium was removed and upper compartment of transwell chambers were cleaned from unmigrated cells with cotton swabs. Cells of the bottom part were fixed with 70% ethanol for 10' and then allow to air dry. Cells were stained with 0,1% crystal violet for 10'. The migrated cells on the lower surface of the filters were photographed under inverted microscope Leica ICC50. Crystal violet was then eluted with acetic acid and quantified using Victor Spectrophotometer at 590 nm.

In vitro permeability assay

Permeability was measured across the HA or HA.VEC.FVIII BOECs or iECs monolayer using Transwell polycarbonate membrane cell culture inserts (8 µm pore, 24-well format, Corning). Cells were plated on 0.1% gelatin-coated transwell inserts at a density of 80,000 cells/well and cultured in complete medium for 2 days. For FVIII stimulation, HA BOECs were cultured in serum free medium with 1U/ml of one of the two recombinant form of FVIII (rBDD-FVIII or rFL-FVIII) for 2 days. Completing the culture, 50 µl of FITC-conjugated 40-kDa dextran (Sigma-Aldrich) was added to the upper chamber and the media fluorescence of the lower chamber was measured after 30 min of incubation at 37 °C, 5% CO2 using Victor Spectrophotometer at 490 nm (excitation)/520 nm (emission). Fluorescence readings were normalized to dextran permeability in transwell inserts without cells.

RNA-seq

RNA from the different EC was purified as previously described (Incarnato et al., 2014) and its integrity was measured using Fragment Analyzer™ (Advanced Analytical). Library preparation was performed from PolyaAplus RNA using Illumina TruSeq RNA prep-kit. Samples were run in the Illumina sequencer NextSeq 500. Reads were mapped using TopHat239 and RPKM and were calculated using cuffdiff tool from Cufflinks software (Trapnell et al., 2010). Data analysis and plotting were performed using custom R scripts (url, https://www.R-project.org/, 2016).

Sequencing reads were aligned to human reference genome (version GRCh38.p13) using STAR v2.7.7a0 (Dobin et al., 2013) (with parameters --outFilterMismatchNmax 999 --outFilterMismatchNoverLmax 0.04) and providing a list of known splice sites extracted from GENCODE comprehensive annotation (version 32). Gene expression levels were quantified with featureCounts v1.6.3 (Liao et al., 2014) (options: -t exon -g gene_name) using GENCODE gene annotation (version 32 basic). Multi-mapped reads were excluded from quantification. Gene expression counts were next analyzed using the edgeR package (Robinson et al., 2009). Normalization factors were calculated using the trimmed-mean of M-values (TMM) method (implemented in the calcNormFactors function) and RPKM were obtained using normalized library sizes and gene lengths. After filtering lowly expressed genes (below 1 CPM in 4 or more samples), differential expression analysis was carried out by fitting a GLM to all groups and performing LF test for the interesting pairwise contrasts. Genes were considered as significantly differentially expressed (DEGs) when having |logFC| >1 and raw.pvalue < 0.01 in each reported comparison.

RPKM values were scaled as Z-scores across samples before computing distances, both in heatmap and PCA plot.

The selection of gene in heatmap in Fig.10A is unsupervised (most variable genes), the one in Fig. 13A is supervised, filtering on DEGs in HA BOECs vs LV-VEC.FVIII HA BOECs.

The PCA were computed with prcomp in R (version 4.0.2) using the top 500 most variable genes selected in an unsupervised way, for the plot in Fig. 13B the data were previously batch corrected with combat R package using patient as covariate.

After the identification of the dataset of differentially expressed genes (DEGs), Enrichr online tool was used to identify pathways and gene ontology (GO) terms enriched using DEGs as input. A term is defined as significantly enriched if the reported adjusted pvalue is < 0.01.

RNA isolation and RT-qPCR for RNA-seq validation

Total RNA was isolated by Isol-RNA Lysis Reagent (Invitrogen). One µg of RNA was treated with DNase I (Thermo Scientific), and cDNAs were obtained using the RevertAid First Strand cDNA Synthesis Kit (Thermo Scientific). All real time quantitative PCR were performed using the StepOnePlus™ Real-Time PCR System (Applied Biosystems). Amplifications were carried out in 20 µL reaction solutions containing SYBR™ green PCR master mix (Thermo Fisher Scientific), first-stranded cDNA (diluted 1:10) and specific primer, listened in Table 3. PCR conditions were 95 °C for 10 min followed by 40 cycles of 95 °C for 15 s and 60 °C for 1 min. The specificity of each pair of primers was checked by melting curve analysis (95 °C for 15 s, 60 °C for 1 min and a continuous raise in temperature to 95 °C at 0.3 °C/s ramp rate followed by 95 °C for 15 s). To check reproducibility, each assay was performed with technical triplicates for each of the biological samples. Analyzed mRNA levels were normalized to Beta actin levels using the formula 2−ΔΔCt by the comparative ΔΔCt method (Livak and Schmittgen, 2001).

Animal procedures

NOD.Cg-Prkdc^{scid}Il2rg^{tm1Wjl}/SzJ (Jackson stock No 005557) mice with hemophilic phenotype (NSG-HA) were previously generated and maintained in our laboratory (Zanolini et al., 2015) All animals' procedures on NSG-HA mice were performed under sterile hood. Eight-week-old BALB/C mice were used for Evans Blue injection and NSG mice for Matrigel plug assays.

In vivo permeability assay

Evans blue extravasation was used to quantify the capillary permeability in 8 weeks old BALB/C WT and BALB/C HA. A 10 g/L Evans Blue solution (Sigma-Aldrich) was injected into the tail vein of mice. After 15 minutes mice were killed and was evaluated the extravasation in the interstitial space and at joint level.

Matrigel Plugs

Matrigel plugs were prepared on ice by re-suspending 2*10^6 healthy, HA or LV-VEC.FVIII HA BOECs 500 µL of Matrigel (Corning). The mixture was implanted intradermal in 8-week-old NSG or NSG-HA mice. After 10 days, the plugs were removed, fixed, and embedded in paraffin for histological analysis**.** For FVIII stimulation, HA BOECs were resuspended in 500 µL of Matrigel (Corning) containing 3U/ml of one of the two recombinant form of FVIII (rBDD-

FVIII or rFL-FVIII). Matrigel plugs were implanted intradermal in 8-week-old NSG-HA mice and every 2 days 2U/ml of rBDD-FVIII or rFL-FVIII were injected within Matrigel plug.
For assays performed using Matrigel not mixed with cells, 500 µL of Matrigel were prepared on ice. For FVIII stimulation, 3U/ml of one of the two recombinant form of FVIII (rBDD-FVIII or rFL-FVIII) were added to Matrigel (Corning) and every 2 days 2U/ml of rBDD-FVIII or rFL-FVIII were injected within Matrigel plug. After subcutanous implantation in 8-week-old NSG or NSG-HA mice, plugs were removed, fixed, and embedded in paraffin for histological analysis**.**

Immunostaining

Mouse Matrigel plugs were harvested and fixed in 4% PFA for 2h at 4°C, equilibrated in sucrose, and embedded in cryostat embedding medium (Bio-Optica). Cryostat sections of 4µm thickness were blocked in buffer containing 5% goat serum, 1% BSA, and 0.1% Triton X-100 in PBS, incubated with primary antibody at RT and then incubated for 45’ in the dark at RT with the secondary antibody. For nuclei detection DAPI were added to the secondary antibodies’ solution. Primary and secondary antibodies and dilutions are reported in Table 4.

Statistical Analysis

All data were expressed as mean ± SD. Graphs were generated, and statistical analysis was performed with Prism 5 (Graph Pad). The p values were calculated using Student's t test with two-tailed distribution, assuming equal standard deviation distribution, one-way ANOVA with Bonferroni post-hoc test; $p < 0.05$ values were considered statistically significant. $*p < 0.05$, $**p < 0.01$, $***p < 0.001$.

Table 3. Primers used in RT-qPCR.

Gene	Synthetic oligonucleotides	
	Forward primer	Reverse primer
COL1A1	TCTGCGACAACGGCAAGGTG	GACGCCGGTGGTTTCTTGGT
COL1A2	GCCCCCCAGGCAGAGA	CCAACTCCTTTTCCATCATACTGA
COL16A1	CACAATGCCCACCTTCACAG	CTTGGGGTTGCGGATCTTCT
COL18A1	GTGCCCATCGTCAACCTCAA	CCGTCAAAGGAGAAGATGCGT
COL24A1	GGCACACGAGATAACCCAGC	ATGTCTGGCCACCAGCACTG
ICAM5	CACCCGGTATCTACGTCTGC	CTGGTGACTTGGGCAGGTAG
ITGA2	GGAACGGGACTTTCGCAT	GGTACTTCGGCTTTCTCATCA
ITGA4	TGTTGAATGTTCCCCACCGA	GCACCCACTAGGAGCCATC
ITGA11	GACCGCCTTCTTTGGCTACAC	GGTTGGTGGCGAGACTAAGG
NID2	GGAGGAGGGATGGTGTTGTA	AGGGTCCAGGTTCTGATTGT
FBN1	TCTCCGCGTGTATCGACATC	AAATCCCGGCTGACAGCTAC
FAT1	GGGCCAACTTTGCGATTCCC	CCTTACTTCCCACGCTGGAT
VCAN	TCGAGGAGGCTGCAAAAGAG	TGGTTGTAGCCTCTTTAGGTTT
NRG1	TTTTCCCAAACCCGATCCGA	GGGGAGGCAAGGCTGG
DOCK10	TGGAGTACCAGGAAGAACTG	TCAGACTTCAGCACTAGATG
NOTCH2	ATGACTGCCCTAACCACAGG	TGCAGTCATCTCCACTCCAG
F2RL1	TGCTAGCAGCCTCTCTCTCC	CCAGTGAGGACAGATGCAGA
F3	AACCTCGGACAGCCAACAAT	GTTTGTTTTGGCTGTTTTCTTTCCT
KITLG	AGCCAGCTCCCTTAGGAATG	GACTTGGCTGTCTCTTCTTCCA
ALK5	GACAACGTCAGGTTCTGGCTCA	CCGCCACTTTCCTCTCCAAACT
ADGRL4	CTATCTAAGCCCAGCCGTGG	GCTCCTCTTGCACAAGACCTTA
TFPI2	CCAGATGAAGCTACTTGTATG	GCACATGCACGTTTGCAATC

Table 4. Antibodies used.

Antibody	Reactivity	Manufacturer	Format
CD31	mouse	Clone Mec 13.3 Biolegend	Biotin
αSMA	mouse	Clone 1A4 Abcam	Not conjugated
Anti -mouse IgG	/	Thermo Scientific	488
Streptavidin	/	eBioscience	PE
Anti-GFP	/	Thermo Scientific	Not conjugated
Anti -rabbit IgG	/	Thermo Scientific	488

Results

In vitro impaired functionality of hemophilic iPSC-derived endothelial cells

iPSCs obtained from HA patients and healthy donors were differentiated in ECs and the characterization is described in Olgasi et al. 2018. To evaluate the acquisition of endothelial functionality, a tubulogenesis assay was performed. The assay mimics the reorganization stage of angiogenesis by measuring the ability of ECs to form capillary-like structures when plated on an extracellular matrix support such as Matrigel. Healthy iECs formed a complete and stable network when cultured on Matrigel while HA iECs built a thin and incomplete network which improved after the LV-VEC.FVIII correction (**Fig. 8A**), suggesting a potential involvement of coagulation FVIII in tubule formation. Quantification of the formed network using ImageJ software showed a significant increase in the number of nodes, junctions, branches, and total length of the tubules formed by LV-VEC.FVIII HA iECs, compared to HA and healthy iECs, demonstrating that FVIII has an evident effect on tubule morphogenesis. It is curious to explore the mechanism leading to this effect (**Fig. 8B**). Furthermore, as shown in Fig. 8A, healthy iECs display a different morphology when cultured in Matrigel, establishing segments with a bigger diameter. This can influence the quantification and result in a non-significative difference in the number of nodes, junctions, and total length compared to LV-VEC.FVIII HA iECs. However, the number of branches is significantly higher compared to both HA and LV-corrected HA iECs indicating a more stable vessel-like tubular structures.

Another key function of endothelial cells is their ability to migrate. Therefore, cells were cultured on transwell and their ability to trans-migrate in the bottom of the chamber in presence of VEGF was tested. As shown in figure 8C, cells lacking FVIII have a reduced migration capability which was recovered following correction with LV-VEC.FVIII (**Fig. 8C**). Quantification of the eluted crystal violet dye, as an estimation of the total number of migrating cells, confirmed a significant increasing of motogenesis of healthy and LV-VEC.FVIII HA iECs compared to the HA iECs (**Fig. 8D**). Surprisingly, healthy iECs showed lower migration ability compared to LV-corrected HA iECs but might be due to their bigger size morphologically observed at the microscope.

Besides tubulogenesis and migration abilities, endothelial cells serve as a barrier between circulating blood and the surrounding tissues, making EC permeability a crucial factor in tissue homeostasis. This ability was evaluated by the extravasation of fluorescein isothiocyanate (FITC)-conjugated dextran (40 kDa, FITC-dextran) into gelatin matrix when

cells are cultured as an intact endothelial monolayer into transwell inserts. Quantification of permeate fluorescence showed an enhanced permeability of HA iECs compared to healthy and LV-VEC.FVIII HA iECs (**Fig. 8E**). Since the permeability assay requires an intact monolayer and the difference in cell morphology does not affect the quantification, the healthy iECs monolayer was significantly less permeable compared to the HA iECs one (**Fig. 8E**).

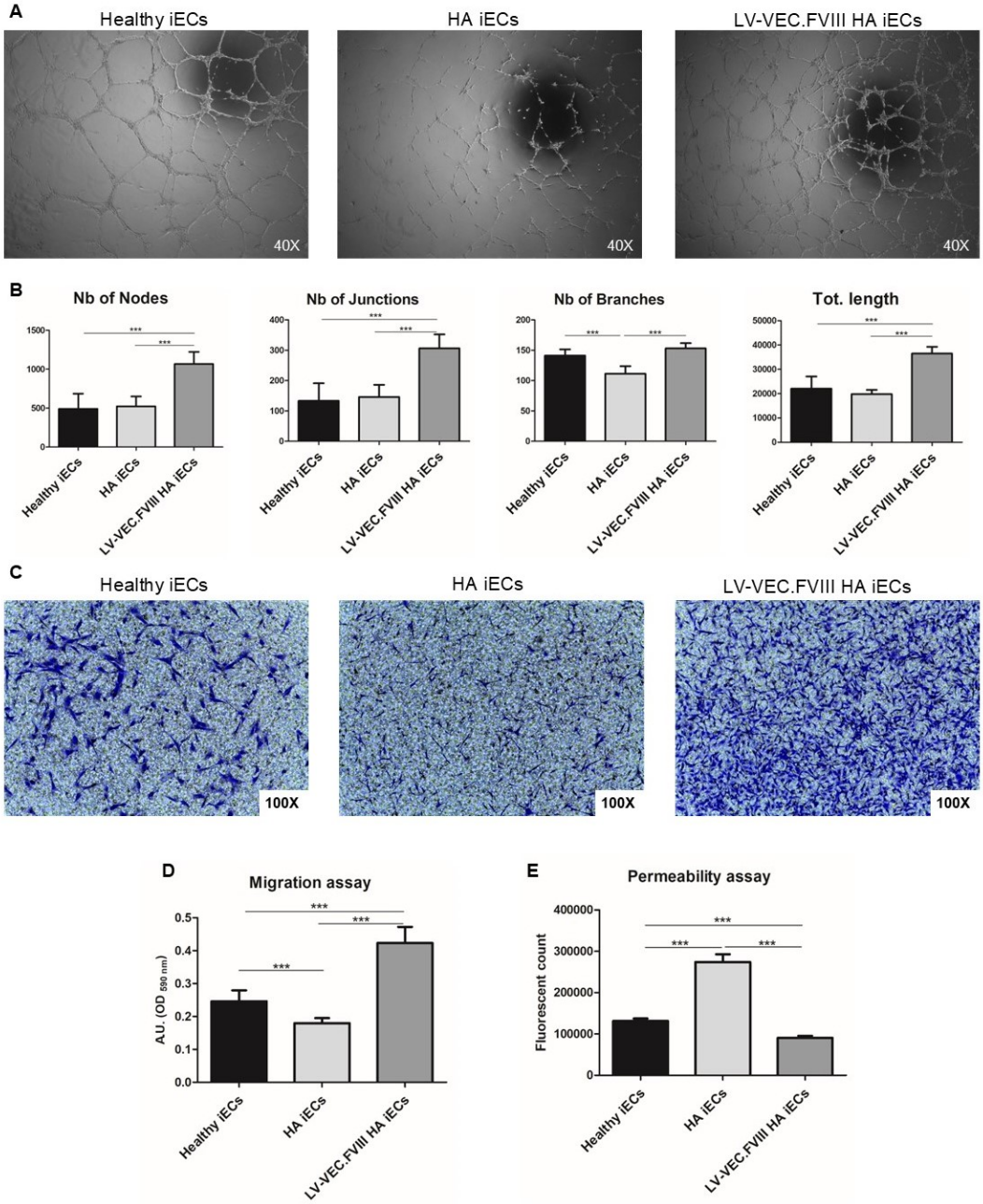

Figure 8. Evaluation of endothelial functionality on healthy, HA and LV-VEC.FVIII corrected iPSCs-derived ECs. A) Representative images of tubulogenic assay on healthy, HA and LV-VEC.FVIII HA iECs **B)** Quantification of number of nodes, junctions, branches and total length of tubule network formed in healthy, HA and LV-VEC.FVIII HA iECs **C)** Representative images of migration assay on healthy, HA and LV-VEC.FVIII HA iECs. **D)** Quantification of cell migration by elution of crystal violet staining **E)** Permeability assay quantification calculated on the extravasation of FITC-dextran through an intact monolayer of healthy, HA or LV-VEC.FVIII HA iECs (***p < 0.0001). Data are expressed as mean ± SD and are representative of three independent experiments (n = 3).

In vivo evaluation of vessel permeability in wild type and hemophilic mice

Based on *in vitro* functional endothelial assay results, we evaluated the differences in vascular stability between wild type (WT) and hemophilic mice. For this purpose, mice were intravenous injected with Evans Blue, a dye that binds albumin. Under physiologic conditions the endothelium is impermeable to albumin and Evans blue remains restricted within blood vessels. On the contrary, in case of vascular leakage, the endothelium becomes permeable to small proteins such as albumin allowing the extravasation of Evans Blue in tissues. Therefore, accumulation of Evans blue was particularly noticeable in the joints of BALB/C HA but not in WT mice (**Fig 9A**). This event could correlate with the reported recurrent vascular ruptures at joint levels in HA patients (Bhat et al., 2015). Likewise, extensive vascular leakage was observed under the skin of HA mice (**Fig 9B**) indicating a vascular fragility of hemophilic mice, leading to a general increased vascular permeability.

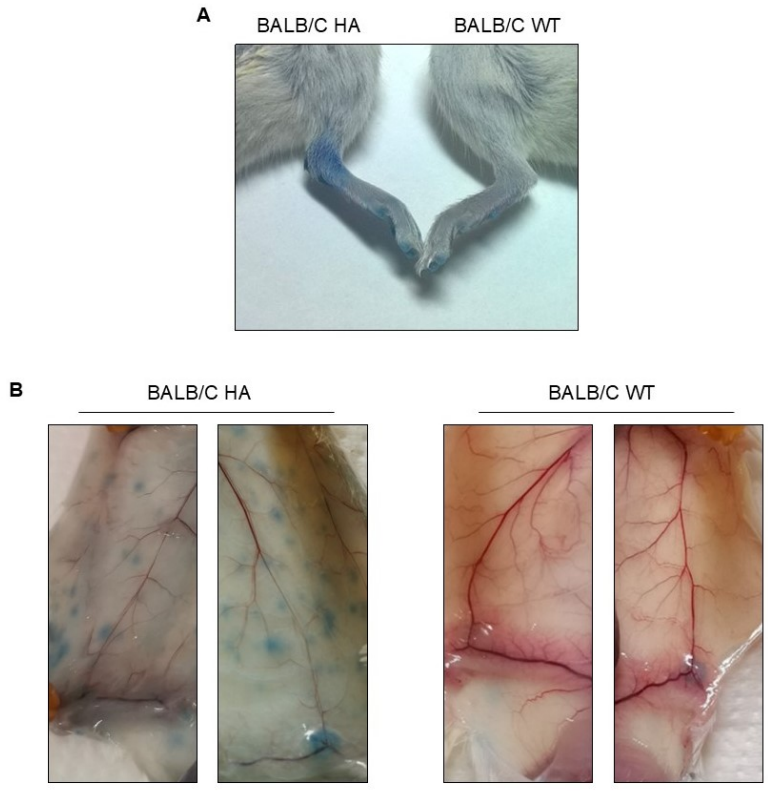

Figure 9. Permeability assay in hemophilic and wild-type BALB/C mice by Evans Blue dye tail vein injection. A) Representative picture of Evans Blue dye extravasation in interstitial tissues of HA mice accumulating in ankle joint. **B)** Macroscopically evaluation of Evans Blue dye distribution at skin level in injected HA and WT BALB/C mice. Data are representative of three independent experiments (n = 3 for BALB/C HA and 3 for BALB/C WT).

Explorative RNA-seq analysis of HA iECs healthy and LV.VEC-FVIII HA iECs

Both the *in vitro* and *in vivo* assays testing the endothelial cell's function demonstrated a negative impact of FVIII absence in ECs. Therefore, we explored by RNA-seq the differential gene expression of healthy (n=1), HA (n=2) and LV-VEC.FVIII HA (n=2) iEC. We observed marked changes between healthy and HA iECs in gene-level expression patterns, as depicted in the generated heatmap (**Fig. 10A**). In contrast, LV-VEC.FVIII HA iECs shared most of the differential expressed genes (DEGs) with the HA iECs, indicating only a partial correction of the transduced cells. This result was confirmed by principal component analysis (PCA) plot (**Fig. 10B**). The plot was built using the gene expression profiles of the three conditions (healthy, HA and LV-corrected) for their representation on a three-dimensional graphic. Each point in a PCA plot represents the gene expression profile of a sample and the distance between two plotted points is proportional to the degree of similarity between the gene expression profiles. Therefore, figure 10B shows that the variance, expressed as PC2 (5,2%) between HA and LV-VEC.FVIII HA iECs was low and that they belong to the same cluster, unlike healthy iECs that clustered apart and showed a high variance compared to the other 2 sample groups.

A total of 5614 genes with log2FC > 1 and < -1, were identified as DEGs of HA iECs compared to healthy iECs as showed in the Volcano plot (**Fig. 10C**). Between all the 5614 genes filtered, 2986 were up-regulated and 2628 down-regulated in HA iECs compared to healthy iECs. Subsequently, pathway enrichment analysis and a gene ontology (GO) of DEGs was performed with Enrichr online tool. In the downregulated set of genes, the pathway analysis identified more than 100 significantly enriched pathways. Based on our *in vivo* and *in vitro* results we focused our attention on pathways that could explain the differences in endothelial functionality among the 3 groups. Figure 10D shows that by comparing HA *versus* (*vs*) healthy iECs there was an enrichment of 10 pathways belonging to extracellular matrix organization, focal adhesion, and angiogenesis. For the gene onthology (GO), more than 200 GO terms were significantly enriched, including biological processes such as regulation of cell migration, molecular functions such as integrin binding, and cellular components such as focal adhesion (**Fig. 10E**). Finally, analysis of HA *vs* LV-transduced HA iECs showed similar enrichment pathways and GO terms of HA *vs* healthy iECs, even though the FVIII correction is only partial, as showed in the PCA plot (**Fig. 10F** and **10G**). On the other side, analysis of upregulated DEGs of both comparisons, HA *vs* healthy and HA *vs* corrected iECs, did not produce biologically relevant enriched pathways and GO terms.

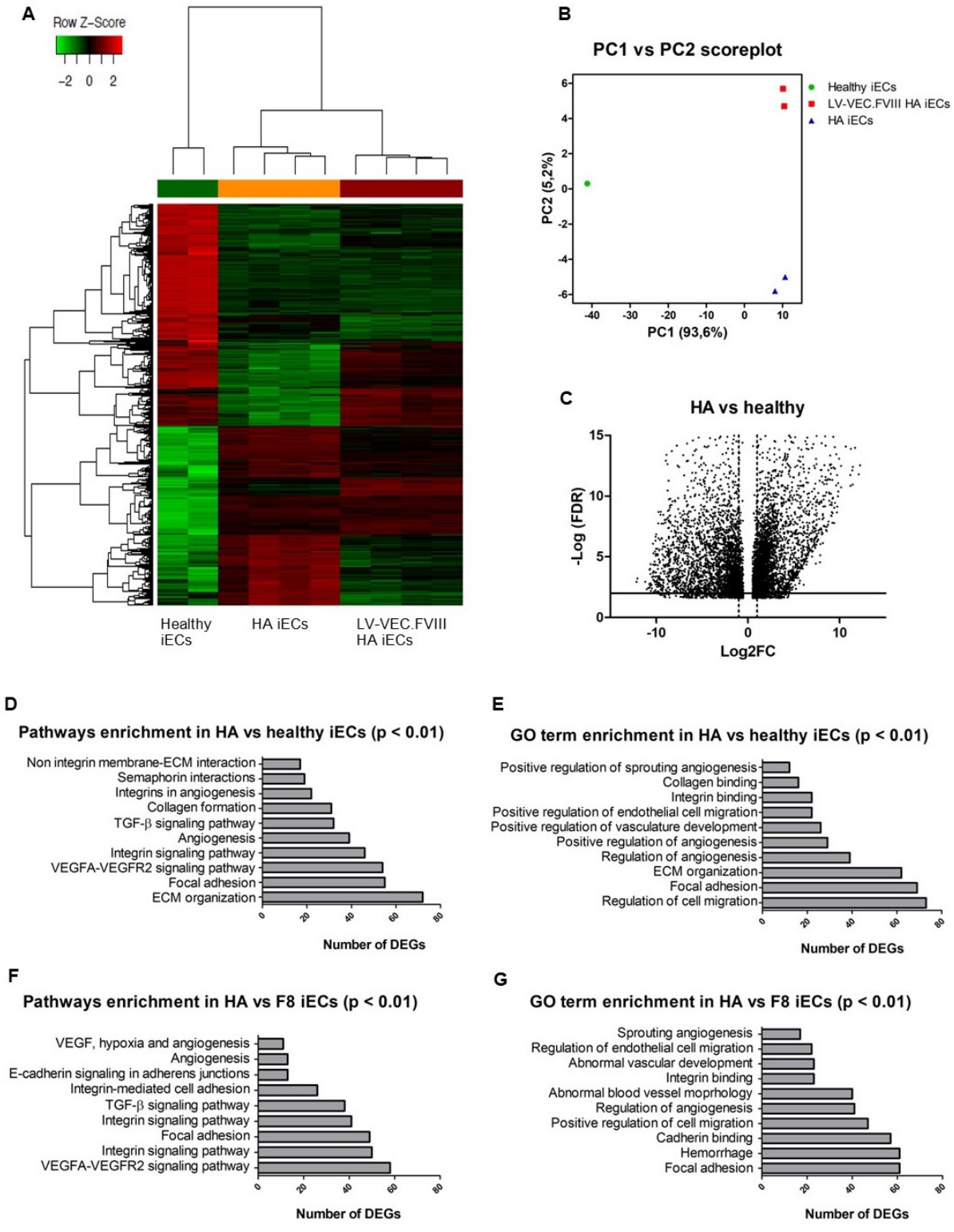

Figure 10. Transcriptomic analysis of healthy, HA and LV-VEC.FVIII HA iECs. A) Heatmap showing the gene expression profile of healthy, HA and LV-VEC.FVIII HA iECs. **B)** Principal component analysis (PCA) describing the variation within the dataset. **C)** Volcano plot representing differential expressed genes in HA *vs* healthy iECs. Black line represents the considered cut off (p <0.01). **D)** Ten of most enriched endothelial related pathways according to the downregulated DEGs in HA *vs* healthy iECs. **E)** Ten of most significant gene ontology (GO) terms for endothelial cells in downregulated DEGs in HA *vs* healthy iECs **F)** Ten of most enriched endothelial related pathways according to the downregulated DEGs in HA *vs* LV-VEC.FVIII (F8) HA iECs. **G**) Ten of most significant GO terms in downregulated DEGs of HA versus F8 iECs. DEGs: differentially expressed genes

Differential gene expression of extracellular matrix markers

The pathway of ECM organization was the most significant enriched one with more than 70 DEGs. Numerous genes relating ECM remodeling, including collagens and adamalysins, were downregulated in HA *vs* healthy iECs (**Fig. 11A**). The modulation of those genes in the comparison of HA *vs* LV-VEC.FVIII HA iECs, did not recapitulate the previous comparison HA *vs* healthy iECs (**Fig. 11A**). Some of the downregulated genes with the log2Fold Change (log2FC) ranging from -10 to -8 were further validated in RT-qPCR (**Fig. 11B** and **11C**). Interestingly, it was reported that high levels of collagen XVIII in HA patients correlates to high annual bleeding rates (Kjeld et al., 2018). This observation also correlates with the upregulation of *COL18A1* (log2FC 2.2) in HA iECs compared to healthy and LV-VEC.FVIII iECs (**Fig. 11D**).

***In vitro* evaluation of endothelial functionality between healthy and hemophilic BOECs**

Based on the results obtained in iECs from both the *in vitro* experiments and the transcriptomic analysis, we aimed to verify if the impaired endothelial functionality occurred not only in ECs derived from iPSCs, but also in primary endothelial cells. Therefore, as endothelial model we used BOECs isolated both from healthy donors and HA patients (Olgasi et al., under revision, see attached manuscript in appendix for further details). The endothelial functionality of BOECs was assessed by tubulogenesis, migration and permeability assays.

Like HA iECs, HA BOECs showed a reduced vessel formation capability compared to healthy BOECs (**Fig. 12A**). However, the exogenous expression of FVIII through LV transduction allowed HA BOECs to restore the capability to form more stable vessel-like structures, as indicated by the quantification of tubules in terms of nodes, junctions, branches and total length (**Fig. 12B**). Unlike iECs, healthy BOECs and LV-corrected HA BOECs shared the same size, therefore there was not the same significant difference observed in iECs. As further characterization, we performed the same migration assay carried out on iECs. As shown in **figure 12C** and **12D**, HA BOECs demonstrated a significant reduction in the migration capability compared to both healthy and LV-transduced BOECs.

Finally, extravasation of dextran-FITC from BOECs monolayer showed an increased permeability of HA BOECs that was reversed after transduction with LV-VEC.FVIII reaching comparable levels to healthy BOECs (**Fig. 12E**).

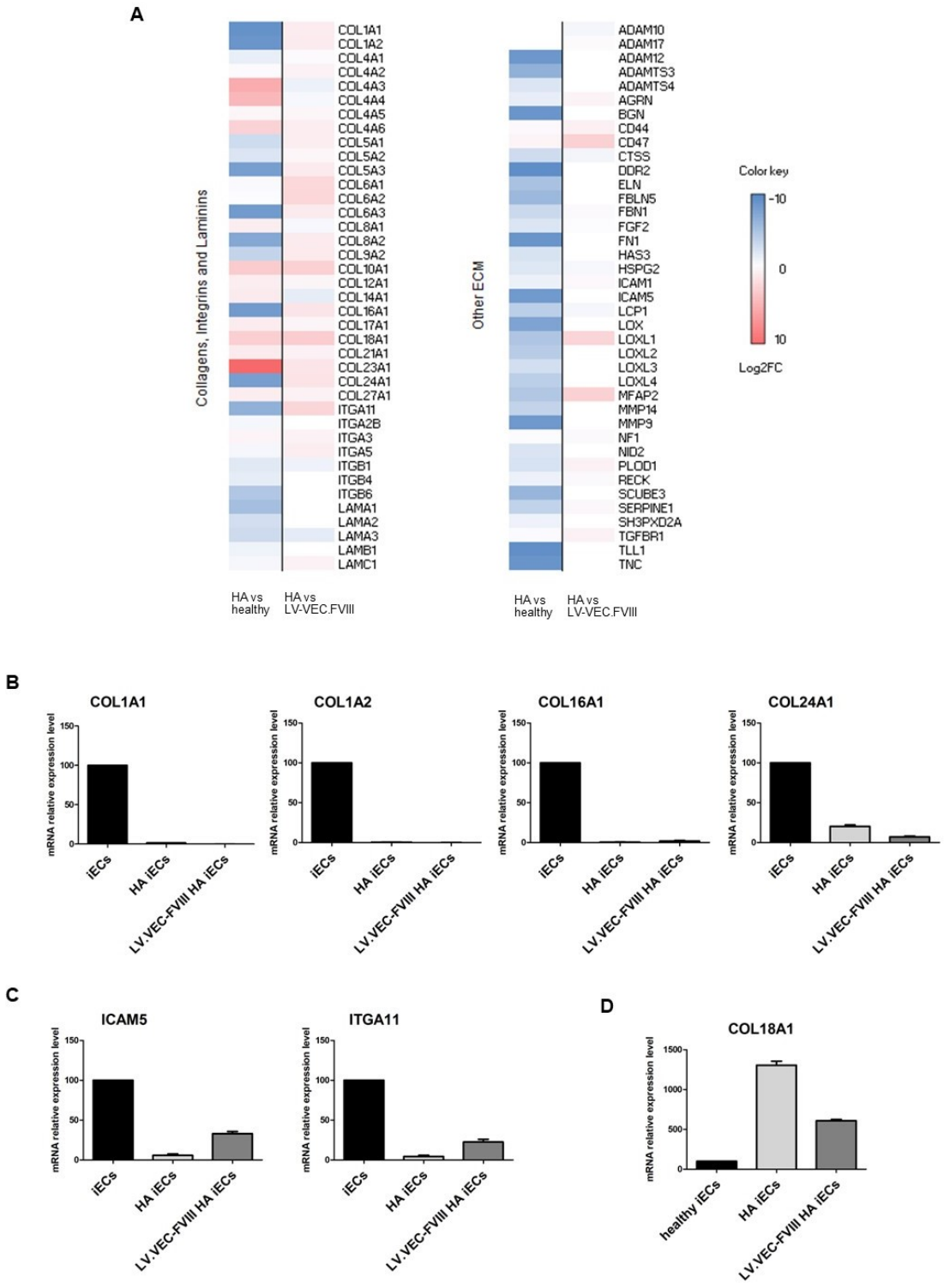

Figure 11. Relative expression of collagens, integrins and other extracellular matrix (ECM) markers in HA *vs* healthy and HA vs LV.VEC-FVIII HA iECs A) Heatmap showing differentially expressed collagen, integrins, laminins and other ECM genes in HA iECs compared to healthy and LV-VEC.FVIII HA iECs expressed as Log2FC. **B)** Relative mRNA expression level of some of the downregulated collagen genes validated by RT-qPCR. **C**) Relative mRNA expression level of some downregulated ECM genes validated by RT-qPCR. **D)** Relative mRNA expression level of *COL18A1* gene by RT-qPCR. Data are expressed as mean ± SD and are representative of three independent experiments.

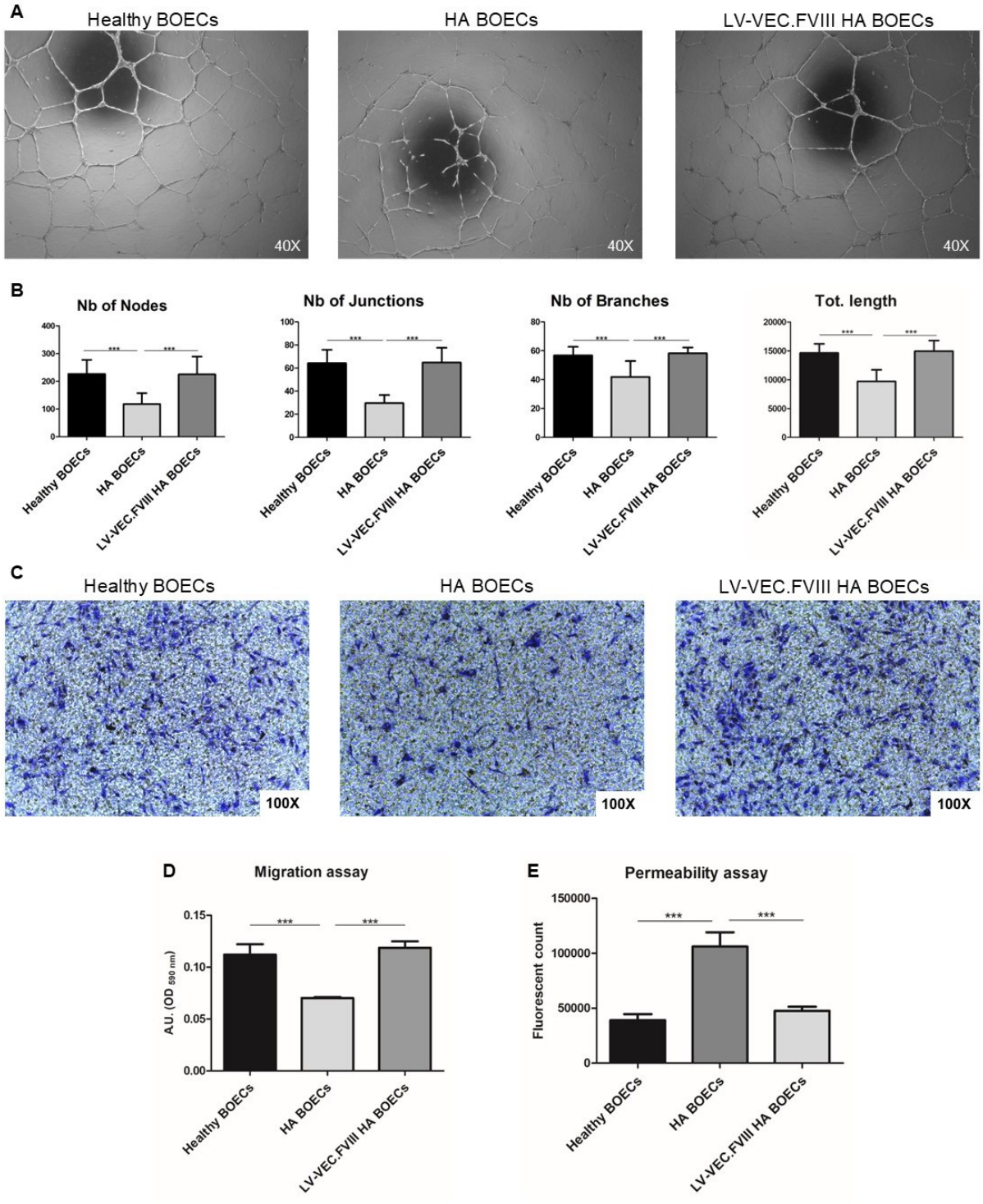

Figure 12. Evaluation of endothelial functionality on healthy, HA and LV-VEC.FVIII corrected BOECs. A) Representative images of tubulogenic assay between healthy, HA and LV-VEC.FVIII BOECs. **B)** Quantification of number of nodes, junctions, branches and total length of the tubule network of healthy, HA and LV-VEC.FVIII HA BOECs. **C)** Representative images of migration assay on healthy, HA and LV-VEC.FVIII HA BOECs. **D)** Quantification of cell migration assay by elution of crystal violet staining. **E)** Extravasation of FITC-dextran through an intact monolayer of BOECs (***p < 0.0001). Data are expressed as mean ± SD and are representative of three independent experiments.

RNA-seq analysis of healthy, HA and LV-VEC.FVIII HA BOECs

A heatmap from gene expression of healthy, HA and LV-VEC.FVIII BOECs was generated (**Fig. 13A**) showing that most of the genes down regulated in HA BOECs were upregulated in healthy BOECs, while their expression was mostly restored after correction with LV-VEC.FVIII. This result was also confirmed by PCA plot showing that the three HA BOECs samples clustered together and differed from LV-VEC.FVII HA BOECs (n=3) that clustered closer to healthy BOECs (n=2) (**Fig. 13B**). RNA-seq analysis found a total of 1667 DEGs of which only 197 had a $p < 0.01$ and a log2FC < -1 and >1 (**Fig. 13C**). To obtain a larger subset of genes, we used as cut off a log2FC < -0.9 and >0.9 with a $p < 0.02$ and we found 386 modulated genes that were analyzed by the Enrichr web tool. The downregulated genes in HA *vs* healthy BOECs had a pattern like the HA *vs* healthy iECs comparison described above. Despite the low number of genes, enriched pathways were found modulated also in this EC model, such as angiogenesis and ECM organization (**Fig.13D**) and gene ontologies like focal adhesion and regulation of cell migration (**Fig. 13E**).

Transcriptomic analysis of healthy, HA and LV-VEC.FVIII corrected BOECs

The RNA-seq data analysis found similar expression profiles in iECs and BOECs samples, starting from the ECM organization pathway. Moreover, genes relating with focal and cells adhesion, angiogenesis and migration were downregulated in HA *vs* healthy BOECs (**Fig. 14A**). Since for BOECs analysis we enlarged the cut off (log2FC < -0.9 and >0.9 with a $p < 0.02$) compared to the one used with iECs, we validated by RT-qPCR some of the genes within the enriched pathways. As depicted in figure 14B, most of the genes were validated showing a significant decrease mRNA expression of HA BOECs compared to heathy BOECs. Meanwhile, LV-VEC.FVIII HA BOECs did not display a significant increase of mRNA expression, showing only a partial rescue (**Fig. 14B**).

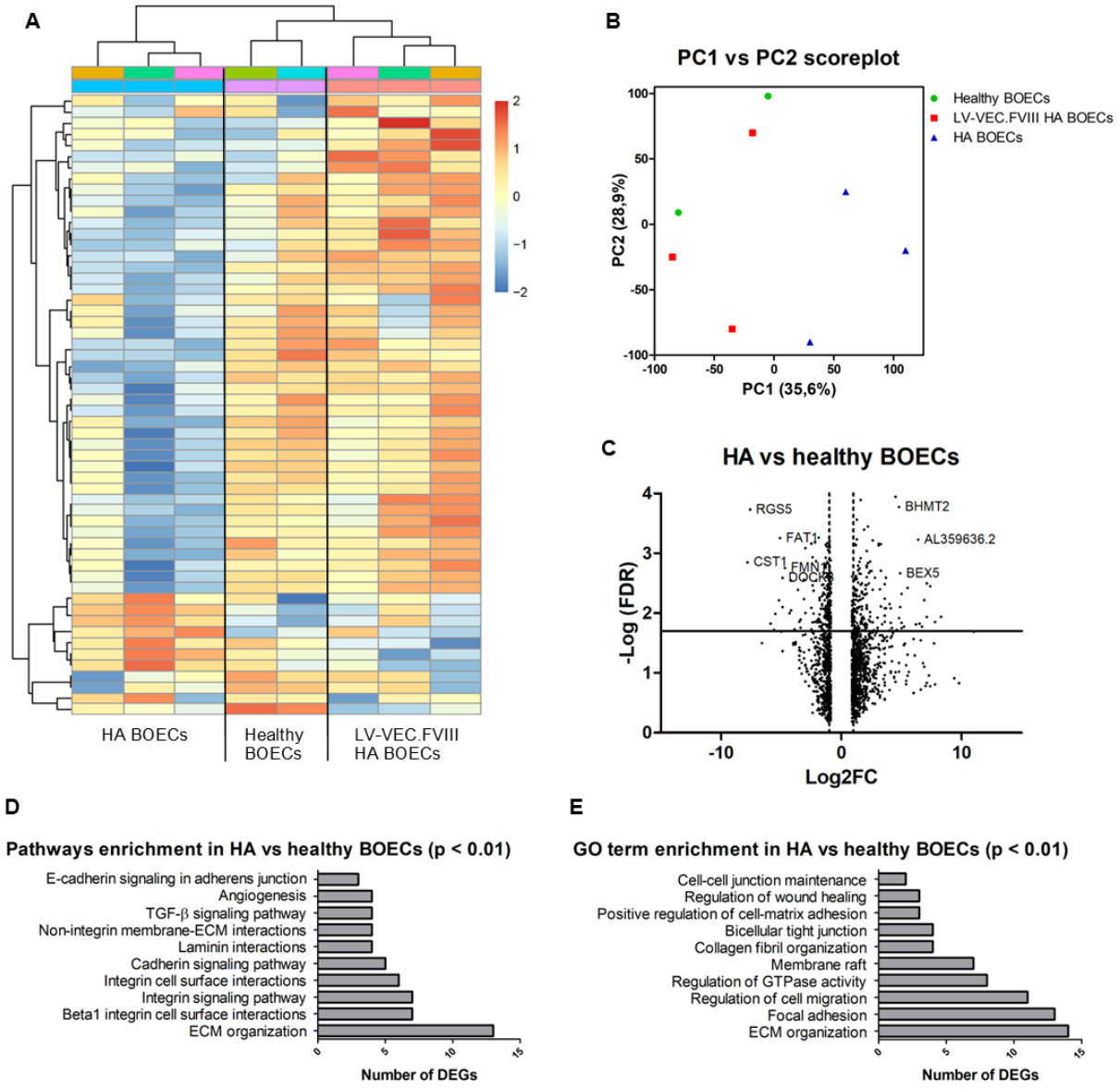

Figure 13. Transcriptomic analysis of healthy, HA and LV-VEC.FVIII corrected BOECs. A) Heatmap showing the gene expression profile among healthy, HA and LV-VEC.FVIII HA BOECs. **B)** Principal component analysis (PCA) describing the variation within the dataset. **C)** Volcano plot representing differential expressed genes in HA *vs* healthy BOECs. Black line represents the cut off considered ($p < 0.02$). **D)** Ten of the most enriched pathways according to the downregulated DEGs in HA *vs* healthy BOECs. **E)** Ten of the most significant gene ontology (GO) terms enriched in the downregulated DEGs in HA *vs* healthy BOECs.

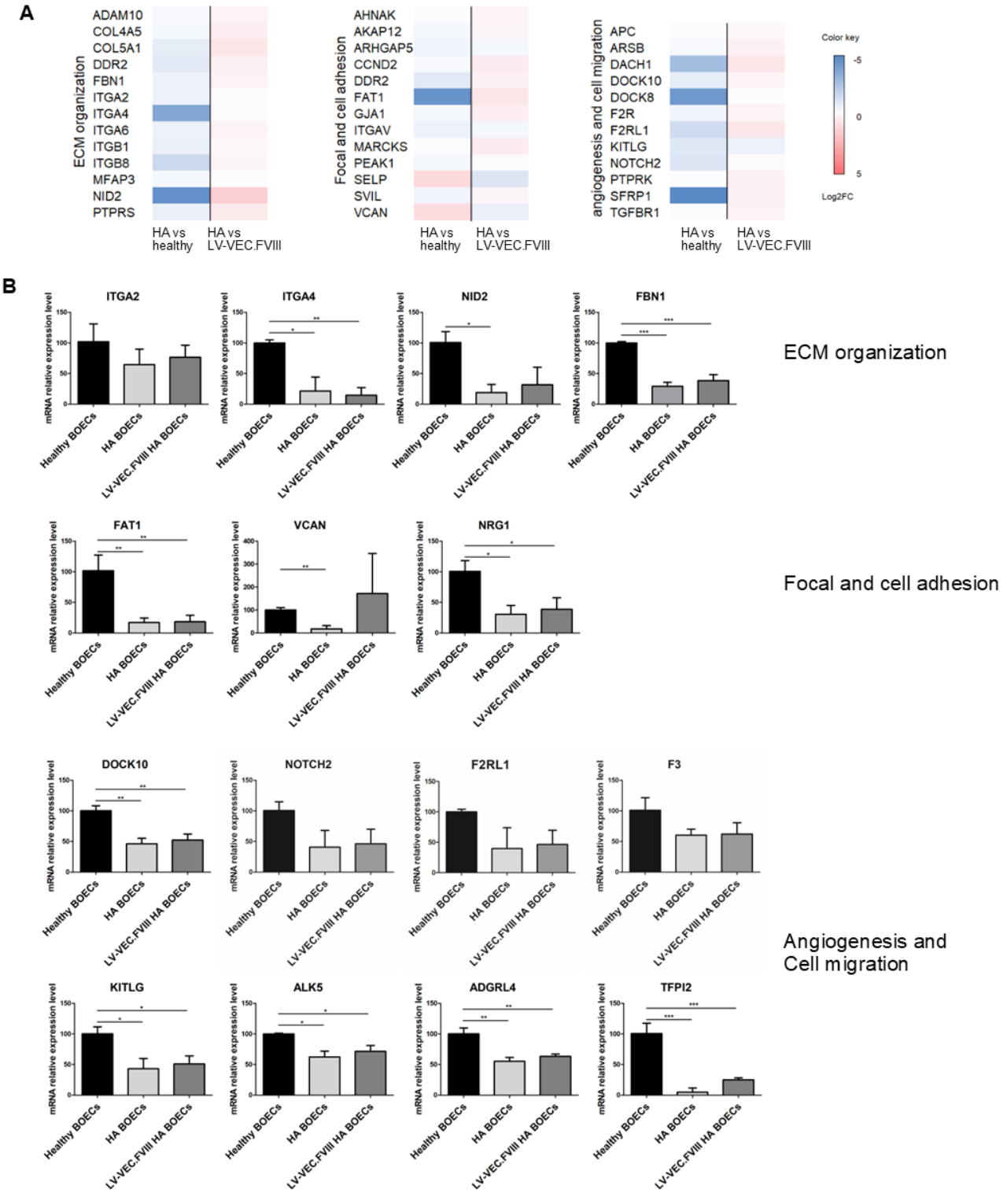

Figure 14. Transcriptomic analysis of healthy, HA and LV-VEC.FVIII corrected BOECs. A) Heatmap of selected genes belonging to downregulated enriched pathways in HA vs healthy BOECs, showing the Log2FC of HA vs healthy and HA vs LV-VEC.FVIII HA BOECs. **B)** RT-qPCR results for gene validation involved in ECM organization, focal and cell adhesion, angiogenesis, and cell migration pathways (***p < 0.0001; ** p < 0.001; * p < 0.05). Data are expressed as mean ± SD and are representative of three independent experiments.

In vitro administration of recombinant FVIII partially enhances endothelial functionality of hemophilic BOECs

To further assess FVIII involvement on ECs functionality, we performed a tubulogenic assay by stimulating HA BOECs with 1U/ml of commercial recombinant BDD or full length (FL) FVIII. A significant enhancing of the tubule network formation was observed in both conditions compared to HA BOECs (**Fig. 15A**). The quantification of nodes, junctions, branches and total length of the vessel-like structures confirmed the observation that the treatment of HA BOECs with either rBDD or rFL-FVIII improved the HA BOEC functions (**Fig. 15B**). Nevertheless, LV-VEC.FVIII HA BOECs performed better than the rFVIII-treated HA BOECs in tubule network building. Moreover, migration assay of HA BOECs treated with rBDD or rFL-FVIII slightly helped the cells to transmigrate towards the low compartment in which VEGF acts as a chemoattractant (**Fig. 16A**). Quantification of migrated cells showed that migration ability of HA BOECs was improved in a comparable way after treatment with rBDD-FVIII or rFL-FVIII (**Fig. 16B**). Finally, we evaluated if FVIII could also ameliorate the cell permeability. When treated with rFVIII, the HA BOECs monolayer was less permeable to FITC-dextran compared to non-treated HA BOECs (**Fig. 16C**). These results indicate that an endogenous expression of FVIII in HA BOECs could be required for building a complex vessel network, to obtain a tight cell monolayer and to enhance the ability to transmigrate towards appropriate stimuli.

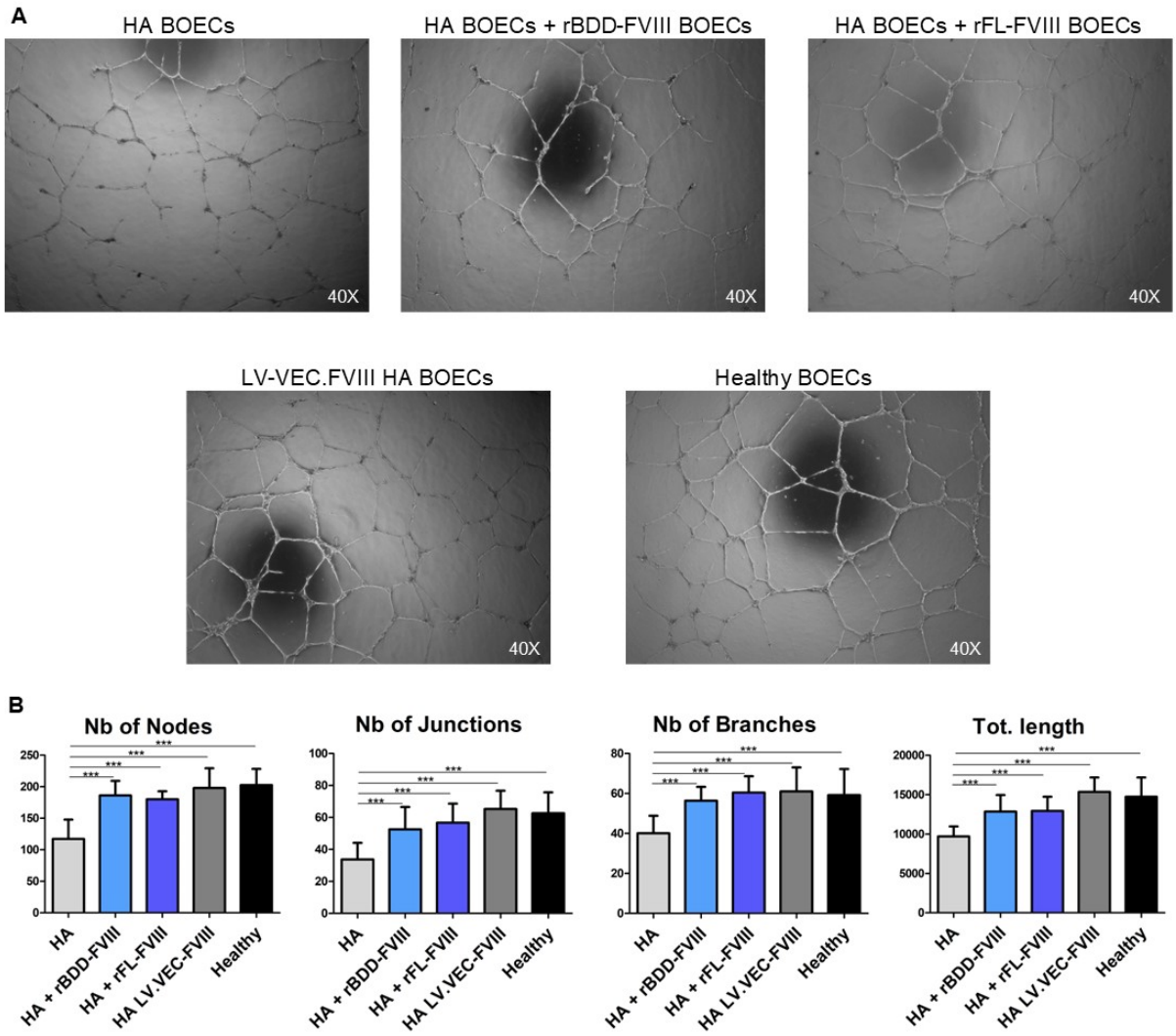

Figure 15. Effects of recombinant B domain deleted (BDD) and full length (FL) FVIII on network formation by healthy, HA and LV-VEC.FVIII BOECs. A) Representative images of tubulogenic assay on HA BOECs in basal condition and after treatment with 1U/ ml of recombinant B domain deleted (BDD) FVIII or full length (FL) FVIII. B) Quantification of number of nodes, junctions, branches and total length showing on HA BOECs treated or not with recombinant FVIII (***p < 0.0001). Data are expressed as mean ± SD and are representative of three independent experiments.

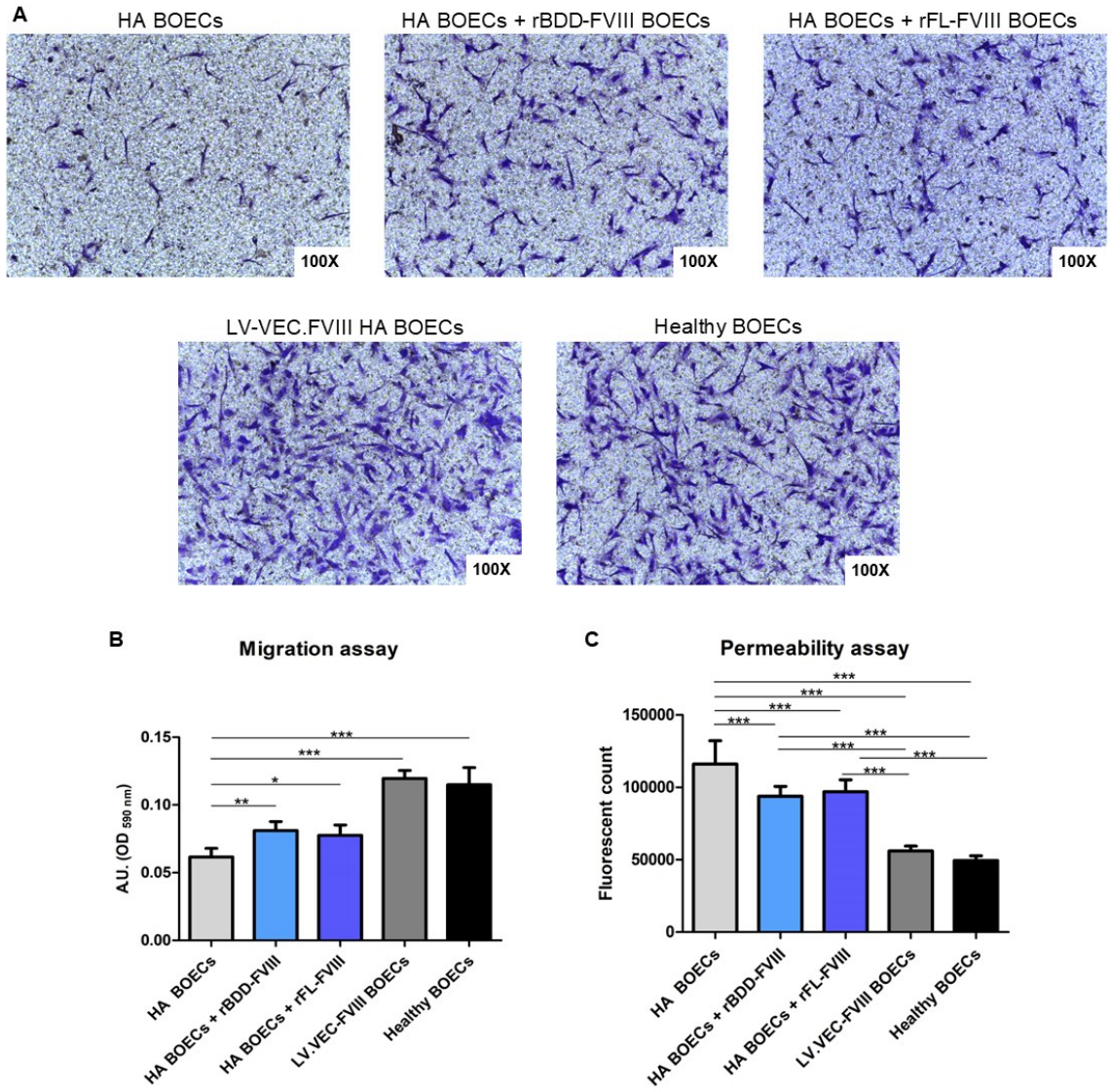

Figure 16. Effects of recombinant B domain deleted (BDD) and full length (FL) FVIII on migration and permeability assay of healthy, HA and LV-VEC.FVIII corrected BOECs. A) Representative images of migration assay performed on healthy, HA treated or not with rBDD-FVIII or rFL-FVIII and LV-VEC.FVIII BOECs. **B)** Quantification of cell migration by elution of crystal violet staining. **C)** Extravasation of FITC-dextran through an intact monolayer of BOECs (***$p < 0.0001$; ** $p < 0.001$; * $p < 0.05$). Data are expressed as mean ± SD and are representative of three independent experiments.

In vivo evaluation of new vessel formation in Matrigel plugs

According to *in vitro* tubulogenic assays performed both with iECs and BOECs, HA cells failed to build a robust and stable vessel-like network. In contrast, when HA BOECs were stimulated with rFVIII in culture, their ability to form tubules markedly improved. Based on these results, we performed *in vivo* angiogenesis assay to evaluate the formation of vessel structures in presence or absence of FVIII by subcutaneous injecting ECM hydrogel (pure Matrigel) in NSG and NSG-HA mice. We first compared the endothelial angiogenic potential of hemophilic and NSG mice by immunofluorescence staining of Matrigel plug sections removed from the mice 10 days after subcutaneous injection (**Fig. 17A**). As shown in **Fig. 17B**, in NSG mice newly formed $CD31^+$ vessels were organized, elongated, and sustained by capillary pericytes, as confirmed by the positivity to the αSMA marker. Conversely, NSG-HA mice formed smaller vessels with lower expression of αSMA (**Fig. 17C**). To investigate the possible role of FVIII in vessel stability, we subcutaneously injected NSG-HA mice with Matrigel containing rBDD-FVIII or rFL-FVIII (**Fig. 17A**). Remarkably, vessels formed within Matrigel plug containing rFVIII were more stable and organized compared to pure Matrigel plugs, as confirmed by mCD31 and αSMA co-staining (**Fig. 17D** and **17E**). Quantification of vessel density and diameter confirmed that the ability to form stable vessels was impaired in NSG-HA mice compared to NSG and that rFVIII addition significantly restored angiogenesis (**Fig.18A** and **18B**). Interestingly, rFL-FVIII within the Matrigel plug significantly enhanced the density of the newly formed vessels, but not their diameter when compared with rBDD-FVIII (**Fig.18A** and **18B**).

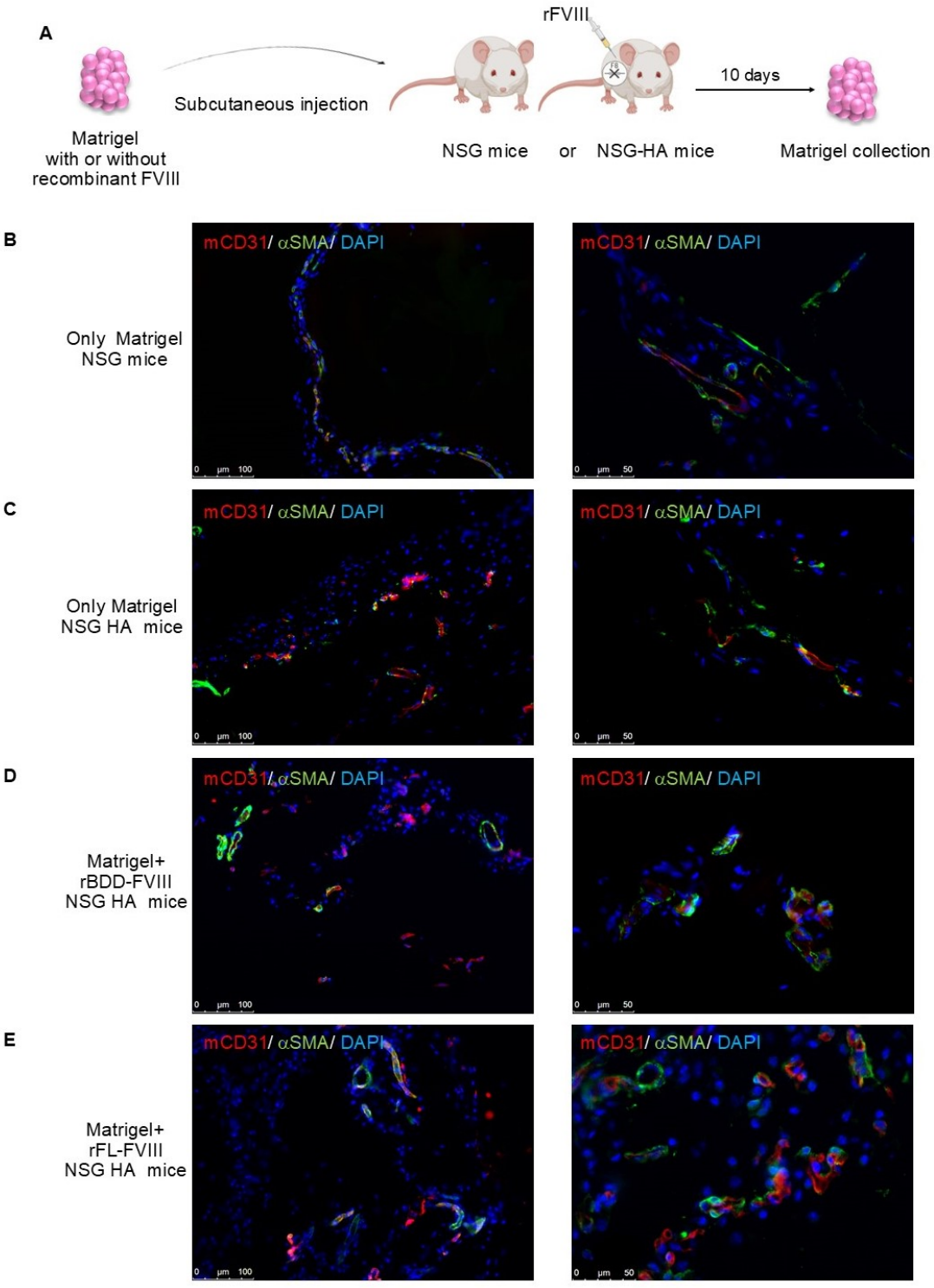

Figure 17. Vessel formation in Matrigel plugs transferred in NSG or NSG-HA mice after recombinant FVIII injection. A) Schematic representation of Matrigel injection in NSG and NSG-HA mice. **B)** Immunofluorescence staining for mCD31 (red) and αSMA (green) on vessels formed within Matrigel plug harvested from NSG mice and **C)** from NSG-HA mice. **D)** Immunofluorescence staining or mCD31 (red) and αSMA (green) on vessels formed within Matrigel plug harvested from NSG-HA mice injected with rBDD-FVIII or **E)** rFL-FVIII. Data are representative of two independent experiments (n=3 each condition).

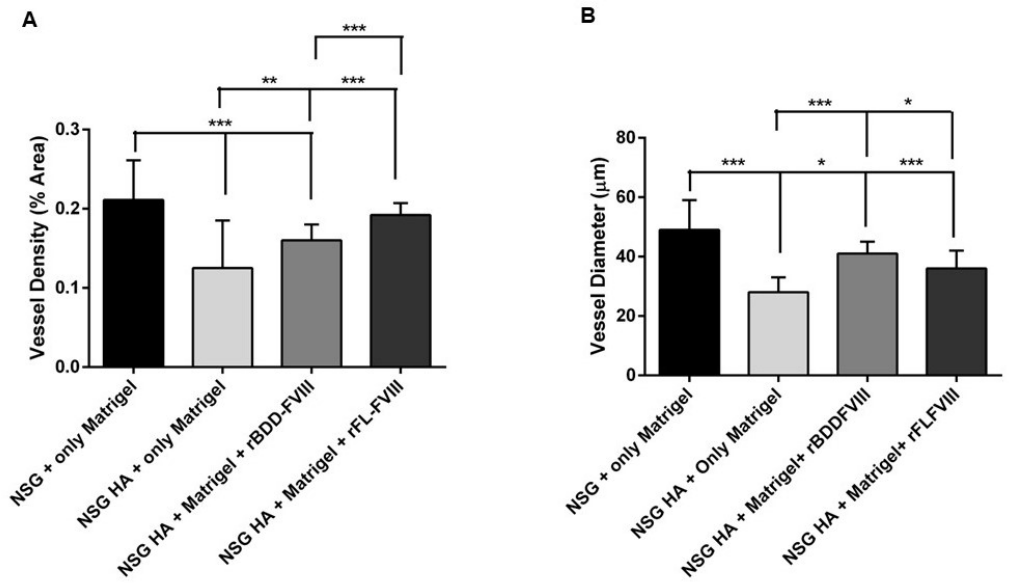

Figure 18. Quantification of angiogenic potential of NSG and NSG-HA mice after recombinant FVIII injection. A) Quantification of vessel density in Matrigel plugs. **B)** Quantification of vessel diameter in Matrigel plugs. (***p < 0.0001; ** p 0.001; * p < 0.05). Data are expressed as mean ± SD and are representative of two independent experiments.

In vivo evaluation of healthy, HA and LV-VEC.FVIII HA BOECs organization in Matrigel plugs of NSG-HA mice

To evaluate *in vivo* the difference in angiogenic capability of healthy, HA and LV-VEC.FVIII HA BOECs were transduced with a LV carrying the green fluorescent protein (GFP) under the control of VEC promoter and more than 90% were GFP+ before injection (**Fig. 19A**). LV-transduced BOECs were mixed Matrigel and subcutaneously injected into NSG-HA mice (**Fig. 19B**). Ten days later the Matrigel plugs were harvested and IF staining showed that healthy BOECs built new vessel structures better organized compared to HA BOECs (**Fig. 20A**). FVIII-corrected HA BOECs, conversely, produced new structures similar to healthy BOECs. This was confirmed by the quantification of vessel density showing a higher number of vessels in healthy BOECs compared to HA BOECs that increased after LV correction of the cells (**Fig. 20B**). Likewise, vessel diameter analysis showed smaller vessel size by HA BOECs compared to healthy and LV-VEC.FVIII HA BOECs and notably, LV-VEC.FVIII HA BOECs formed vessels with a slightly smaller diameter than healthy BOECs (**Fig. 20C**).

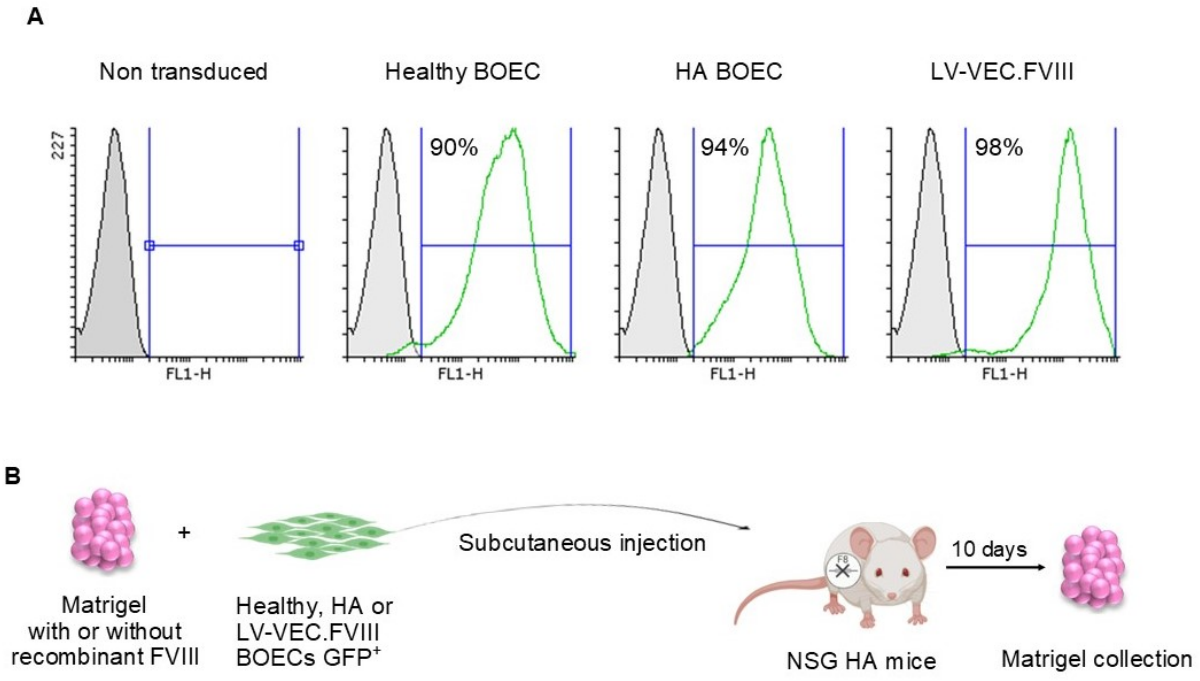

Figure 19. Healthy, HA and LV-VEC.FVIII HA BOECs embedded in Matrigel and injected in NSG-HA mice. A) Representative histograms for GFP evaluation by FACS analysis in healthy, HA BOECs and LV-VEC.FVIII HA BOECs transduced with LV-VEC.GFP with an MOI of 20. **B)** Schematic representation of BOECs embedded in Matrigel and injected in NSG-HA mice.

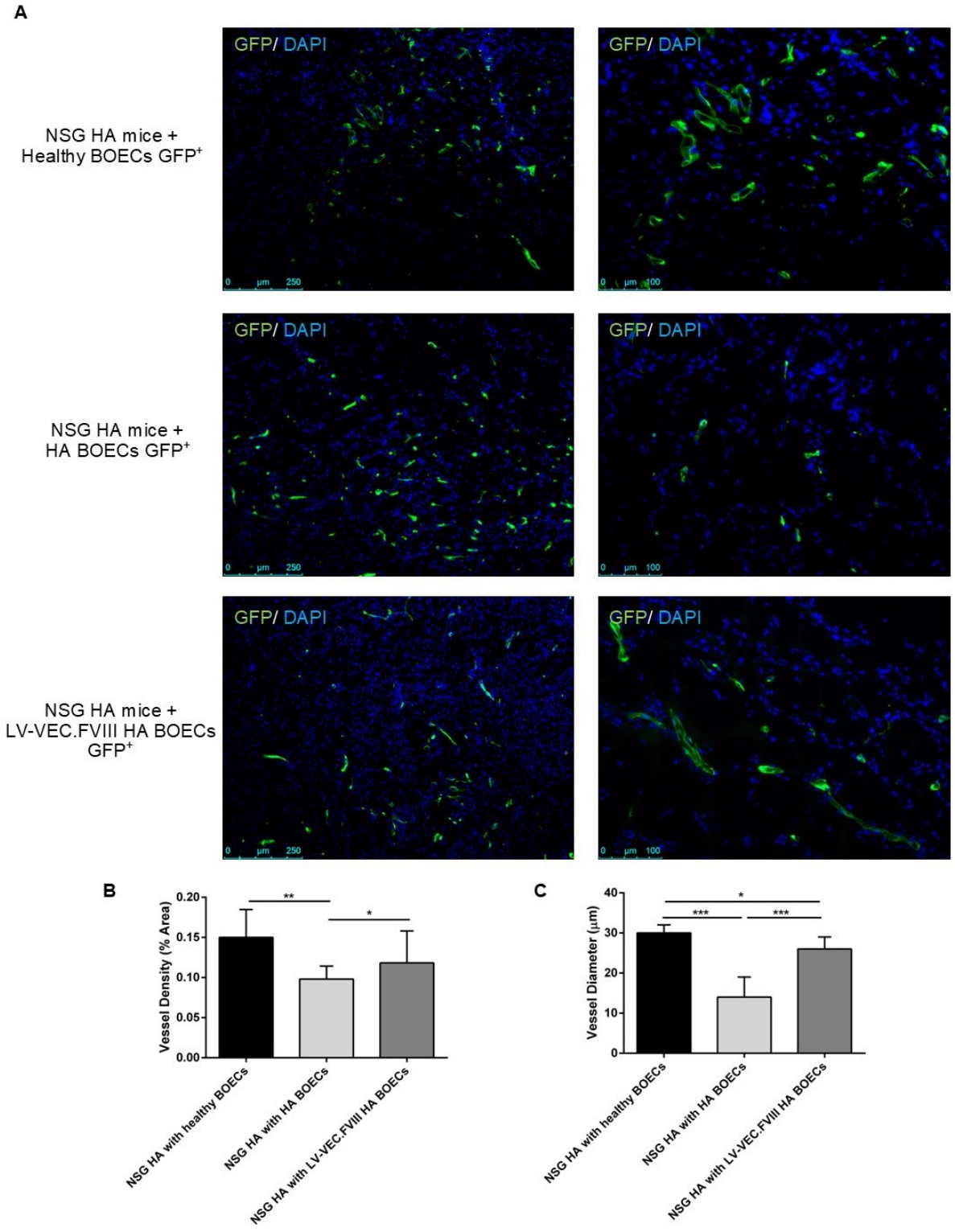

Figure 20. Angiogenic potential of healthy, HA and LV-VEC.FVIII HA BOECs embedded in Matrigel and injected in NSG-HA mice A) Schematic representation of BOECs embedded in Matrigel and injected in NSG-HA mice. **B)** Immunofluorescence staining for mCD31 (red) and αSMA (green) on vessels by healthy, HA and LV-VEC.FVIII HA BOECs. **C)** Quantification of vessel density in Matrigel plugs. **B)** Quantification of vessel diameter in Matrigel plugs. (***p < 0.0001; ** p 0.001; * p < 0.05). Data are expressed as mean ± SD and are representative of two independent experiments (n=3 each condition).

In vivo evaluation of HA BOECs organization in presence of recombinant FVIII in Matrigel plugs of NSG and NSG-HA mice

Considering the potential effect of FVIII on vessel formation and stability on BOECs, we investigated *in vivo* whether rFVIII could improve these processes in HA BOECs included in Matrigel plugs. We subcutaneously injected GFP^+ HA BOECs/Matrigel mix with or without rFVIII into NSG or NSG-HA mice (**Fig. 21A**). As showed in **figure 21B** and **21C**, HA BOECs were not able to form structured vessels neither in NSG nor in HA NSG mice. Interestingly, the administration of rFVIII (rBDD-FVIII and rFL-FVIII) into the Matrigel plug of NSG-HA mice every 2 days until harvesting, greatly improved the ability of HA BOECs to form well-organized vessels (**Fig. 21D** and **21E**). Vessel density and diameter were significant higher in presence of rFVIII, where rBDD-FVIII was more efficient in increasing vessel density than rFL-FVIII (**Fig. 22A** and **22B**). These results indicate that despite the presence of physiological level of mouse FVIII in NSG mice, HA BOECs failed to form well-organized vessels in Matrigel plugs, as well as in NSG-HA mice. Conversely, the constant presence of exogenous human rFVIII in the matrix led to the formation of newly and larger vessels. It will be interesting to explore the level in which mFVIII in NSG mice is able to stimulate transplanted human HA BOECs in the Matrigel plug.

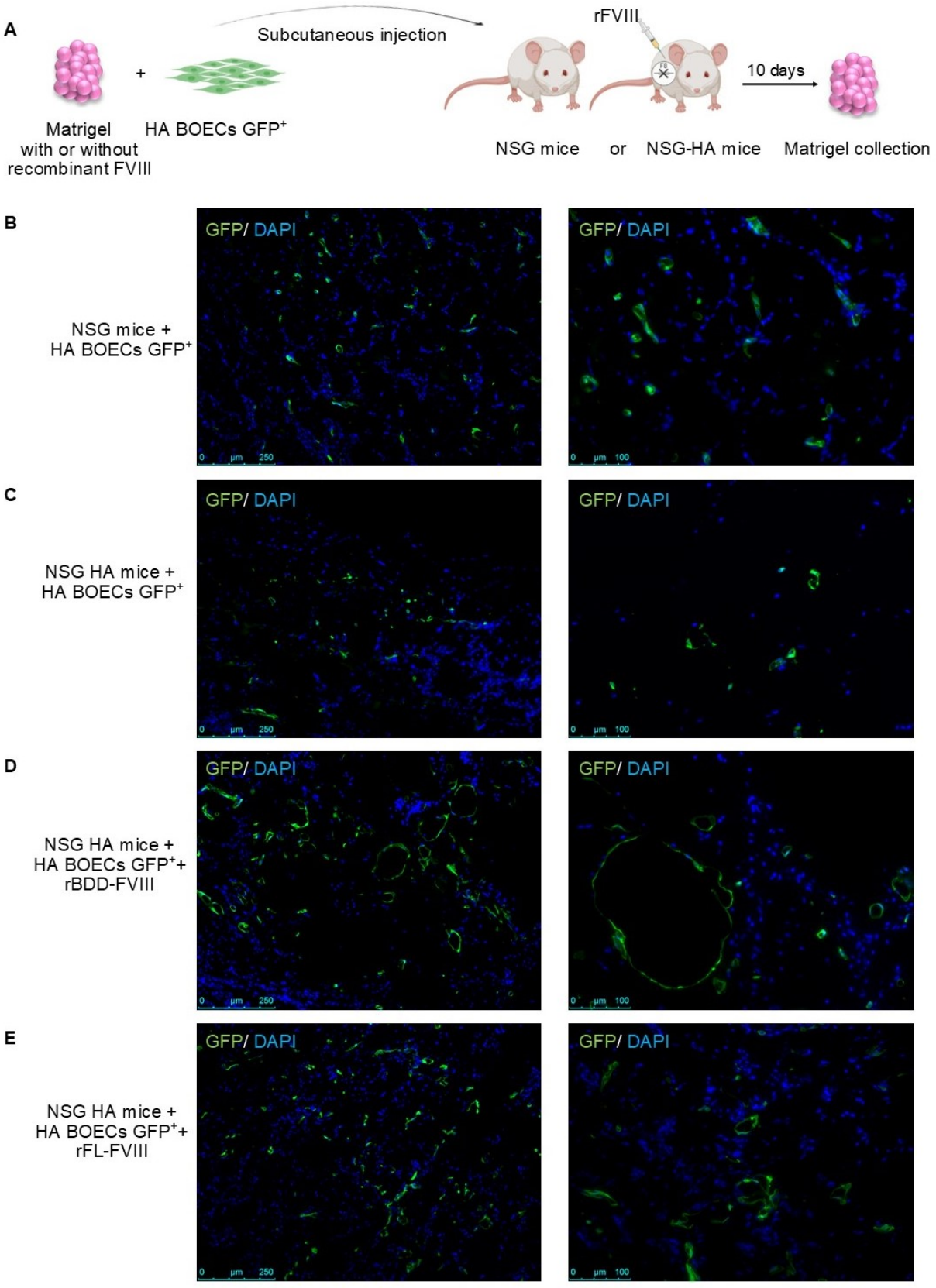

Figure 21. Angiogenic potential of HA BOEC GFP$^+$ treated or not with recombinant FVIII, embedded in Matrigel and injected in NSG or NSG-HA mice A) Schematic representation of the experiment. **B)** Immunofluorescence staining for HA BOEC GFP$^+$ forming vessels in NSG mice and **C)** NSG-HA mice. **D)** Immunofluorescence staining for HA BOEC GFP$^+$ forming vessels in Matrigel plugs treated with rBDD-FVIII or **E)** rFL-FVIII. Data are expressed representative of two independent experiments (n=3 each condition).

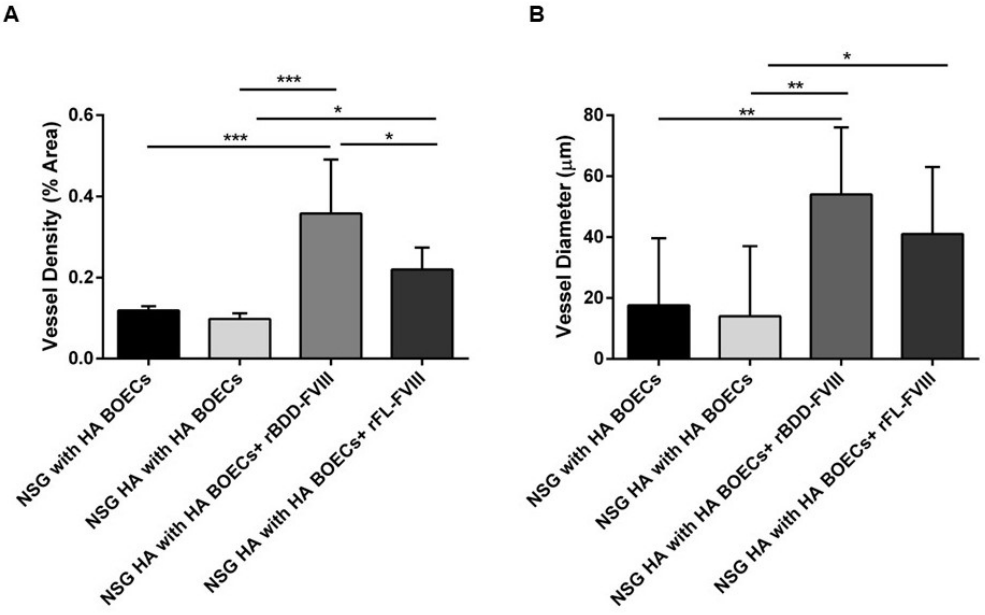

Figure 22. Quantification of angiogenic potential BOEC treated or not with recombinant FVIII, embedded in Matrigel and injected in NSG-HA mice A) Quantification of vessel density. **B)** Quantification of vessel diameter (***p < 0.0001; ** p 0.001; * p < 0.05). Data are expressed as mean ± SD and are representative of two independent experiments (n=3 each condition).

Discussion

Hemophilia A (HA) is a genetic coagulation disease with an impairment of FVIII activity caused by mutation in FVIII gene leading to a lifelong bleeding tendency, whose clinical severity is proportional to FVIII reduction (Bolton-Maggs and Pasi, 2003).

Currently, there is no definitive cure for HA and patients are prophylactic treated with infusions of FVIII concentrate to treat or prevent bleeding episodes. Primary prophylaxis, which is initiated prior to or immediately following the first bleeding, is used to prevent joint destruction or to halt its progression. In the absence of primary prophylaxis patients will develop a first hemarthrosis and repeated hemarthrosis are responsible for arthropathy. However, the pathological mechanism underlying the development of hemophilic arthropathy is not yet fully understood. The mechanism is multifactorial, involving cartilage degradation and inflammation of the synovial membrane due to the toxic effects related to blood effusions. However, vascular development and angiogenesis are an essential component of blood-induced joint disease (Acharya et al., 2011).

Spontaneous bleeding into muscles and joints are the typical symptoms in HA patients, but another event that can occur in HA severe patients is spontaneous intracranial hemorrhage (ICH) resulting in high rates of mortality and disability (Hay et al., 2021).

The manifestation of ICH is often spontaneous, and it mainly occurs in children and in patients that do not adhere to prophylaxis. Although the cause of the development of spontaneous ICH is still unknown, a correlation between the severe form of hemophilia and ICH in children has been described highlighting the importance of prophylaxis in reducing the risk of ICH development (Zanon and Pasca, 2019).

In adult HA patients the major risk factor for ICH is hypertension as well as cardiovascular diseases. Indeed, it has been demonstrated a higher risk of developing hypertension and cardiovascular diseases in hemophilic patients compared to healthy subjects, but also in this case the mechanism again is not fully understood yet (Kamphuisen and Ten Cate, 2014).

During the years, the development of extended half-life recombinant FVIII allowed a better HA patients quality of life, but some concerns are still present. The main complication is the development of FVIII inhibitors that occur in 20-40% of severe HA patients making the treatment ineffective (Van Den Berg et al., 2019). To overcome these issues, alternative strategies such as non-replacement therapy have been established resulting in a longer duration of FVIII effect that leads to a more stable hemostatic effect. However, even if the level of hemostatic correction is comparable to that of patients with mild hemophilia, bleeding

events can still occur after trauma and the long-term bone and joint health complications related to hemophilia condition continue to not be solved (Pipe et al., 2019b).

On the other hand, gene and cell therapy approaches can offer an opening for one-time intervention providing long-term expression of FVIII that could result in enormous advantages for HA patients. Thus, it is necessary to identify cells able to effectively secrete FVIII and, at the same time, to meet the necessary conditions to ensure the success of the therapy. It is well established that FVIII is largely secreted by endothelial cells (ECs) and we demonstrated that LSECs produce and secrete FVIII, although not exclusively (Follenzi et al., 2008; Fomin et al., 2013; Shahani et al., 2014; Zanolini et al., 2015). Plasma FVIII may originate from additional sources, e.g., peripheral blood mononuclear cells, blood derived outgrowth endothelial cells (BOECs) or lung microvascular endothelial cells (Jacquemin et al., 2006; Tatsumi et al., 2013).

We successfully reprogrammed both healthy and hemophilic human CD34+ cells into iPSCs and differentiate them in endothelial cells (iECs), equivalent to blood endothelial cells (Olgasi et al., 2018). Evaluating the endothelial functionality of generated iECs, we surprisingly observed a reduced capacity of HA iECs compared to healthy ones in terms of tubule formation, migration, and permeability. The transduction of HA iECs with a LV carrying the B deleted- domain (BDD) form of coagulation FVIII under the control of an endothelial promoter, VE-cadherin (LV-VEC.FVIII) partially restored the impaired capabilities of these cells (Olgasi et al., 2018). Notably, by morphological observation, HA iECs seems to have a smaller size compared to healthy iECs and after LV-correction, the morphology is unaltered. This difference in size is quite noteworthy and deserve further investigation.

Based on *in vitro* functional assays results, we hypothesized that the impaired endothelial functionality could also occur *in vivo*. Increased vascular permeability is one of the major indicators of blood vessel damage and it has been reported in systemic diseases such as diabetes and hypertension (Rask-Madsen and King, 2013; Viazzi et al., 2008). Increased vascular permeability and remodeling is also associated with hemarthrosis that could lead to recurrent joint bleedings (Cooke et al., 2018).

In a mouse model of HA, we observed an altered permeability of HA mice vessels compared to healthy ones. Extensive vascular leakage occurred under the skin and at joint level of HA mice indicating a general vascular fragility of HA mice.

As the vascular network is indispensable for homeostasis in the human body, it is important to understand whether coagulation FVIII plays a role in ECs functionality. Actually, the molecular changes at gene expression level between healthy and HA ECs has never been

investigated. Thus, we proceed with gene expression and pathway analyses in healthy, HA and LV-VEC.FVIII HA iECs by RNAseq. We identified marked transcriptional changes between healthy and HA iECs finding several genes highly expressed in healthy iECs and downregulated in HA ECs and vice-versa. RNA-seq analysis highlighted that many genes downregulated in HA iECs are implicated in ECM organization, focal adhesion, and angiogenesis pathways that could explain the differences in endothelial functionality of HA *vs* healthy cells. Whether FVIII deficiency have such an impact on the regulation or expression of many genes on ECs remain still unknown and object of intense investigations. In contrast, LV-VEC.FVIII HA iECs showed an intermediate transcriptional profile indicating only a partial phenotypic correction after LV transduction. This result correlates with the levels of FVIII expression detectable in LV-corrected cells when transplanted in HA mice reaching a 6% of FVIII activity (Olgasi et al., 2018). Despite minimal transcriptional changes are observed in HA iECs compared to LV-VEC.FVIII HA, the downregulated pathways found significantly enriched are similar to HA iECs versus healthy iECs indicating that, even if moderate, FVIII increase can ameliorate the expression of some genes involved in ECM organization, focal adhesion, and angiogenesis.

Among ECM proteins, collagens are the most abundant. Collagens can preserve physiologic hemostasis by maintaining the integrity and stability of vascular wall and counteract blood extravasations upon vascular injury. The vascular ECM is an important structural and functional component of all blood vessels, with a determining role in the progression of several diseases, such as collagenopathies (Manon-Jensen et al., 2016). Ehlers–Danlos syndromes (EDS) include a heterogeneous group of connective tissue diseases that share clinical manifestations in skin, ligaments and joints, blood vessels and internal organs. Despite the mutations occur in genes coding for collagens and for enzymes involved in the biosynthesis of those proteins, easy bruising and bleeding to a variable degree are present in all subtypes of EDS. Because of fragility of the capillaries and the perivascular connective tissues, complications such as intracranial hemorrhage and arterial aneurysms can occur (Jesudas et al., 2019).

Among the collagens mutated in EDS, type I collagen is a heterodimer encoded by the *COL1A1*- and *COL1A2* genes and resides in the ECM of bone, ligaments, dermis, and blood vessel walls. Collagen fibrils result from the lateral fusion of collagen, which are stabilized by the formation of intra- and intermolecular crosslinks, catalyzed by enzymes of the lysyl oxidase (LOX) and LOX-like 1-4 family. *COL5A1* and *COL5A2* are mutated in another EDS subtype in which cardiovascular fragility is associated. Similar vascular defects arise from

the mutation of *PLOD1* gene that encode for the lysyl-hydroxylase 1 that hydroxylate lysyl residues in the collagen triple helix as the first step necessary for the formation of intra-and intermolecular collagen crosslinks (Malfait, 2018).

All the above-mentioned mutated genes are surprisingly found downregulated (LogFC < -3) in HA *vs* healthy iECs in RNAseq. These indications could represent a starting point to understand how lack of coagulation FVIII can affect ECM organization and remodeling.

Recent studies demonstrated a correlation between vascular basal membrane degradation with the development of hemophilic arthropathy (Cooke et al., 2019; Kjeld et al., 2018). Moreover, Kjield et al. demonstrated the correlation of serum level of the endothelial specific isoform of type XVIII collagen with HA patients annual bleeding rate. RNAseq analysis revealed an upregulation of *COL18A1* gene in HA iECs and a partial reduction in LV-VEC.FVIII HA iECs that was validated by RT-qPCR. It is worth noting that proteolytic cleavage within collagen XVIII C-terminal domain releases a fragment called endostatin, which has been reported to have anti-angiogenesis effects. Endostatin regulates also endothelial cell cytoskeletal organization, disturbs cell-matrix adhesion, and attenuates endothelial cell migration through an unknown mechanism (Walia et al., 2015). From our perspective, the role of collagen XVIII in correlation with FVIII deficiency will be further investigate.

Besides iECs, we aimed to verify if the impaired endothelial functionality occurred in primary endothelial cells. Therefore, as endothelial model we used BOECs isolated both from healthy donors and HA patients (Olgasi et al., under revision). Remarkably, HA BOECs showed the same dysfunction in endothelial functionality, that was restored by LV-VEC.FVIII transduction. Transcriptomic profile analysis of healthy, HA and LV-corrected BOECs did not put in evidence many differentially expressed genes as in iECs. However, the analysis of the pathways involved in HA condition showed a similar trend of iECs, with a remarked enrichment of downregulated genes belonging to ECM markers, integrins, focal adhesion and angiogenesis. Moreover, in contrast to iECs, LV transduced HA BOECs clustered closer to healthy ones with a more similar transcriptomic profile. Among the downregulated genes, *VCAN* has been validated by RT-qPCR and was found downregulated in HA BOECs compared to healthy BOECs and LV-corrected BOECs. The protein encoded is a large proteoglycan and is a major component of the extracellular matrix. This protein is involved in cell adhesion, proliferation, migration and angiogenesis and can also influence endothelial cell phenotype. The mechanism responsible for versican's effect on endothelial cells is not

described, but probably versican interacts with hyaluronic acid, a well-known ECM regulator of angiogenesis in vascular system (Wight et al., 2020; Yang and Yee, 2013).

To further demonstrate the possible extra-coagulative role of FVIII, we investigated if the presence of FVIII in proximity of the basal membrane of ECs lining the vessels could improve HA ECs functionality. Therefore, we first demonstrated, *in vitro*, that the treatment of HA BOECs with two different recombinant human forms of FVIII (rhFVIII), rhBDD and rhFL, increased their ability to form tubule network, cell migration, and ameliorate the permeability of HA BOECs. This enhancement resembles the abilities observed in LV-VEC.FVIII HA BOECs and healthy BOECs and correlate with RNAseq data analysis indicating an impairment in ECM organization and angiogenesis. The same effect of FVIII on angiogenesis improvement was also observed *in vivo*, after injection of healthy, HA or LV-corrected HA BOECs mixed with Matrigel in NSG-HA mice, confirming the hypothesized role of FVIII in maintaining ECs stability and functionality. Noteworthy, it was not observed an improvement in vessel diameter and density when HA BOEC were injected in NSG mice. These results indicate that despite the presence of physiological level of mouse FVIII (mFVIII) in NSG mice, HA BOECs failed to form well-organized vessels in Matrigel plugs, as well as in NSG-HA mice.

Finally, we injected Matrigel plugs, with or without rhFVIII, in NSG-HA mice to further demonstrate that HA mice have a dysfunctional endothelium and that rhFVIII can restore their functionality. The treatment of Matrigel plugs with the two forms of rhFVIII (rhBDD-FVIII and rhFL-FVIII) in NSG-HA mice induce a significant increase in vessel density and diameter compared to NSG-HA injected with Matrigel alone. Moreover, it was observed a significant enhanced density of the newly formed vessels, but not their diameter, with rhFL-FVIII. These results indicate that the constant presence of exogenous human rhFVIII in the matrix led to the formation of newly and larger vessels. It will be interesting to explore the level in which mFVIII in NSG mice is able to stimulate transplanted human HA BOECs in the Matrigel plug. Moreover, the different behavior of the two forms of rhFVIII needs further investigations, to evaluate if the different length of FVIII, and especially the presence of the B-domain, could play an extra-coagulative role in enhancing vessel stability.

Currently, the use of BDD-FVIII is prominent in HA gene therapy as it bypasses the inability of most viral vectors to carry the FL-FVIII transgene. Nonetheless, questions about the implications of using a truncated BDD-FVIII instead of the full-length version remain. No studies were carried out to compare, side-by-side, the performance of BDD-FVIII vs FL-FVIII in the correction of the bleeding phenotype with a particular focus on the endothelial

stabilization. Further investigation will be also needed to understand the differences of FVIII role in EC biology when FVIII is exogenously provided by rFVIII intravenous infusion or endogenously produced after LV gene therapy. Moreover, *in vivo* studies of joint hemarthrosis in combination with the presence/absence of FVIII would be helpful to support the role of FVIII beyond coagulation in EC function.

The advancement of non-replacement therapy allowed the treatment of HA patients that develop inhibitors using recombinant or blood derived FVIII. Despite the hemostatic effect, bleeding events can still occur, suggesting that non replacement therapy may not ameliorate vessel fragility. Non-replacement therapy, indeed, is based on humanized antibodies that bridges FX and FIX, thus they do not contain FVIII protein. Based on the effect of rhFVIII observed in our *in vivo* experiment, we can speculate that the presence of the protein can be fundamental for vessel stabilization. Considering that the use of rhFVIII has side effects as inhibitors development, the gene and cell therapy approach can possibly overcome the limitations and be successful in reducing the side effects of both strategies.

In conclusion, we paved the way to study the differences in the genetic profile between healthy and hemophilic ECs. This information can be crucial to understand if key molecular targets are missing in HA patients at the cellular level impairing EC functionality. The study of the extra-coagulative role of FVIII can offer new therapeutic gene and cell therapy strategies for the management of HA and can lay the basis for the development of a combined strategy that can result in a safer and more efficient treatment of HA.

References

Acharya, S.S., Kaplan, R.N., Macdonald, D., Fabiyi, O.T., DiMichele, D., and Lyden, D. (2011). Neoangiogenesis contributes to the development of hemophilic synovitis. Blood *117*, 2484–2493.

Adamson, R. (1994). Design and operation of a recombinant mammalian cell manufacturing process for rFVIII. Annals of Hematology *68*.

Aird, W.C. (2012). Endothelial cell heterogeneity. Cold Spring Harbor Perspectives in Medicine *2*.

Andersson, N.G., Auerswald, G., Barnes, C., Carcao, M., Dunn, A.L., Fijnvandraat, K., Hoffmann, M., Kavakli, K., Kenet, G., Kobelt, R., et al. (2017). Intracranial haemorrhage in children and adolescents with severe haemophilia A or B – the impact of prophylactic treatment. British Journal of Haematology *179*, 298–307.

Annoni, A., Battaglia, M., Follenzi, A., Lombardo, A., Sergi-Sergi, L., Naldini, L., and Roncarolo, M.G. (2007). The immune response to lentiviral-delivered transgene is modulated in vivo by transgene-expressing antigen-presenting cells but not by CD4 +CD25+ regulatory T cells. Blood *110*, 1788–1796.

Asahara, T., Murohara, T., Sullivan, A., Silver, M., Van Der Zee, R., Li, T., Witzenbichler, B., Schatteman, G., and Isner, J.M. (1997). Isolation of putative progenitor endothelial cells for angiogenesis. Science *275*, 964–967.

Balami, J.S., and Buchan, A.M. (2012). Complications of intracerebral haemorrhage. The Lancet Neurology *11*, 101–118.

Barnes, C., Wong, P., Egan, B., Speller, T., Cameron, F., Jones, G., Ekert, H., and Monagle, P. (2004). Reduced bone density among children with severe hemophilia. Pediatrics *114*.

Barnes, R.F.W., Cramer, T.J., Sait, A.S., Kruse-Jarres, R., Quon, D.V.K., and Von Drygalski, A. (2016). The Hypertension of Hemophilia Is Not Explained by the Usual Cardiovascular Risk Factors: Results of a Cohort Study. International Journal of Hypertension *2016*.

Baud'huin, M., Duplomb, L., Téletchéa, S., Charrier, C., Maillasson, M., Fouassier, M., and Heymann, D. (2009). Factor VII-von Willebrand factor complex inhibits osteoclastogenesis and controls cell survival. Journal of Biological Chemistry *284*, 31704–31713.

Van Den Berg, H.M., Fischer, K., Carcao, M., Chambost, H., Kenet, G., Kurnik, K., Königs, C., Male, C., Santagostino, E., and Ljung, R. (2019). Timing of inhibitor development in more than 1000 previously untreated patients with severe hemophilia A. Blood *134*, 317–320.

Berntorp, E. (1997). Second generation, B-domain deleted recombinant factor VIII. In Thrombosis and Haemostasis, (Schattauer GmbH), pp. 256–260.

Bhat, V., Olmer, M., Joshi, S., Durden, D.L., Cramer, T.J., Barnes, R.F.W., Ball, S.T., Hughes, T.H., Silva, M., Luck, J. V., et al. (2015). Vascular remodeling underlies rebleeding in hemophilic arthropathy. American Journal of Hematology *90*, 1027–1035.

Bhopale, G.M., and Nanda, R.K. (2003). Blood coagulation factor VIII: An overview. Journal of Biosciences *28*, 783–789.

Bierhansl, L., Conradi, L.C., Treps, L., Dewerchin, M., and Carmeliet, P. (2017). Central role of metabolism in endothelial cell function and vascular disease. Physiology *32*, 126–140.

Biffi, A., Bartholomae, C.C., Cesana, D., Cartier, N., Aubourg, P., Ranzani, M., Cesani, M., Benedicenti, F., Plati, T., Rubagotti, E., et al. (2011). Lentiviral vector common integration sites in preclinical models and a clinical trial reflect a benign integration bias and not oncogenic selection. Blood *117*, 5332–5339.

Bladen, M., Main, E., Khair, K., Hubert, N., Koutoumanou, E., and Liesner, R. (2016). The incidence, risk and functional outcomes of intracranial haemorrhage in children with inherited bleeding disorders at one haemophilia center. Haemophilia *22*, 556–563.

Bolton-Maggs, P.H.B., and Pasi, K.J. (2003). Haemophilias A and B. In Lancet, (Elsevier B.V.), pp. 1801–1809.

Bontempo, F.A., Lewis, J.H., Gorenc, T.J., Spero, J.A., Ragni, M. V, Scott, J.P., and Starzl, T.E. (1987). Liver transplantation in hemophilia A. Blood *69*, 1721–1724.

Brown, B.D., Venneri, M.A., Zingale, A., Sergi, L.S., and Naldini, L. (2006). Endogenous microRNA regulation suppresses transgene expression in hematopoietic lineages and enables stable gene transfer. Nature Medicine *12*, 585–591.

Calcaterra, I., Iannuzzo, G., Dell'Aquila, F., and Di Minno, M.N.D. (2020). Pathophysiological Role of Synovitis in Hemophilic Arthropathy Development: A Two-Hit Hypothesis. Frontiers in Physiology *11*, 541.

Cardinal, M., Kantaridis, C., Zhu, T., Sun, P., Pittman, D.D., Murphy, J.E., and Arkin, S. (2018). A first-in-human study of the safety, tolerability, pharmacokinetics and pharmacodynamics of PF-06741086, an anti-tissue factor pathway inhibitor mAb, in healthy volunteers. Journal of Thrombosis and Haemostasis *16*, 1722–1731.

Chalmers, E.A., Alamelu, J., Collins, P.W., Mathias, M., Payne, J., Richards, M., Tunstall, O., Williams, M., Palmer, B., and Mumford, A. (2018). Intracranial haemorrhage in children with inherited bleeding disorders in the UK 2003-2015: A national cohort study. Haemophilia *24*, 641–647.

Collins, P.W., Blanchette, V.S., Fischer, K., Björkman, S., Oh, M., Fritsch, S., Schroth, P., Spotts, G., Astermark, J., and Ewenstein, B. (2009). Break-through bleeding in relation to predicted factor VIII levels in patients receiving prophylactic treatment for severe hemophilia A. Journal of Thrombosis and Haemostasis *7*, 413–420.

Cooke, E.J., Zhou, J.Y., Wyseure, T., Joshi, S., Bhat, V., Durden, D.L., Mosnier, L.O., and Drygalski, A. Von (2018). Vascular Permeability and Remodelling Coincide with Inflammatory and Reparative Processes after Joint Bleeding in Factor VIII-Deficient Mice. Thrombosis and Haemostasis *118*, 1036–1047.

Cooke, E.J., Wyseure, T., Zhou, J.Y., Gopal, S., Nasamran, C.A., Fisch, K.M., Manon-Jensen, T., Karsdal, M.A., Mosnier, L.O., and von Drygalski, A. (2019). Mechanisms of vascular permeability and remodeling associated with hemarthrosis in factor VIII-deficient mice. Journal of Thrombosis and Haemostasis *17*, 1815–1826.

Cramer, T.J., and Gale, A.J. (2011). Function of the activated protein C (APC) autolysis loop in activated FVIII inactivation. British Journal of Haematology *153*, 644–654.

Danoy, M., Poulain, S., Koui, Y., Tauran, Y., Scheidecker, B., Kido, T., Miyajima, A., Sakai, Y., Plessy, C., and Leclerc, E. (2020). Transcriptome profiling of hiPSC-derived LSECs with nanoCAGE. Molecular Omics *16*, 138–146.

Deyle, D.R., and Russell, D.W. (2009). Adeno-associated virus vector integration. Current Opinion in Molecular Therapeutics *11*, 442–447.

Dimichele, D. (2002). Inhibitors: Resolving diagnostic and therapeutic dilemmas. Haemophilia *8*, 280–287.

Dobin, A., Davis, C.A., Schlesinger, F., Drenkow, J., Zaleski, C., Jha, S., Batut, P., Chaisson, M., and Gingeras, T.R. (2013). STAR: Ultrafast universal RNA-seq aligner. Bioinformatics *29*, 15–21.

Donath, M.J.S.H. (1996). Kinetics of factor VIII light-chain cleavage by thrombin and factor Xa A regulatory role of the factor VIII heavy-chain region Lys713-Arg740. European Journal of Biochemistry *240*, 365–372.

Von Drygalski, A., Kolaitis, N.A., Bettencourt, R., Bergstrom, J., Kruse-Jarres, R., Quon, D. V., Wassel, C., Li, M.C., Waalen, J., Elias, D.J., et al. (2013). Prevalence and risk factors for hypertension in hemophilia. Hypertension *62*, 209–215.

Du, L.M., Nurden, P., Nurden, A.T., Nichols, T.C., Bellinger, D.A., Jensen, E.S., Haberichter, S.L., Merricks, E., Raymer, R.A., Fang, J., et al. (2013). Platelet-targeted gene therapy with human factor VIII establishes haemostasis in dogs with haemophilia A. Nature Communications *4*.

DUNN, A.L. (2011). Pathophysiology, diagnosis and prevention of arthropathy in patients with haemophilia. Haemophilia *17*, 571–578.

Eaton, D., Rodriguez, H., and Vehar, G.A. (1986). Proteolytic Processing of Human Factor VIII. Correlation of Specific Cleavages by Thrombin, Factor Xa, and Activated Protein C with Activation And Inactivation of Factor VIII Coagulant Activity. Biochemistry *25*, 505–512.

Ebbert, P.T., Xavier, F., Seaman, C.D., and Ragni, M. V. (2020). Emicizumab prophylaxis in patients with haemophilia A with and without inhibitors. Haemophilia *26*, 41–46.

Famà, R., Borroni, E., Merlin, S., Airoldi, C., Pignani, S., Cucci, A., Corà, D., Bruscaggin, V., Scardellato, S., Faletti, S., et al. (2020). Deciphering the Ets-1/2-mediated transcriptional regulation of F8 gene identifies a minimal F8 promoter for hemophilia A gene therapy. Haematologica haematol.2019.239202.

Fang, H., Wang, L., and Wang, H. (2007). The protein structure and effect of factor VIII. Thrombosis Research *119*, 1–13.

Fay, P.J. (2004). Activation of factor VIII and mechanisms of cofactor action. Blood Reviews *18*, 1–15.

Filali, E. El, Hiralall, J.K., Van Veen, H.A., Stolz, D.B., and Seppen, J. (2013). Human Liver Endothelial Cells, But Not Macrovascular or Microvascular Endothelial Cells, Engraft in the Mouse Liver. Cell Transplantation *22*, 1801–1811.

Finn, J.D., Ozelo, M.C., Sabatino, D.E., Franck, H.W.G., Merricks, E.P., Crudele, J.M., Zhou, S., Kazazian, H.H., Lillicrap, D., Nichols, T.C., et al. (2010). Eradication of neutralizing antibodies to factor VIII In canine hemophilia a after liver gene therapy. Blood *116*, 5842–5848.

Follenzi, A., Battaglia, M., Lombardo, A., Annoni, A., Roncarolo, M.G., and Naldini, L. (2004). Targeting lentiviral vector expression to hepatocytes limits transgene-specific immune response and establishes long-term expression of human antihemophilic factor IX in mice. Blood *103*, 3700–3709.

Follenzi, A., Benten, D., Novikoff, P., Faulkner, L., Raut, S., and Gupta, S. (2008). Transplanted endothelial cells repopulate the liver endothelium and correct the phenotype of hemophilia A mice. The Journal of Clinical Investigation *118*, 935–945.

Follenzi, A., Raut, S., Merlin, S., Sarkar, R., and Gupta, S. (2012). Role of bone marrow transplantation for correcting hemophilia A in mice. Blood *119*, 5532–5542.

Fomin, M.E., Zhou, Y.C., Beyer, A.I., Publicover, J., Baron, J.L., and Muench, M.O. (2013). Production of Factor VIII by Human Liver Sinusoidal Endothelial Cells Transplanted in Immunodeficient uPA Mice. PloS One *8*.

Franchini, M., and Mannucci, P.M. (2014). The history of hemophilia. Seminars in Thrombosis and Hemostasis *40*, 571–576.

Franchini, M., Favaloro, E.J., and Lippi, G. (2010). Mild hemophilia A. Journal of Thrombosis and Haemostasis *8*, 421–432.

Gao, K., Kumar, P., Cortez-Toledo, E., Hao, D., Reynaga, L., Rose, M., Wang, C., Farmer, D., Nolta, J., Zhou, J., et al. (2019). Potential long-term treatment of hemophilia A by neonatal co-transplantation of cord blood-derived endothelial colony-forming cells and placental mesenchymal stromal cells. Stem Cell Research and Therapy *10*.

Gay, N.D., Lee, S.C., Liel, M.S., Sochacki, P., Recht, M., and Taylor, J.A. (2015). Increased fracture rates in people with haemophilia: A 10-year single institution retrospective analysis. British Journal of Haematology *170*, 584–586.

Giangrande, P., Andreeva, T., Chowdary, P., Ehrenforth, S., Hanabusa, H., Leebeek, F.W.G., Lentz, S.R., Nemes, L., Poulsen, L.H., Santagostino, E., et al. (2017). Clinical evaluation of glycoPEGylated recombinant FVIII: Efficacy and safety in severe haemophilia A. Thrombosis and Haemostasis *117*, 252–261.

Gooding, R., Thachil, J., Alamelu, J., Motwani, J., and Chowdary, P. (2021). Asymptomatic joint bleeding and joint health in hemophilia: A review of variables, methods, and biomarkers. Journal of Blood Medicine *12*, 209–220.

Graf, L. (2018). Extended Half-Life Factor VIII and Factor IX Preparations. Transfusion Medicine and Hemotherapy *45*, 86–91.

Graw, J., Brackmann, H.-H., Oldenburg, J., Schneppenheim, R., Spannagl, M., and Schwaab, R. (2005). Haemophilia A: from mutation analysis to new therapies. Nature Reviews Genetics *6*, 488–501.

Grieger, J.C., and Samulski, R.J. (2012). Adeno-associated virus vectorology, manufacturing, and clinical applications. In Methods in Enzymology, (Academic Press Inc.), pp. 229–254.

Gu, J.M., Zhao, X.Y., Schwarz, T., Schuhmacher, J., Baumann, A., Ho, E., Subramanyan, B., Tran, K., Myles, T., Patel, C., et al. (2017). Mechanistic Modeling of the Pharmacodynamic and Pharmacokinetic Relationship of Tissue Factor Pathway Inhibitor-Neutralizing Antibody (BAY 1093884) in Cynomolgus Monkeys. AAPS Journal *19*, 1186–1195.

Hay, C.R.M., Nissen, F., and Pipe, S.W. (2021). Mortality in congenital hemophilia A – a systematic literature review. Journal of Thrombosis and Haemostasis *19*, 6–20.

Hebbel, R.P. (2017). Blood endothelial cells: Utility from ambiguity. Journal of Clinical Investigation *127*, 1613–1615.

Hewett, P.W. (2016). Isolation and culture of human endothelial cells from micro- and macro-vessels. In Methods in Molecular Biology, (Humana Press Inc.), pp. 61–76.

High, K.A. (2012). The gene therapy journey for hemophilia: Are we there yet? Blood *120*, 4482–4487.

High, K.A., George, L.A., Eyster, M.E., Sullivan, S.K., Ragni, M. V., Croteau, S.E., Samelson-Jones, B.J., Evans, M., Joseney-Antoine, M., Macdougall, A., et al. (2018). A Phase 1/2 Trial of Investigational Spk-8011 in Hemophilia a Demonstrates Durable Expression and Prevention of Bleeds. Blood *132*, 487–487.

Hollestelle, M.J., Thinnes, T., Crain, K., Stiko, A., Kruijt, J.K., Van Berkel, T.J.C., Loskutoff, D.J., and Van Mourik, J.A. (2001). Tissue distribution of factor VIII gene expression in vivo - A closer look. Thrombosis and Haemostasis *86*, 855–861.

Hooiveld, M.J.J., Roosendaal, G., van den Berg, H.M., Bijlsma, J.W.J., and Lafeber, F.P.J.G. (2003). Haemoglobin-derived iron-dependent hydroxyl radical formation in blood-induced joint damage: An in vitro study. Rheumatology *42*, 784–790.

Hoots, W.K. (2006). Pathogenesis of hemophilic arthropathy. In Seminars in Hematology, (Semin Hematol), p.

Ilić, K., Obradović, N., and Vujasinović-Stupar, N. (2013). The relationship among hypertension, antihypertensive medications, and osteoporosis: A narrative review. Calcified Tissue International *92*, 217–227.

Incarnato, D., Neri, F., Anselmi, F., and Oliviero, S. (2014). Genome-wide profiling of mouse RNA secondary structures reveals key features of the mammalian transcriptome. Genome Biology *15*.

Iorio, A., Stonebraker, J.S., Chambost, H., Makris, M., Coffin, D., Herr, C., Germini, F., Stonebraker, J.S., Iorio, A., Byams, V., et al. (2019). Establishing the prevalence and prevalence at birth of hemophilia in males a meta-analytic approach using national registries. Annals of Internal Medicine *171*, 542–546.

Jacquemin, M., Neyrinck, A., Hermanns, M.I., Lavend'homme, R., Rega, F., Saint-Remy, J.M., Peerlinck, K., Van Raemdonck, D., and Kirkpatrick, C.J. (2006). FVIII production by human lung microvascular endothelial cells. Blood *108*, 515–517.

Jesudas, R., Chaudhury, A., and Laukaitis, C.M. (2019). An update on the new classification of Ehlers-Danlos syndrome and review of the causes of bleeding in this population. Haemophilia *25*, 558–566.

Jia, B., Chen, S., Zhao, Z., Liu, P., Cai, J., Qin, D., Du, J., Wu, C., Chen, Q., Cai, X., et al. (2014). Modeling of hemophilia A using patient-specific induced pluripotent stem cells derived from urine cells. Life Sciences *108*, 22–29.

Kamphuisen, P.W., and Ten Cate, H. (2014). Cardiovascular risk in patients with hemophilia. Blood *123*, 1297–1301.

Katsarou, O., Terpos, E., Chatzismalis, P., Provelengios, S., Adraktas, T., Hadjidakis, D., Kouramba, A., and Karafoulidou, A. (2010). Increased bone resorption is implicated in the pathogenesis of bone loss in hemophiliacs: Correlations with hemophilic arthropathy and HIV infection. Annals of Hematology *89*, 67–74.

Kitazawa, T., Igawa, T., Sampei, Z., Muto, A., Kojima, T., Soeda, T., Yoshihashi, K., Okuyama-Nishida, Y., Saito, H., Tsunoda, H., et al. (2012). A bispecific antibody to factors IXa and X restores factor VIII hemostatic activity in a hemophilia A model. Nature Medicine *18*, 1570–1574.

Kjalke, M., Heding, A., Talbo, G., Persson, E., Thomsen, J., and Ezban, M. (1995). Amino Acid Residues 721–729 are Required for Full Factor VIII Activity. European Journal of Biochemistry *234*, 773–779.

Kjeld, N.G., Hua, B., Karsdal, M.A., Sun, S., and Manon-Jensen, T. (2018). The endothelial specific isoform of type XVIII collagen correlates to annual bleeding rate in haemophilia patients. PloS One *13*, e0190375.

Klamroth, R., Pollmann, H., Hermans, C., Faradji, A., Yarlas, A.S., Epstein, J.D., and Ewenstein, B.M. (2011). The relative burden of haemophilia A and the impact of target joint development on health-related quality of life: Results from the ADVATE Post-Authorization Safety Surveillance (PASS) study. Haemophilia *17*, 412–421.

Knobe, K., and Berntorp, E. (2011). Haemophilia and Joint Disease: Pathophysiology, Evaluation, and Management. Journal of Comorbidity *1*, 51–59.

Knolle, P.A., and Wohlleber, D. (2016). Immunological functions of liver sinusoidal endothelial cells. Cellular and Molecular Immunology *13*, 347–353.

Konkle, B.A., Stasyshyn, O., Chowdary, P., Bevan, D.H., Mant, T., Shima, M., Engl, W., Dyck-Jones, J., Fuerlinger, M., Patrone, L., et al. (2015). Pegylated, full-length, recombinant factor VIII for prophylactic and on-demand treatment of severe hemophilia A. Blood *126*, 1078–1085.

Konkle, B.A., Stine, K., Visweshwar, N., Harrington, T.J., Leavitt, A.D., Giermasz, A., Arkin, S., Di Russo, G., Snyder, A., Woolfson, A., et al. (2019). Updated Follow-up of the Alta Study, a Phase 1/2, Open Label, Adaptive, Dose-Ranging Study to Assess the Safety and Tolerability of SB-525 Gene Therapy in Adult Patients with Severe Hemophilia A. Blood *134*, 2060–2060.

Koui, Y., Kido, T., Ito, T., Oyama, H., Chen, S.W., Katou, Y., Shirahige, K., and Miyajima, A. (2017). An In Vitro Human Liver Model by iPSC-Derived Parenchymal and Non-parenchymal Cells. Stem Cell Reports *9*, 490–498.

Kovacs, C.S. (2008). Hemophilia, low bone mass, and osteopenia/osteoporosis. Transfusion and Apheresis Science *38*, 33–40.

Kuether, E.L., Schroeder, J.A., Fahs, S.A., Cooley, B.C., Chen, Y., Montgomery, R.R., Wilcox, D.A., and Shi, Q. (2012). Lentivirus-mediated platelet gene therapy of murine hemophilia A with pre-existing anti-factor VIII immunity. Journal of Thrombosis and Haemostasis *10*, 1570–1580.

Kulkarni, R., Presley, R.J., Lusher, J.M., Shapiro, A.D., Gill, J.C., Manco-Johnson, M., Koerper, M.A., Abshire, T.C., DiMichele, D., Hoots, W.K., et al. (2017). Complications of haemophilia in babies (first two years of life): a report from the Centers for Disease Control and Prevention Universal Data Collection System. Haemophilia *23*, 207–214.

Kumaran, V., Benten, D., Follenzi, A., Joseph, B., Sarkar, R., and Gupta, S. (2005). Transplantation of endothelial cells corrects the phenotype in hemophilia A mice. Journal of Thrombosis and Haemostasis *3*, 2022–2031.

Lampugnani, M.G., Dejana, E., and Giampietro, C. (2018). Vascular Endothelial (VE)-Cadherin, Endothelial Adherens Junctions, and Vascular Disease. Cold Spring Harbor Perspectives in Biology *10*, a029322.

Leavitt, A. (2020). Updated Follow-up of the Alta Study, a Phase 1/2 Study of Giroctocogene Fitelparvovec (SB-525) Gene Therapy in Adults with Severe Hemophilia a.

Lenting, P.J., Denis, C. V., and Christophe, O.D. (2017). Emicizumab, a bispecific antibody recognizing coagulation factors IX and X: How does it actually compare to factor VIII? Blood *130*, 2463–2468.

Lentz, S.R., Janic, D., Kavakli, K., Miljic, P., Oldenburg, J., C. Ozelo, M., Santagostino, E., Suzuki, T., Zupancic Šalek, S., Korsholm, L., et al. (2018). Long-term safety and efficacy of turoctocog alfa in prophylaxis and treatment of bleeding episodes in severe haemophilia A: Final results from the guardian 2 extension trial. Haemophilia *24*, e391–e394.

Liao, Y., Smyth, G.K., and Shi, W. (2014). FeatureCounts: An efficient general purpose program for assigning sequence reads to genomic features. Bioinformatics *30*, 923–930.

Lin, Y., Weisdorf, D.J., Solovey, A., and Hebbel, R.P. (2000). Origins of circulating endothelial cells and endothelial outgrowth from blood. Journal of Clinical Investigation *105*, 71–77.

Lin, Y., Chang, L., Solovey, A., Healey, J.F., Lollar, P., and Hebbel, R.P. (2002). Use of blood outgrowth endothelial cells for gene therapy for hemophilia A. Blood *99*, 457–462.

Lissitchkov, T., Rusen, L., Georgiev, P., Windyga, J., Klamroth, R., Gercheva, L., Nemes, L., Tiede, A., Bichler, J., Knaub, S., et al. (2017). PK-guided personalized prophylaxis with Nuwiq® (human-cl rhFVIII) in adults with severe haemophilia A. Haemophilia *23*, 697–704.

Livak, K.J., and Schmittgen, T.D. (2001). Analysis of relative gene expression data using real-time quantitative PCR and the 2-ΔΔCT method. Methods *25*, 402–408.

Ljung, R.C.R. (2008). Intracranial haemorrhage in haemophilia A and B. British Journal of Haematology *140*, 378–384.

Lobet, S., Hermans, C., and Lambert, C. (2014). Optimal management of hemophilic arthropathy and hematomas. Journal of Blood Medicine *5*, 207.

Luck, J. V, Silva, M., Rodriguez-Merchan, E.C., Ghalambor, N., Zahiri, C.A., and Finn, R.S. Hemophilic arthropathy. The Journal of the American Academy of Orthopaedic Surgeons *12*, 234–245.

Lynch, C.M., Israel, D.I., Kaufman, R.J., and Miller, A.D. (1993). Sequences in the Coding Region of Clotting Factor VIII Act as Dominant Inhibitors of RNA Accumulation and Protein Production. Human Gene Therapy *4*, 259–272.

Mahlangu, J., Powell, J.S., Ragni, M. V., Chowdary, P., Josephson, N.C., Pabinger, I., Hanabusa, H., Gupta, N., Kulkarni, R., Fogarty, P., et al. (2014). Phase 3 study of recombinant factor VIII Fc fusion protein in severe hemophilia A. Blood *123*, 317–325.

Mahlangu, J., Kuliczkowski, K., Karim, F.A., Stasyshyn, O., Kosinova, M. V., Lepatan, L.M., Skotnicki, A., Boggio, L.N., Klamroth, R., Oldenburg, J., et al. (2016). Efficacy and safety of rVIII-Singlechain: Results of a phase 1/3 multicenter clinical trial in severe hemophilia A. Blood *128*, 630–637.

Mahlangu, J., Young, G., Hermans, C., Blanchette, V., Berntorp, E., and Santagostino, E. (2018). Defining extended half-life rFVIII—A critical review of the evidence. Haemophilia *24*, 348–358.

Malfait, F. (2018). Vascular aspects of the Ehlers-Danlos Syndromes. Matrix Biology *71–72*, 380–395.

Manon-Jensen, T., Kjeld, N.G., and Karsdal, M.A. (2016). Collagen-mediated hemostasis. Journal of Thrombosis and Haemostasis *14*, 438–448.

Margaglione, M., Castaman, G., Morfini, M., Rocino, A., Santagostino, E., Tagariello, G., Tagliaferri, A., Zanon, E., Bicocchi, M.P., Castaldo, G., et al. (2008). The Italian AICE-Genetics hemophilia a database: Results and correlation with clinical phenotype. Haematologica *93*, 722–728.

Matsui, H., Shibata, M., Brown, B., Labelle, A., Hegadorn, C., Andrews, C., Hebbel, R.P., Galipeau, J., Hough, C., and Lillicrap, D. (2007). Ex Vivo Gene Therapy for Hemophilia A That Enhances Safe Delivery and Sustained In Vivo Factor VIII Expression from Lentivirally Engineered Endothelial Progenitors. Stem Cells *25*, 2660–2669.

Matsui, H., Hegadorn, C., Ozelo, M., Burnett, E., Tuttle, A., Labelle, A., McCray, P.B., Naldini, L., Brown, B., Hough, C., et al. (2011). A MicroRNA-regulated and GP64-pseudotyped lentiviral vector mediates stable expression of FVIII in a murine model of hemophilia a. Molecular Therapy *19*, 723–730.

Matsui, H., Fujimoto, N., Sasakawa, N., Ohinata, Y., Shima, M., Yamanaka, S., Sugimoto, M., and Hotta, A. (2014). Delivery of Full-Length Factor VIII Using a piggyBac Transposon Vector to Correct a Mouse Model of Hemophilia A. PLoS ONE *9*, e104957.

McIntosh, J., Lenting, P.J., Rosales, C., Lee, D., Rabbanian, S., Raj, D., Patel, N., Tuddenham, E.G.D., Christophe, O.D., McVey, J.H., et al. (2013). Therapeutic levels of FVIII following a single peripheral vein administration of rAAV vector encoding a novel human factor VIII variant. Blood *121*, 3335–3344.

Medina, R.J., O'Neill, C.L., Sweeney, M., Guduric-Fuchs, J., Gardiner, T.A., Simpson, D.A., and Stitt, A.W. (2010). Molecular analysis of endothelial progenitor cell (EPC) subtypes reveals two distinct cell populations with different identities. BMC Medical Genomics *3*.

Merlin, S., Cannizzo, E.S., Borroni, E., Bruscaggin, V., Schinco, P., Tulalamba, W., Chuah, M.K., Arruda, V.R., VandenDriessche, T., Prat, M., et al. (2017). A Novel Platform for Immune Tolerance Induction in Hemophilia A Mice. Molecular Therapy *25*, 1815–1830.

Merlin, S., Famà, R., Borroni, E., Zanolini, D., Bruscaggin, V., Zucchelli, S., and Follenzi, A. (2019). FVIII expression by its native promoter sustains long-term correction avoiding immune response in hemophilic mice. Blood Advances *3*, 825–838.

Mingozzi, F., and High, K.A. (2013). Immune responses to AAV vectors: Overcoming barriers to successful gene therapy. Blood *122*, 23–36.

Naldini, L. (2019). Genetic engineering of hematopoiesis: current stage of clinical translation and future perspectives. EMBO Molecular Medicine *11*.

Nathwani, A.C., Rosales, C., McIntosh, J., Rastegarlari, G., Nathwani, D., Raj, D., Nawathe, S., Waddington, S.N., Bronson, R., Jackson, S., et al. (2011). Long-term safety and efficacy following systemic administration of a self-complementary AAV vector encoding human FIX pseudotyped with serotype 5 and 8 capsid proteins. Molecular Therapy *19*, 876–885.

Nathwani, A.C., Reiss, U.M., Tuddenham, E.G.D., Rosales, C., Chowdary, P., McIntosh, J., Della Peruta, M., Lheriteau, E., Patel, N., Raj, D., et al. (2014). Long-Term Safety and Efficacy of Factor IX Gene Therapy in Hemophilia B. New England Journal of Medicine *371*, 1994–2004.

Nathwani, A.C., Tuddenham, E., Chowdary, P., McIntosh, J., Lee, D., Rosales, C., Phillips, M., Pie, J., Junfang, Z., Meagher, M.M., et al. (2018). GO-8: Preliminary Results of a Phase I/II Dose Escalation Trial of Gene Therapy for Haemophilia a Using a Novel Human Factor VIII Variant. Blood *132*, 489–489.

NCT03513939 A Safety, Tolerability and Efficacy Study of Sernova's Cell Pouch™ for Clinical Islet Transplantation - Full Text View - ClinicalTrials.gov.

Neumeyer, J., Lin, R.Z., Wang, K., Hong, X., Hua, T., Croteau, S.E., Neufeld, E.J., and Melero-Martin, J.M. (2019). Bioengineering hemophilia a-specific microvascular grafts for delivery of full-length factor VIII into the bloodstream. Blood Advances *3*, 4166–4176.

Ngo, J.C.K., Huang, M., Roth, D.A., Furie, B.C., and Furie, B. (2008). Crystal Structure of Human Factor VIII: Implications for the Formation of the Factor IXa-Factor VIIIa Complex. Structure *16*, 597–606.

Nguyen, G.N., Everett, J.K., Raymond, H., Kafle, S., Merricks, E.P., Kazazian, H.H., Nichols, T.C., Bushman, F.D., and Sabatino, D.E. (2019). Long-Term AAV-Mediated Factor VIII Expression in Nine Hemophilia A Dogs: A 10 Year Follow-up Analysis on Durability, Safety and Vector Integration. Blood *134*, 611–611.

Nieuwenhuizen, L., Roosendaal, G., Coeleveld, K., Lubberts, E., Biesma, D.H., Lafeber, F.P.J.G., and Schutgens, R.E.G. (2013). Haemarthrosis stimulates the synovial fibrinolytic system in haemophilic mice. Thrombosis and Haemostasis *110*, 173–183.

Nogami, K., Shima, M., Nishiya, K., Hosokawa, K., Saenko, E.L., Sakurai, Y., Shibata, M., Suzuki, H., Tanaka, I., and Yoshioka, A. (2002). A novel mechanism of factor VIII protection by von Willebrand factor from activated protein C-catalyzed inactivation. Blood *99*, 3993–3998.

Nogami, K., Wakabayashi, H., and Fay, P.J. (2003). Mechanisms of factor Xa-catalyzed cleavage of the factor VIIIa A1 subunit resulting in cofactor inactivation. In Journal of Biological Chemistry, (Elsevier), pp. 16502–16509.

Ohashi, K., Waugh, J.M., Dake, M.D., Yokoyama, T., Kuge, H., Nakajima, Y., Yamanouchi, M., Naka, H., Yoshioka, A., and Kay, M.A. (2005). Liver tissue engineering at extrahepatic sites in mice as a potential new therapy for genetic liver diseases. Hepatology *41*, 132–140.

Oldenburg, J., and Pavlova, A. (2006). Genetic risk factors for inhibitors to factors VIII and IX. Haemophilia *12*, 15–22.

Oldenburg, J., Mahlangu, J.N., Kim, B., Schmitt, C., Callaghan, M.U., Young, G., Santagostino, E., Kruse-Jarres, R., Negrier, C., Kessler, C., et al. (2017). Emicizumab Prophylaxis in Hemophilia A with Inhibitors. New England Journal of Medicine *377*, 809–818.

Olgasi, C., Talmon, M., Merlin, S., Cucci, A., Richaud-Patin, Y., Ranaldo, G., Colangelo, D., Di Scipio, F., Berta, G.N., Borsotti, C., et al. (2018). Patient-Specific iPSC-Derived Endothelial Cells Provide Long-Term Phenotypic Correction of Hemophilia A. Stem Cell Reports *11*.

Ozelo, M.C., Vidal, B., Brown, C., Notley, C., Hegadorn, C., Webster, S., Harpell, L., Ahlin, J., Winterborn, A., Handforth, J., et al. (2014). Omental implantation of BOECs in hemophilia dogs results in circulating FVIII antigen and a complex immune response. Blood *123*, 4045–4053.

Park, C.-Y., Kim, J., Kweon, J., Son, J.S., Lee, J.S., Yoo, J.-E., Cho, S.-R., Kim, J.-H., Kim, J.-S., and Kim, D.-W. (2014). Targeted inversion and reversion of the blood coagulation factor 8 gene in human iPS cells using TALENs. Proceedings of the National Academy of Sciences *111*, 9253–9258.

Park, C.-Y., Kim, D.H., Son, J.S., Sung, J.J., Lee, J., Bae, S., Kim, J.-H., Kim, D.-W., and Kim, J.-S. (2015). Functional Correction of Large Factor VIII Gene Chromosomal Inversions in Hemophilia A Patient-Derived iPSCs Using CRISPR-Cas9. Cell Stem Cell *17*, 213–220.

Park, C.Y., Sung, J.J., Cho, S.R., Kim, J., and Kim, D.W. (2019). Universal Correction of Blood Coagulation Factor VIII in Patient-Derived Induced Pluripotent Stem Cells Using CRISPR/Cas9. Stem Cell Reports *12*, 1242–1249.

Paschou, S.A., Anagnostis, P., Karras, S., Annweiler, C., Vakalopoulou, S., Garipidou, V., and Goulis, D.G. (2014). Bone mineral density in men and children with haemophilia A and B: a systematic review and meta-analysis. Osteoporosis International *25*, 2399–2407.

Pasi, K.J., Rangarajan, S., Georgiev, P., Mant, T., Creagh, M.D., Lissitchkov, T., Bevan, D., Austin, S., Hay, C.R., Hegemann, I., et al. (2017). Targeting of Antithrombin in Hemophilia A or B with RNAi Therapy. New England Journal of Medicine *377*, 819–828.

Pasi, K.J., Rangarajan, S., Mitchell, N., Lester, W., Symington, E., Madan, B., Laffan, M., Russell, C.B., Li, M., Pierce, G.F., et al. (2020). Multiyear Follow-up of AAV5-hFVIII-SQ Gene Therapy for Hemophilia A. New England Journal of Medicine *382*, 29–40.

Payne, A.B. The CDC Hemophilia A Mutation Project (CHAMP) F8 Mutation List:.... ISTH Academy. Payne A. Jul 11 2020; 295642.

Dela Paz, N.G., and D'Amore, P.A. (2009). Arterial versus venous endothelial cells. Cell and Tissue Research *335*, 5–16.

Pipe, S., Becka, M., Detering, E., Vanevski, K., and Lissitchkov, T. (2019a). First-in-human Gene Therapy Study of AAVhu37 Capsid Vector Technology in Severe Hemophilia A. Blood *134*, 4630–4630.

Pipe, S.W., Shima, M., Lehle, M., Shapiro, A., Chebon, S., Fukutake, K., Key, N.S., Portron, A., Schmitt, C., Podolak-Dawidziak, M., et al. (2019b). Efficacy, safety, and pharmacokinetics of emicizumab prophylaxis given every 4 weeks in people with haemophilia A (HAVEN 4): a multicentre, open-label, non-randomised phase 3 study. The Lancet Haematology *6*, e295–e305.

Pittman, D., Alderman, E., Tomkinson, K., Wang, J., Giles, A., and Kaufman, R. (1993). Biochemical, immunological, and in vivo functional characterization of B-domain-deleted factor VIII. Blood *81*, 2925–2935.

Rabinowitz, J., Chan, Y.K., and Samulski, R.J. (2019). Adeno-associated Virus (AAV) versus immune response. Viruses *11*.

Ran, G., Chen, X., Xie, Y., Zheng, Q., Xie, J., Yu, C., Pittman, N., Qi, S., Yu, F.X., Agbandje-McKenna, M., et al. (2020). Site-Directed Mutagenesis Improves the Transduction Efficiency of Capsid Library-Derived Recombinant AAV Vectors. Molecular Therapy - Methods and Clinical Development *17*, 545–555.

Rangarajan, S., Walsh, L., Lester, W., Perry, D., Madan, B., Laffan, M., Yu, H., Vettermann, C., Pierce, G.F., Wong, W.Y., et al. (2017). AAV5–Factor VIII Gene Transfer in Severe Hemophilia A. New England Journal of Medicine *377*, 2519–2530.

Rask-Madsen, C., and King, G.L. (2013). Vascular complications of diabetes: Mechanisms of injury and protective factors. Cell Metabolism *17*, 20–33.

Reding, M.T., Ng, H.J., Poulsen, L.H., Eyster, M.E., Pabinger, I., Shin, H.J., Walsch, R., Lederman, M., Wang, M., Hardtke, M., et al. (2017). Safety and efficacy of BAY 94-9027, a prolonged-half-life factor VIII. Journal of Thrombosis and Haemostasis *15*, 411–419.

Renna, N.F., De Las Heras, N., and Miatello, R.M. (2013). Pathophysiology of vascular remodeling in hypertension. International Journal of Hypertension *2013*.

Ribatti, D., Tamma, R., Ruggieri, S., Annese, T., and Crivellato, E. (2020). Surface markers: An identity card of endothelial cells. Microcirculation *27*, e12587.

Robinson, M.D., McCarthy, D.J., and Smyth, G.K. (2009). edgeR: A Bioconductor package for differential expression analysis of digital gene expression data. Bioinformatics *26*, 139–140.

Rohban, R., Reinisch, A., Etchart, N., Schallmoser, K., Hofmann, N.A., Szoke, K., Brinchmann, J.E., Rad, E.B., Rohde, E., and Strunk, D. (2013). Identification of an Effective Early Signaling Signature during Neo-Vasculogenesis In Vivo by Ex Vivo Proteomic Profiling. PLoS ONE *8*.

Roosendaal, G., and Lafeber, F.P.J.G. (2003). Blood-induced joint damage in hemophilia. Seminars in Thrombosis and Hemostasis *29*, 37–42.

Rosen, S., Tiefenbacher, S., Robinson, M., Huang, M., Srimani, J., Mackenzie, D., Christianson, T., John Pasi, K., Rangarajan, S., Symington, E., et al. (2020). Activity of transgene-produced B-domain–deleted factor VIII in human plasma following AAV5 gene therapy. Blood *136*, 2524–2534.

Rossetti, L.C., Radic, C.P., Abelleyro, M.M., Larripa, I.B., and de Brasi, C. (2011). Eighteen years of molecular genotyping the hemophilia inversion hotspot: From southern blot to inverse shifting-PCR. International Journal of Molecular Sciences *12*, 7271–7285.

Samuelson Bannow, B., Recht, M., Négrier, C., Hermans, C., Berntorp, E., Eichler, H., Mancuso, M.E., Klamroth, R., O'Hara, J., Santagostino, E., et al. (2019). Factor VIII: Long-established role in haemophilia A and emerging evidence beyond haemostasis. Blood Reviews *35*, 43–50.

Santagostino, E., Mancuso, M.E., Novembrino, C., Solimeno, L.P., Tripodi, A., and Peyvandi, F. (2019). Rescue factor VIII replacement to secure hemostasis in a patient with hemophilia A and inhibitors on emicizumab prophylaxis undergoing hip replacement. Haematologica *104*, e380–e382.

Saxena, K., Lalezari, S., Oldenburg, J., Tseneklidou-Stoeter, D., Beckmann, H., Yoon, M., and Maas Enriquez, M. (2016). Efficacy and safety of BAY 81-8973, a full-length recombinant factor VIII: results from the LEOPOLD I trial. Haemophilia *22*, 706–712.

Schuerwegh, A.J., Dombrecht, E.J., Stevens, W.J., Van Offel, J.F., Bridts, C.H., and De Clerck, L.S. (2003). Influence of pro-inflammatory (IL-1α, IL-6, TNF-α, IFN-γ) and anti-inflammatory (IL-4) cytokines on chondrocyte function. Osteoarthritis and Cartilage *11*, 681–687.

Sehgal, A., Barros, S., Ivanciu, L., Cooley, B., Qin, J., Racie, T., Hettinger, J., Carioto, M., Jiang, Y., Brodsky, J., et al. (2015). An RNAi therapeutic targeting antithrombin to rebalance the coagulation system and promote hemostasis in hemophilia. Nature Medicine *21*, 492–497.

Sen, D., Chapla, A., Walter, N., Daniel, V., Srivastava, A., and Jayandharan, G.R. (2013). Nuclear factor (NF)-κB and its associated pathways are major molecular regulators of blood-induced joint damage in a murine model of hemophilia. Journal of Thrombosis and Haemostasis *11*, 293–306.

Senapati, S., Mishra, S., Dhir, M., and Das, S. (2016). Intracerebellar haemorrage in a haemophilia child. Asian Journal of Neurosurgery *11*, 179.

Shahani, T., Covens, K., Lavend'homme, R., Jazouli, N., Sokal, E., Peerlinck, K., and Jacquemin, M. (2014). Human liver sinusoidal endothelial cells but not hepatocytes contain factor VIII. J Thromb Haemost *12*, 36–42.

Shahi, M., Peymani, A., and Sahmani, M. (2017). Regulation of bone metabolism. Reports of Biochemistry and Molecular Biology *5*, 73–82.

Shapiro, A.D., Mitchell, I.S., and Nasr, S. (2018). The future of bypassing agents for hemophilia with inhibitors in the era of novel agents. Journal of Thrombosis and Haemostasis *16*, 2362–2374.

Sheppard, D. (2002). Endothelial integrins and angiogenesis: not so simple anymore. Journal of Clinical Investigation *110*, 913–914.

Shi, Q., Wilcox, D.A., Fahs, S.A., Fang, J., Johnson, B.D., Du, L.M., Desai, D., and Montgomery, R.R. (2007). Lentivirus-mediated platelet-derived factor VIII gene therapy in murine haemophilia A. Journal of Thrombosis and Haemostasis *5*, 352–361.

Shi, Q., Mattson, J.G., Fahs, S.A., Geurts, A.M., Weiler, H., and Montgomery, R.R. (2020). The severe spontaneous bleeding phenotype in a novel hemophilia A rat model is rescued by platelet FVIII expression. Blood Advances *4*, 55–65.

Simioni, P., Cagnin, S., Sartorello, F., Sales, G., Pagani, L., Bulato, C., Gavasso, S., Nuzzo, F., Chemello, F., Radu, C.M., et al. (2021). Partial F8 gene duplication (factor VIII Padua) associated with high factor VIII levels and familial thrombophilia . Blood *137*, 2383–2393.

Simpson, M.L., and Valentino, L.A. (2012). Management of joint bleeding in hemophilia. Expert Review of Hematology *5*, 459–468.

Solovey, A., Lin, Y., Browne, P., Choong, S., Wayner, E., and Hebbel, R.P. (1997). Circulating Activated Endothelial Cells in Sickle Cell Anemia. New England Journal of Medicine *337*, 1584–1590.

Srivastava, A., Santagostino, E., Dougall, A., Kitchen, S., Sutherland, M., Pipe, S.W., Carcao, M., Mahlangu, J., Ragni, M. V., Windyga, J., et al. (2020). WFH Guidelines for the Management of Hemophilia, 3rd edition. Haemophilia : The Official Journal of the World Federation of Hemophilia *26*, 1–158.

Stephensen, D., Tait, R., Brodie, N., Collins, P., Cheal, R., Keeling, D., Melton, K., Dolan, G., Haye, H., Hayman, E., et al. (2009). Changing patterns of bleeding in patients with severe haemophilia A. Haemophilia *15*, 1210–1214.

Stieltjes, N., Calvez, T., Demiguel, V., Torchet, M.F., Briquel, M.E., Fressinaud, E., Claeyssens, S., Coatmelec, B., Chambost, H., Peynet, J., et al. (2005). Intracranial haemorrhages in French haemophilia patients (1991-2001): Clinical presentation, management and prognosis factors for death. Haemophilia *11*, 452–458.

Sung, J.J., Park, S., Choi, S.H., Kim, J., Cho, M.S., and Kim, D.W. (2020). Generation of a gene edited hemophilia A patient-derived iPSC cell line, YCMi001-B-1, by targeted insertion of coagulation factor FVIII using CRISPR/Cas9. Stem Cell Research *48*.

Takahashi, K., Yamanaka, S., Randle, D.H., Kamijo, T., Cleveland, J.L., Sherr, C.J., Roussel, M.F., Kraft, A.S., Yang, V.W., Farese, R.V., et al. (2006). Induction of Pluripotent Stem Cells from Mouse Embryonic and Adult Fibroblast Cultures by Defined Factors. Cell *126*, 663–676.

Tatsumi, K., Sugimoto, M., Lillicrap, D., Shima, M., Ohashi, K., Okano, T., and Matsui, H. (2013). A novel cell-sheet technology that achieves durable factor VIII delivery in a mouse model of hemophilia a. PLoS ONE *8*.

Thompson, A.R. (2003). Structure and function of the factor VIII gene and protein. Seminars in Thrombosis and Hemostasis *29*, 11–22.

Trapnell, C., Williams, B.A., Pertea, G., Mortazavi, A., Kwan, G., Van Baren, M.J., Salzberg, S.L., Wold, B.J., and Pachter, L. (2010). Transcript assembly and quantification by RNA-Seq reveals unannotated transcripts and isoform switching during cell differentiation. Nature Biotechnology *28*, 511–515.

Valentino, L.A. (2010). Blood-induced joint disease: The pathophysiology of hemophilic arthropathy. Journal of Thrombosis and Haemostasis *8*, 1895–1902.

VandenDriessche, T., Vanslembrouck, V., Goovaerts, I., Zwinnen, H., Vanderhaeghen, M.L., Collen, D., and Chuah, M.K. (1999). Long-term expression of human coagulation factor VIII and correction of hemophilia A after in vivo retroviral gene transfer in factor VIII-deficient mice. Proceedings of the National Academy of Sciences of the United States of America *96*, 10379–10384.

Vehar, G.A., Keyt, B., Eaton, D., Rodriguez, H., O'brien, D.P., Rotblat, F., Oppermann, H., Keck, R., Wood, W.I., Harkins, R.N., et al. (1984). Structure of human factor VIII. Nature *312*, 337–342.

Verma, I.M., and Weitzman, M.D. (2005). Gene therapy: Twenty-first century medicine. Annual Review of Biochemistry *74*, 711–738.

Viazzi, F., Leoncini, G., Ratto, E., Parodi, A., Falqui, V., Conti, N., Tomolillo, C., Ravera, G., Deferrari, G., and Pontremoli, R. (2008). Vascular permeability, blood pressure, and organ damage in primary hypertension. Hypertension Research *31*, 873–879.

Vigna, E., Amendola, M., Benedicenti, F., Simmons, A.D., Follenzi, A., and Naldini, L. (2005). Efficient Tet-dependent expression of human factor IX in vivo by a new self-regulating lentiviral vector. Molecular Therapy *11*, 763–775.

Walia, A., Yang, J.F., Huang, Y.H., Rosenblatt, M.I., Chang, J.H., and Azar, D.T. (2015). Endostatin's emerging roles in angiogenesis, lymphangiogenesis, disease, and clinical applications. Biochimica et Biophysica Acta - General Subjects *1850*, 2422–2438.

Wang, H., and Bai, X. (2021). Mechanisms of Bone Remodeling Disorder in Hemophilia. Seminars in Thrombosis and Hemostasis *47*, 43–52.

Wang, X., Shin, S.C., Chiang, A.F.J., Khan, I., Pan, D., Rawlings, D.J., and Miao, C.H. (2015). Intraosseous delivery of lentiviral vectors targeting factor VIII expression in platelets corrects murine hemophilia A. Molecular Therapy *23*, 617–626.

White, G.C., Rosendaal, F., Aledort, L.M., Lusher, J.M., Rothschild, C., Ingerslev, J., and Factor VIII and Factor IX Subcommittee (2001). Definitions in hemophilia. Recommendation of the scientific subcommittee on factor VIII and factor IX of the scientific and standardization committee of the International Society on Thrombosis and Haemostasis. Thrombosis and Haemostasis *85*, 560.

Wight, T.N., Kang, I., Evanko, S.P., Harten, I.A., Chang, M.Y., Pearce, O.M.T., Allen, C.E., and Frevert, C.W. (2020). Versican—A Critical Extracellular Matrix Regulator of Immunity and Inflammation. Frontiers in Immunology *11*.

Wion, K.L., Kelly, D., Summerfield, J.A., Tuddenham, E.G.D., and Lawn, R.M. (1985). Distribution of factor VIII MRNA and antigen in human liver and other tissues. Nature *317*, 726–729.

Wise, R.J., Dorner, A.J., Krane, M., Pittman, D.D., and Kaufman, R.J. (1991). The role of von Willebrand factor multimers and propeptide cleavage in binding and stabilization of factor VIII. Journal of Biological Chemistry *266*, 21948–21955.

Xu, J., and Shi, G.P. (2014). Vascular wall extracellular matrix proteins and vascular diseases. Biochimica et Biophysica Acta - Molecular Basis of Disease *1842*, 2106–2119.

Xu, D., Alipio, Z., Fink, L.M., Adcock, D.M., Yang, J., Ward, D.C., and Ma, Y. (2009). Phenotypic correction of murine hemophilia A using an iPS cell-based therapy. Proceedings of the National Academy of Sciences of the United States of America *106*, 808–813.

Xu, L., Nichols, T.C., Sarkar, R., McCorquodale, S., Bellinger, D.A., and Ponder, K.P. (2005). Absence of a desmopressin response after therapeutic expression of factor VIII in hemophilia A dogs with liver-directed neonatal gene therapy. Proceedings of the National Academy of Sciences *102*, 6080–6085.

Yang, W., and Yee, A.J. (2013). Versican V2 isoform enhances angiogenesis by regulating endothelial cell activities and fibronectin expression. FEBS Letters *587*, 185–192.

Yoder, M.C., Mead, L.E., Prater, D., Krier, T.R., Mroueh, K.N., Li, F., Krasich, R., Temm, C.J., Prchal, J.T., and Ingram, D.A. (2007). Redefining endothelial progenitor cells via clonal analysis and hematopoietic stem/progenitor cell principals. In Blood, (Blood), pp. 1801–1809.

Zanolini, D., Merlin, S., Feola, M., Ranaldo, G., Amoruso, A., Gaidano, G., Zaffaroni, M., Ferrero, A., Brunelleschi, S., Valente, G., et al. (2015). Extrahepatic sources of factor VIII potentially contribute to the coagulation cascade correcting the bleeding phenotype of mice with hemophilia A. Haematologica *100*, 881–892.

Zanon, E., and Pasca, S. (2019). Intracranial haemorrhage in children and adults with haemophilia A and B: A literature review of the last 20 years. Blood Transfusion *17*, 378–384.

Zanon, E., Iorio, A., Rocino, A., Artoni, A., Santoro, R., Tagliaferri, A., Coppola, A., Castaman, G., Mannucci, P.M., Barillari, G., et al. (2012). Intracranial haemorrhage in the Italian population of haemophilia patients with and without inhibitors. Haemophilia *18*, 39–45.

Zhang, S., Dutton, J.R., Su, L., Zhang, J., and Ye, L. (2014). The influence of a spatiotemporal 3D environment on endothelial cell differentiation of human induced pluripotent stem cells. Biomaterials *35*, 3786–3793.

Zhao, Y., Hu, Y., Jin, J., Zhao, X., Wang, X., Wu, R., Wu, D., Yang, R., Yang, F., Hu, Q., et al. (2021). Phase 4 Safety and Efficacy Study of Antihemophilic Factor (Recombinant) in Previously Treated Chinese Patients With Severe/Moderately Severe Hemophilia A. Clinical and Applied Thrombosis/Hemostasis *27*.

Zimowski, K.L., Batsuli, G.M., Bryant, P., McDaniel, J., Tickle, K., Meeks, S.L., and Sidonio, R.F. (2019). Severe Bleeding Events in Hemophilia A Patients Receiving Emicizumab Prophylaxis. Blood *134*, 1126–1126.

Appendix

[Manuscript under revision]

Efficient and safe correction of hemophilia A by lentiviral vector-transduced BOECs in an implantable device

Cristina Olgasi[1*], Chiara Borsotti[1*], Simone Merlin[1*], Thorsten Bergmann[2], Patrick Bittorf[2], Adeolu Badi Adewoye[3], Nicholas Wragg[4], Kelcey Patterson[5], Andrea Calabria[6], Fabrizio Benedicenti[6], Alessia Cucci[1], Alessandra Borchiellini[7], Berardino Pollio[8], Eugenio Montini[6], Delfina M. Mazzuca[5], Martin Zierau[9], Alexandra Stolzing[10, 11], Philip. M. Toleikis[5], Joris Braspenning[2], Antonia Follenzi[1§]

[1]Department of Health Sciences, University of Piemonte Orientale, Novara. Italy

[2]Department of Tissue Engineering and Regenerative Medicine, University Hospital Würzburg, Würzburg, Germany

[3]Institute of Inflammation and Ageing, College of Medical and Dental Sciences, University of Birmingham, Birmingham, United Kingdom

[4]Guy Hilton Research Centre, School of Pharmacy and Bioengineering, Keele University, Staffordshire, Stoke-on-Trent, UK

[5]Sernova Corp., London, Ontario, Canada

[6]TIGET-HSR, Milan, Italy

[7] Haematology Unit Regional Center for Hemorrhagic and Thrombotic Diseases, City of Health and Science University Hospital of Molinette Turin Italy.

[8] Immune-Haematology and Transfusion Medicine, Regina Margherita Children Hospital, City of Health and Science University Hospital of Molinette, Turin, Italy.

[9]IMS Integrierte Management Systeme e. K., Heppenheim, Germany

[10]Centre for Biological Engineering, School of Mechanical, Electrical and Manufacturing Engineering, Loughborough University, UK

[11]SENS Research Foundation, Mountain View, CA, USA

*Co-first Authors

Short title: **BOECs within a medical device to cure hemophilia A**

Abstract

Hemophilia A (HA) is a rare bleeding disorder caused by deficiency/dysfunction of the FVIII protein. As current therapies based on frequent FVIII infusions are not a definitive cure, long-term expression of FVIII in endothelial cells through lentiviral vector (LV)-mediated gene transfer holds the promise of a one-time treatment. Thus, here we sought to determine whether LV-corrected blood outgrowth endothelial cells (BOECs) implanted through a prevascularized medical device (Cell Pouch™) would rescue the bleeding phenotype of HA mice. To this end, BOECs from HA patients and healthy donors were isolated, expanded and transduced with an LV carrying FVIII driven by an endothelial-specific promoter employing GMP-like procedures. FVIII-corrected HA-BOECs were either directly transplanted into the peritoneal cavity or injected into a Cell Pouch™ implanted subcutaneously in NSG-HA mice. In both cases, FVIII secretion was detected and sufficient to improve the mouse bleeding phenotype. Indeed, FVIII-corrected HA-BOECs reached a long-term engraftment, and their genomic integration profile did not show enrichment for oncogenes, confirming the process safety. Overall, this is the first pre-clinical study showing the safety and feasibility of transplantation of GMP-like produced LV-corrected BOECs within an implantable device for the long-term treatment of HA.

Introduction

Hemophilia A (HA) is an X-linked disorder caused by mutations in the *F8* gene. [1,2] These mutations result in deficiency or reduced activity of the coagulation factor VIII (FVIII), leading to a lifelong bleeding tendency, whose clinical severity is proportional to FVIII reduction.[1] Although the current standard of care is to infuse intravenously HA patients with clotting factor concentrates, the short half-life of FVIII requires frequent and multiple infusions, with a negative impact on the patient's quality of life (QoL). The management of HA is further complicated by the development of anti-FVIII antibodies (i.e., inhibitors), which occurs in 20-40% of patients with the severe form of the disease.[3] This has led researchers to explore innovative cell and gene therapy strategies that may ensure continuous endogenous FVIII expression with only a one-time treatment. Another good reason for choosing gene therapy over traditional approaches is that HA is a monogenic disease i.e., entirely ascribable to the lack of one protein, FVIII and that a small increase in FVIII plasma levels is enough to ameliorate the bleeding phenotype of HA patients.

Given the growing number of cell and gene therapy approaches being developed, it is becoming increasingly important to identify the most suitable cell target. Even though FVIII mRNA is expressed in different human and mouse organs, such as liver, spleen, lymph nodes, kidney,[4–7] and in hematopoietic cells,[8,9] transplantation studies in hemophilic animal models have shown FVIII expression to be mainly localized in liver sinusoidal endothelial cells (LSECs),[10–12] making these cells attractive targets for HA gene therapy. This is also supported by the fact that endothelial cells (ECs) secrete FVIII and can act as tolerogenic cells.[13,14]

Over the years, several gene therapy approaches for HA have been attempted using adeno-associated virus (AAV) vectors to induce FVIII expression in the desired cell type. Despite

the encouraging preliminary results obtained in few ongoing clinical trials testing the efficacy of AAV-mediated hepatocyte-targeted FVIII expression in HA patients,[15–17] some medical issues still need to be addressed, such as the use of these vectors in patients with pre-existing immunity to AAV or with FVIII inhibitors. As AAV vectors do not actively integrate into the host cell genome, they are lost upon cell division during liver growth or in case of liver disease, thus potentially limiting their use in pediatric patients and questioning their life-long maintenance. Therefore, lentiviral vectors (LVs) could represent a viable approach able to overcome some AAV limitations. Moreover, several studies have demonstrated, by the use of endothelial specific promoters, specific expression of human FVIII in LSECs.[10–12,18] Recently, we have shown that induced pluripotent stem cells (iPSCs) derived from $CD34^+$ HA cells can be differentiated into ECs and genetically corrected by LV to express the FVIII transgene, deleted of the B domain (BDD), driven by the endothelial specific vascular endothelial cadherin (VEC) promoter. After transplanting these cells into the liver of monocrotaline-conditioned NOD-*scid* $IL2Rg^{null}$ HA (NSG-HA) mice, we were able to correct the bleeding phenotype of these mice and maintain a stable FVIII activity over time.[19] Moreover, BDD-FVIII-transduced ECs encapsulated in microcarrier beads have been shown to survive for a prolonged time in the peritoneal cavity of NSG HA mice secreting therapeutic level of FVIII.[19]

Several studies have focused on defining different cell sources and matrices to transplant FVIII-expressing ECs.[20–22] A readily available EC source is represented by patient-derived blood outgrowth endothelial cells (BOECs).[23] BOECs are isolated from adult peripheral blood[24] and can be fully differentiated into mature ECs. They promote neovascularization *in vivo* when transplanted into immunodeficient mice[25] or when cultured on three-dimensional biodegradable vascular scaffolds.[26–28] In addition, they can be considered a valuable source of cells to understand EC biology and model disease and can be used in regenerative medicine due to their ability to promote neovascularization, thus representing an optimal candidate for HA cell and gene therapy. Indeed, BOECs transplanted in NSG-HA mice after gene modification for FVIII expression were able to partially rescue the hemorrhagic phenotype of these mice.[23,29] Moreover, autologous transplantation of FVIII-expressing BOEC cell-sheet allowed long-term phenotypic correction and survival of transplanted cells.[22] Noteworthy, BOECs can promote neovascularization *in vivo* in combination with synthetic or natural materials.[25]

A combination of LV-corrected BOECs with a medical device is classified by the European Union as a combined gene therapy medicinal product (GTMP).[30] The mandatory non-clinical study scheme prior to the first administration of a cell-based GTMP to human subjects includes the comprehensive characterization of the transduced cells and the evaluation of the medical device contribution.[31] Moreover, the proof-of-concept pharmacodynamics along with the molecular mechanism of action must be identified in preclinical models *in vivo* and/or *in vitro*. These studies are deemed essential to determine the GMP cell dose to be used in clinical trials.[32]

Here, we show extensive characterization of LV-transduced BOECs isolated from healthy donors or HA patients for FVIII long-term production *in vivo*. These cells were transplanted in a small scalable, implantable, and prevascularized medical device, namely Cell Pouch™ (Sernova Corp.), previously developed for diabetes treatment[33].

Our findings, showing that Cell Pouch-transplanted LV-corrected HA-BOECs are capable of correcting the bleeding phenotype of HA mice, open new avenues for the treatment of HA in humans.

Results

Characterization of BOECs isolated from HA patients or healthy subjects and LV-mediated FVIII gene transfer

Upon isolation and expansion in culture medium, both BOECs from healthy donors and HA patients showed the classical endothelial cobblestone-like morphology (Figure 1A). Of note, despite being all isolated from severe HA patients, HA BOECs gave rise to many colonies (Supplemental Table 4). For transgene expression, isolated cells were transduced with a lentiviral vector (LV) carrying the BDD form of FVIII driven by the vascular endothelial cadherin promoter (LV-VEC.hBDD-FVIII) or with an LV carrying the green fluorescent protein under the control of the same promoter (LV-VEC.GFP), both at an MOI of 20. FACS analysis showed 98±1% GFP^+ cells after transduction (Supplemental Figure 1), indicating excellent transduction efficiency. The number of integrated LV copies/cell was ~6 and ~3 for LV-VEC.GFP and LV-VEC.hBDD-FVIII-transduced cells, respectively (Supplemental Table 5). Thus, this protocol ensures a very high transduction efficiency while maintaining a safe number of integrated LV copies/cell.[34,35]

We next assessed the endothelial phenotype and functionality of transduced *vs* non-transduced healthy or HA BOECs. As shown in Figure 1B, all cells expressed the classical endothelial markers (e.g., *PECAM1, KDR, TEK, CDH5*, and V*WF*) as well as other genes specific to blood endothelial cells (BECs)[36,37] (Figure 1C). The endothelial phenotype of healthy and HA BOECs was further verified at the protein level (Figure 1D and E, respectively), while the hematopoietic phenotype was ruled out upon CD34 and CD45 staining, which resulted negative (Figure 1D and E).

The endothelial functionality of the transduced cells was confirmed by their ability to form tubule networks upon Matrigel cell culture (Figure 1F). FVIII mRNA expression was measured in transduced BOECs by RT-PCR (Figure 1G), while FVIII protein expression levels were detected by flow cytometry (Figure H and I for healthy and HA BOECs, respectively) and immunofluorescence (IF) (Figure 1J). When cell supernatants were subjected to activated partial thromboplastin time (aPTT) assay, we noticed a consistent shortening in LV-VEC.hBDD-FVIII-transduced BOECs (69± 3.5 sec for transduced healthy BOECs, 66± 4 sec for transduced HA BOECs) compared to non-transduced cells (80± 2.8 sec for healthy BOECs, 84± 2.8 sec for HA BOECs) (Supplemental Figure 2A), in good agreement with the amount of secreted FVIII (35.9± 2.3 ng/ml for LV-VEC.hBDD-FVIII healthy BOECs, 4.5± 1.3 ng/ml for non-transduced healthy BOECs; 54± 7.5 for LV-VEC.hBDD-FVIII HA BOECs*,* 0.15± 2.5 for non-transduced HA BOECs) (Supplemental Figure 2B).

To further confirm the safety of LV transduction, healthy BOECs were transduced with different MOIs (MOI 10, 20, 50, 100), and HIV-1 p24 expression on cell supernatant was assessed. As shown in Supplemental Figure 2C, all LV-transduced BOEC supernatants were negative for HIV-1 p24 at any of the MOIs tested 10 days after transduction, demonstrating the safety of our protocol. HIV-1 p24 on supernatant of HA BOECs

transduced with an MOI of 20 showed comparable results in terms of safety (Supplemental Figure 2C).

Secretion of the FVIII gene product by LV-transduced HA or healthy BOECs in NSG-HA mice

Since healthy and HA BOECs were both able to secrete FVIII *in vitro*, we evaluated their ability to survive and secrete FVIII in NSG-HA mice following intraperitoneal (i.p.) injection in association with Cytodex® 3 microcarrier beads. Following injection, FVIII-transduced GFP^+ healthy BOECs were able to partially restore FVIII activity, which reached a peak of approximately 10% at 4 weeks post injection (pi) and persisted above 5% for up to 10 weeks pi (Figure 2A). As expected, LV-VEC.GFP BOEC controls showed only basal FVIII secretion, which only lasted for 4 weeks. Importantly, mice receiving FVIII-transduced HA BOECs revealed sustained therapeutic FVIII activity (up to 10%) for up to 13 weeks pi, which persisted at a level < 5% throughout the 18 following weeks (Figure 2A). Blood loss assays, run between 7 and 10 weeks pi of FVIII-transduced GFP^+ HA BOECs, demonstrated partial hemostasis restoration (Figure 2B) accompanied by detectable amounts of plasmatic FVIII antigen (12.4±3.9 ng/ml) (Figure 2C). IF staining performed on the recovered beads 13 weeks pi showed GFP^+ cells associated with the beads. Lastly, the endothelial phenotype of the transplanted cells was confirmed by GFP and human CD31 co-staining (Figure 2D).

Large scale expansion of FVIII-transduced cells

With the aim to translate this approach into the clinic, we developed a protocol that would allow us to obtain a large amount of transduced HA BOECs for our *in vivo* experiments. LV-VEC.hBDD-FVIII-transduced HA BOECs from four patients were large-scale expanded to reach 10^8 cells, frozen and sent to the partners in accordance with GMP-like procedures. Upon arrival, cells were re-cultured by simulating a centralized cell production process with long-term cryopreservation. After large-scale expansion and cryopreservation, upon thawing and reseeding, all cells showed normal cobblestone-like morphology (Figure 3A). Even though their size was slightly enlarged, no significant changes in their doubling time, cell density, and length of time required for expansion were noticed (Figure 3B). In addition to maintaining expression of the classical endothelial markers (CD31, KDR, Tie-2, VEC), expanded BOECs became $CD34^+$, a transmembrane phosphoglycoprotein involved in cell adhesion,[38] while they retained the classical $CD45^-$ phenotype (Figure 3C).
Functionally, FVIII-transduced cells preserved their tubulogenesis activity (Figure 3D) and led to partial restoration of FVIII activity once transferred into NSG-HA mice (Figure 3E), similar to the kinetics of non-expanded BOECs. Thus, LV-VEC.hBDD-FVIII HA BOECs maintain their ability to secrete FVIII at therapeutic levels even after large-scale expansion.

Tissue matrix development and safety of LV-VEC.hBDD-FVIII-transduced BOECs within a Cell Pouch™ implanted in NSG-HA mice

The Cell Pouch™ is a medical implantation device specifically designed to enable the development of a vascularized tissue matrix environment that ensures long-term survival and function of transplanted therapeutic cells. Thus, we first evaluated safety and survival

of transduced HA BOECs within the Cell Pouch™ implanted in NSG-HA mice. For this purpose, 4-week implanted Cell Pouches™ were transplanted with one of three doses (2×, 5× or 10×10^6) of LV-VEC.hBDD-FVIII HA BOECs isolated from two separate HA donors. The Cell Pouches™ transplanted with BOECs were explanted at 4, 8, or 12 weeks, and a gross pathological assessment was performed. HA BOECs were safe across doses and time points with no visible tumors observed (n = 60 total; HA1 n = 37; HA2, n = 23) (data not shown).

Overall, the tissue matrix developed within the Cell Pouch™ internal chamber and transplant area was viable among all groups according to time, dose, and cell lot, with no apparent signs of inflammation, hemorrhage, fibrosis, or necrosis (Figure 4A and Supplemental Table 6). The center of the transplanted chamber area showed mild to moderate collagen deposition without any difference due to donor lot, time, or dose. Within the area of pre-vascularization, there was comparatively an increase in established collagen, indicating that the Cell Pouch™ promoted, over time, the development of a natural scaffold to provide strength and structure to the environment irrespective of the transplant. Regarding tissue vascularization, there was moderate neovascularization of the central, transplanted tissue of the Cell Pouch™ that was present in both donor lots, as well as the controls, along with evidence of established vessel growth, indicating that the tissue development within this area included new blood vessel formation (Figure 4B). Established vessels within the central, transplanted zone appeared to be more prominent and donor-dependent at the latest time points (Figure 4A).

Transduced HA BOECs improve the bleeding phenotype and cell survival in mice after transplantation into the vascularized Cell Pouch™

The therapeutic efficacy of LV-VEC.hBDD-FVIII HA BOECs transplanted into the Cell Pouch™ was evaluated by performing a tail bleeding assay on NSG-HA mice four months after the cell transfer. Remarkably, we noticed a significantly improved presence of clotting as judged by a reduction in blood volume recovered in animals transplanted with 20×10^6 LV-VEC.hBDD-FVIII HA BOECs compared to non-transplanted mice (Figure 5A). Notably, this was not significantly different when compared to NSG mice, confirming that correction of the missing coagulation factor had been achieved in the transplanted HA mice. Long-term cell survival (4 months post-transplant) was confirmed by co-staining with anti-HLA-ABC and anti-vWF antibodies as well as by the formation of blood vessels within the transplanted area (Figure 5B and Supplemental Table 7).

Overall, these data indicate that corrected HA BOECs are able to engraft and persist for prolonged periods of time within the tissue matrix supported by the Cell Pouch™ and secret enough FVIII to correct the hemophilia phenotype of the implanted NSG-HA mice.

Complex composition of BOEC clonal populations

Sonication Linker Mediated PCR was performed on 53 samples of genomic DNA extracted from LV-transduced BOECs derived from 3 healthy donors (D45, D2, and D3) and 3 HA patients (pHA1, pA, and pC), collected at different expansion passages or procedure time points. By grouping the samples according to the BOEC source (i.e., healthy donors or HA

patients) and the type of vector used (i.e., LV-VEC.hBDD-FVIII or LV-VEC.GFP), we obtained 4 main groups: HA.FVIII; HA.GFP; Healthy.FVIII; Healthy.GFP. Overall, we retrieved 142,349 integration sites (IS) (HA.FVIII: 28,069; HA.GFP: 106,554; Healthy.FVIII: 5,864; Healthy.GFP: 1,862.) (Supplemental Table 8). We compared the distribution of IS of the 4 groups along the whole human genome and with respect to gene transcription start site (TSS). The profile of LV integrations was similar for all the groups and confirmed the marked tendency of the LV to integrate within gene bodies, without bias for promoter regions (Figure 6A-B), in line with previously published results.[39–42] Following enrichment analysis of genomic position and gene annotations, none of the ontological gene classes showed cancer or tumor suppressor gene enrichment (Supplemental Figure 3).
Common Insertion Site (CIS) analysis showed few highly targeted genes in all datasets (e.g., *NPLOC4, PACS1*, and *MROH1*) (Supplemental Figure 4). The quantification of IS Abundance showed only a few clones with abundance > 10% in LV-VEC.hBDD-FVIII-transduced BOECs from pA and pHA1 (Figure 7). Only 2 IS were retrieved from D45 cells transduced at an MOI of 30, thus resulting in both to be 50% abundant. One clone with an IS in the GNL3 gene, which may interact with p53 and may be involved in tumorigenesis, and with abundance > 25% was also observed in pHA1 BOEC, but only at a single time point (P11-UK). To address the clonality of transduced BOECs, we analyzed the diversity of the clonal population through Shannon diversity index. The highest Shannon diversity index, between 9 and 11, was observed in BOECs from pHA1 and pA, transduced with the VEC.GFP vector. All the other BOECs showed a Shannon diversity index between 4 and 8, which remained constant throughout the various cell passages. A lower diversity index directly correlated with a lower number of IS, in particular for the HA Beads and Cell Pouch™ samples at different time points (Figure 8A). To better understand if, especially in the Cell Pouch™ samples, the clonal diversity was reduced, we compared the H Index between samples grouped by type (Expansion, HA Beads, Cell Pouch™ and LV used (VEC-FVIII, VEC-GFP) (Figure 8B). IS analysis revealed a high level polyclonality of LV-transduced BOECs, with no significant difference between the FVIII- and GFP-transduced samples. The clonal composition heterogeneity of FVIII-transduced samples remained constant over time *in vitro* and *in vivo*. Finally, Cell Pouch™ samples had a significant lower H index when compared to BOECs in expansion.

Discussion

Although the current therapy for HA involves the administration of plasma-derived or recombinant FVIII, there is to date no definitive cure for this inherited bleeding disorder. While several ongoing phase 1-3 clinical trials assessing the feasibility and safety of AAV-mediated hepatocyte-directed HA gene therapy have been able to achieve therapeutic FVIII plasma levels,[43–46] further experiments are in progress to assess the long-term stability of transgene expression. In this regard, the fact that AAV vectors do not actively integrate into the host cell genome and, thus, can be lost upon cell division during liver growth or liver disease questions their life-long maintenance besides limiting their potential use in pediatric patients.

A promising alternative approach is represented by a combination of cell and gene therapy, which would however require the identification of a suitable cell type able to effectively secrete FVIII while meeting all the necessary conditions for successful cell transplantation. In this regard, it is widely acknowledged that the liver is the main organ producing FVIII, where LSECs appear to be the main source of FVIII[47–49] and can play a tolerogenic role. In addition, because of the important role of the interaction between FVIII and vWF in the stability and activity of FVIII, LSECs may represent the most suitable target for cell and gene therapy-based strategies aimed to correct the HA phenotype.[50] Unfortunately**,** LSEC are not easy to obtain and maintain *in vitro*, therefore, in this study we explored the feasibility of using gene-corrected autologous BOECs, more manageable and previously shown to be able to secrete FVIII *in vivo*.[51] Here we show that BOECs isolated from both healthy and HA donors can be efficiently cultured, transduced, expanded, and used to correct the bleeding phenotype of HA mice. In this regard, it is important to point out that the large number of corrected cells we obtained allowed us to reach more quickly FVIII therapeutic concentrations, thus reducing the risk of cell senescence.

The current protocols for BOEC isolation are based on the culture of mononuclear cells (MNCs) from peripheral or umbilical cord blood on collagen-coated cell culture vessels in endothelial specific medium.[52] The fact that MNCs can be isolated directly through density gradient centrifugation of blood makes these cells a safe cell source for hemophilic patients. Normally, BOECs colonies arise after 2-4 weeks of culture, and the colonies are very rare since their number in the normal peripheral blood is quite low.[52] However, here we show that, under GMP-compliant conditions and using a chemically defined medium, it is possible to isolate BOECs from both healthy donors and HA patients with high efficiency and rapidly grow them to the desired amount to prevent the risk of cellular senescence once transplanted in mice.

In addition to being more easily obtainable, BOECs are fully differentiated ECs with a mature endothelial phenotype. Indeed, these cells originate from bone marrow-derived progenitors circulating in the blood or residing in the endothelium, which can be differentiated into BOECs *in vitro*.[53] Thus, the observation that the expanded pools of BOECs from healthy donors or HA patients retained the expression of endothelial markers and were able to form vessels indicates that our GMP-compliant conditions did not alter the endothelial phenotype and function of these cells, as previously shown.[53]

Another important aspect of this study is that we efficiently transduced BOECs with an LV carrying a functional BDD form of FVIII driven by the endothelial-specific promoter VEC. The efficiency and tissue specificity of FVIII transcription under the control of this promoter has been previously demonstrated in gene therapy approaches showing the restriction of FVIII expression in the desired cell type[54] and in cell therapy by secretion of FVIII after genetic correction in target cells.[19] Here, we show that LV-corrected HA BOECs transplanted in association with Cytodex® 3 microcarrier beads into the peritoneum of NSG-HA mice rescues the hemophilic phenotype of these animals for up to 18 weeks, achieving 9% FVIII activity.

Importantly, we reached therapeutic levels of secreted FVIII through LV-VEC.hBDD-FVIII HA BOECs injection into a prevascularized Cell Pouch™ device transplanted into a preclinical murine model of severe HA. Notably, the correction of the bleeding phenotype by

using LV-VEC.hBDD-FVIII HA BOECs injected into the peritoneum lasted up to 13 weeks and then slowly decreased. After 18 weeks FVIII activity was almost absent probably due to the death of BOECs.

Despite the encouraging results presented in this proof-of-concept study in a pre-clinical setting, there still remain several important issues that need to be addressed before our approach can be brought into the clinic. For instance, it will be imperative to characterize the cells within the Cell Pouch™ in terms of cell markers, longevity, and proliferation/senescence status. It will also be important to assess if we can increase the expression levels of FVIII using different EC-specific promoters, and if that would translate into augmented FVIII secretion and functionality *ex-vivo*.

Overall, our findings indicate that cell transfer into a medical device is a suitable solution for cell therapy as it confers a more physiological and protected environment where cells can proliferate at an excellent rate and escape from the immune response of the transplanted organism, all the while allowing nutrient exchange and therapeutic protein secretion. Congruently, the safety and efficacy of the Cell Pouch™ for the transplantation of mouse pancreatic islets has been previously shown to provide insulin independence in diabetic animals in preclinical studies of type 1 diabetes mellitus.[33,55] Furthermore, a phase I/II clinical trial is ongoing for the treatment of T1DM patients whose result may support the potential application of this device to other diseases for cell therapy approaches, such as HA.[56]

The Cell Pouch™ is a biocompatible, safe, implantable device that forms an internal vascularized tissue matrix supporting the transplanted cells. When we analyzed the Cell Pouch™ injected with LV-VEC.hBDD-FVIII HA BOECs after 4 weeks from the cell transfer, we observed the presence of a viable vascularized tissue matrix supporting the cells, with no evidence of fibrosis-associated consequences, including inflammation and necrosis, or hemophilia-related hemorrhage episodes. Moreover, the bleeding assay demonstrated that LV-VEC.FVIII HA BOECs transplanted into the vascularized subcutaneous Cell Pouch™ were able to correct the clotting function of HA mice. As previously shown in a canine model of HA, BOECs transduced with an LV carrying the canine FVIII and implanted subcutaneously allowed secretion of therapeutic levels of FVIII up to 15 weeks in Matrigel scaffolds and up to a year after omental implantation.[51] Moreover, BOECs were shown to form tubule network *in vitro* when plated on Matrigel[57] or on the surface of synthetic vascular scaffolds[58] and to promote neovascularization *in vivo* when transplanted into immunodeficient mice,[25] suggesting that they can be directly involved in vessel formation.

In this context, our data attest the feasibility of a method to correct autologous cells based on a combined cell and gene therapy approach together with the use of a scaffold (i.e., Cell Pouch™) able to guarantee long-term cell survival and, in case of need, a re-injection of new therapeutic cells. In addition to the phenotypical and functional characterization of the transduced HA BOECs, our results demonstrate the pharmacodynamics proof-of-concept in non-clinical models, which is mandatory before any GTMP can be used in human clinical trial.[31,32] Thus, our next step will be to evaluate the safety and toxicity of the GTMP *in vivo* based on these results so as to ensure patient safety and promote product translation. Examples of required non-clinical studies are the evaluation of the potential tumorigenicity and biodistribution of the transduced BOECs with or without the medical device.[59] Our molecular analysis of the integration sites in BOECs shows that no enrichment for

oncogenes or expansion of clones with IS in CIS or biases toward gene classes related to cancer genes occurred. IS analysis suggests a high level of polyclonality of LV-transduced BOECs, with no statistical difference between the FVIII- and GFP-transduced samples. The heterogeneity of the clonal composition of the FVIII-transduced samples remained constant over time (between different cell passages) also when cells were coupled to the micro carrier beads. Furthermore, Cell Pouch™ samples had a statistically significant lower H index when compared to BOECs in expansion.

The process of BOEC engraftment within the subcutaneous space is novel and complex and further studies will provide additional insight into the interactions between the developing tissue and the transplanted cells, elucidating the role played in the kinetics of blood vessel formation and FVIII secretion within the surrounding tissue.

In this study, we could not evaluate the immune response to the secreted factor because we used implanted cells in immunodeficient hemophilic mice. Thus, in future studies it will be interesting to evaluate antibody formation after transplantation of transduced BOECs encapsulated in the Cell Pouch™ into immunocompetent mice. Finally, while several gene therapy clinical trials for HA are ongoing, to our knowledge this is the first therapeutic approach that combines the GMP production of autologous human BOECs with the use of a safe *ex-vivo* approach based on an implantable prevascularized device.

In conclusion, our findings suggest that long-term encapsulation and survival of LV-corrected BOECs by means of an implantable device may prove effective in ameliorating the HA patients' QoL. The therapeutic dose of FVIII released by these autologous genetically modified cells would in fact prevent the need of frequent infusions of FVIII and significantly reduce the morbidity and the frequency of the bleeding episodes in hemophiliacs.

Material and Methods

BOEC isolation form HA patients and healthy donors

Blood sampling from 4 adult severe HA patients, named pHA1, pA, pC, and pD, was performed at the hospital A.O.U Città della Salute e della Scienza, Turin, Italy. The blood was shipped at room temperature to Università del Piemonte Orientale (UPO), Novara, Italy. Blood sampling from adult severe HA patients was approved by the Ethics Committee "Comitato Etico Interaziendale A.O.U. Maggiore della Carità" (Protocol 810/CE, Study n. CE 125/17). Human BOECs were isolated as previously described,[52] with the introduction of an earlier cell passaging step seven days after initial isolation of the peripheral blood mononuclear cells to reduce expansion time and increase the final cell yield.[60] Isolated cells were cultured on CELLCOAT Collagen Type 1-coated tissue culture flasks (Greiner Bio-One) using MCDB 131 medium (Gibco®, Life Technologies) containing proprietary supplements. Primary cells from adult healthy donors (named D45, D2, D3) were isolated at Tissue Engineering and Regenerative Medicine, Würzburg, Germany, under informed consent according to ethical approval granted by the Institutional Ethics Committee of the University Hospital Würzburg (approval number 182/10). Cell viability and count were assessed using the Countess II FL Automated Cell Counter (Thermo Fisher Scientific).

Healthy and HA BOEC transduction

Healthy and HA BOECs were plated at a 10^4 cells/cm^2 density and after 6-8 h transduced with a lentiviral vector carrying the BDD form of FVIII under the control of the VE-cadherin promoter (LV-VEC.hBDD-FVIII) or with a lentiviral vector carrying the green fluorescent protein under the control of the same VE-cadherin promoter (LV-VEC.GFP), using a multiplicity of infection (MOI) of 20. After 14-16 h incubation, fresh medium was added to the cells and, 72 h later, half of the cells were harvested for subsequent analysis, while the other half was further cultured.

GMP-compliant (GMP-like) preclinical development of LV-VEC.hBDD-FVIII-transduced BOECs

BOECs were isolated and expanded using a GMP-compliant standardized approach between all partners, including a quality control strategy. The standardized expansion scheme defined within the project is based on the generation of Master Cell Banks (MCB) and a Working Cell Bank (WCB), which ensures not only a controllable defined expansion for each patient's BOECs but also an in-process quality control at defined crucial steps. After isolation and expansion, cells were transduced with LV lots produced with a GMP-compliant method (TFF, see Supplemental Material section). All freezing steps were performed using a cryopreservation solution based on compounds that are GMP-compliant free of toxic compounds (e.g., DMSO). The Cell Pouch™ was manufactured under GMP-compliant conditions. All steps were designed and conducted according to European GMP-regulations to ensure that the product would fully comply with the quality requirements of the European authorities. The main objectives were to provide sets of design and manufacturing protocols based on current European GMP regulations and to prepare an Investigational Medicinal Product Dossier (IMPD) for an Investigational Medicinal Product (IMP), composed of

therapeutic cells and an implantable medical device (Cell Pouch™), a so-called combined Advanced Therapeutic Medicinal Product (combined ATMP).

Insertion site analysis

Integration sites (IS) were retrieved from genomic DNA of LV-transduced BOEC cells by Sonication Linker Mediated (SLiM)-PCR, an adaptation of a previously described method.[61,62] Genomic DNA (300 ng) was sheared using a Covaris E220 Ultrasonicator (Covaris Inc., Woburn, MA), generating fragments with a target size of 1000 bp. The fragmented DNA was split into 3 parts to generate technical replicates and, by using the NEBNext® Ultra™ DNA Library Prep Kit for Illumina® (New England Biolabs, Ipswich, MA), subjected to end repair, 3' adenylation, and ligation to linker cassettes (Integrated DNA Technologies, Skokie, IL) containing a 8-nucleotide sequence barcode used for sample identification and a 12 random nucleotide sequence necessary for clonal abundance quantification. Ligation products were then subjected to 35 cycles of exponential PCR using primers specific for the lentiviral vector LTR and the linker cassette. The amplification product was then re-amplified with additional 10 PCR cycles using primers specific for the linker cassette and the LTR, with the latter containing a second barcode in order to adopt a double barcode strategy for sample identification. The final PCR products were quantified using a KAPA Library Quantification Kit (Roche, Basil, Switzerland) and pooled in sequencing libraries with equimolar composition, avoiding repeated barcode pairs. Primers incorporate the adapter sequences required for the Illumina paired end sequencing technology (Illumina, San Diego, CA). Sequencing was performed on the Illumina MiSeq and HiSeq. Sample processing and metadata were tracked within our laboratory information management system.[63,64] Sequencing reads were processed by a dedicated bioinformatics pipeline (VISPA2).[64] Briefly, paired sequence reads were filtered for raw reads quality, then cleaned by vector genome, and the resulting cellular genomic sequence mapped on the human genome (version hg19), and the nearest RefSeq gene assigned to each unambiguously mapped IS. Clonal abundance for each IS was estimated using the R package sonicLength,[65] where the number of genomes with the same integration site is calculated by counting the number of fragments with different sizes generated by sonication belonging to each individual IS. Within each group, IS shared between different time points of the same transduction were counted once. The relative abundance of each clone was then calculated as the percentage of genomes with a specific integration site over the total genomes. Common Insertion Sites (CIS) were identified through the Grubbs test for outliers.[66] Enrichment analysis for ontological classes among the targeted genes by vector IS was performed by the Genomic Regions Enrichment of Annotations Tool (G.R.E.A.T.).[67]

Animal procedures

Animal studies were approved by the Animal Care and Use Committee at UPO (Italian Health Ministry Authorization n. 492/2016-PR, No. DBO64.5). NOD.Cg-Prkdc^{scid}Il2rg^{tm1Wjl}/SzJ (Jackson stock No 005557) mice with hemophilic phenotype (NSG-HA) were previously generated and maintained in our laboratory.[9] Eight-10 week old animals were used for cell transplantation studies. Cell Pouch™ implantations were conducted under additional ethical guidelines and approval from the Animal Care Committee

at the University of British Columbia (Vancouver, British Columbia, Canada) in accordance with the Canadian Council on Animal Care Guide to the Care and Use of Experimental Animals.

BOEC transplantation

For cell transplantation with beads, $5x10^6$ FVIII-transduced healthy or HA BOECs were mixed with Cytodex®3 microcarrier beads (GE Healthcare Life Sciences) and intraperitoneally delivered in NSG-HA mice as previously described.[68] For Cell Pouch™ implantation, female NSG and NSG-HA animals were anesthetized and surgically implanted with a Cell Pouch™ in the subcutaneous space of the lower abdomen 4 weeks before cell transplantation, allowing incorporation with vascularized tissue and forming fully developed tissue chambers suitable for cell transplantation upon removal of a space holding plug. LV-VEC.hBDD-FVIII BOECs were cultured for 3 days post-thawing and finally transplanted into the Cell Pouch™. Mice received either a dose of viable BOECs ($2\text{-}20\times10^6$) or remained untreated. All animals received a prophylactic dose (2-4 IU) of recombinant human FVIII by tail vein injection prior to surgical procedures.

FVIII activity

aPTT assay was performed on plasma samples of transplanted mice to assess FVIII activity. Standard curves were generated by serial dilution of recombinant human BDD-FVIII (ReFacto) in hemophilic mouse plasma. Analyses were performed using a Coatron® M4 coagulometer (TECO Medical Instruments) and TEClot APTT-S kit reagents (TECO Medical Instruments).

Bleeding assay

A bleeding assay was performed on anesthetized mice. The distal portion of the tail was cut at a diameter of 2-2.5 mm. Tails were placed in a conical tube containing 14 ml of 37°C pre-warmed saline. Blood was collected for 10 min and, following centrifugation, resuspended in red blood lysis buffer (155 mM NH4Cl, 10 mM KHCO3, and 0.1 mM EDTA). The absorbance of the samples was measured at 575 nm. For cell transplantation experiments with Cell Pouch™, the tail bleeding assay was performed by Sernova, as previously described,[69,70] at the end of the experimental period, 4 months post-transplantation. In brief, mice were anesthetized, and tail tips were placed in a guide, ensuring the same diameter of 1-mm, and severed (~ a distal 10-mm segment) for each animal. The tail was immediately immersed in pre-warmed saline at 37°C. Bleeding was carried out for a maximum of 20 min, after which animals were euthanized as *per* approved animal use protocol (AUP). Blood loss was evaluated by determining hemoglobin concentration by lysing collected red blood cells (ACK Lysing Buffer, Gibco™), and the absorbance measured at 550 nm on a Synergy™ Mx (BioTeck) spectrophotometer. Results were analyzed by comparing the amount of blood loss obtained from treated NSG-HA mice with control mice (untreated NSG-HA and NSG mice).

Statistical analysis

Data were expressed as means ± standard deviation (SD) or means ± standard error mean (SEM). Statistical significance was analyzed using Student's t test with two-tailed distribution, assuming equal standard deviation distribution, two-way analysis of variance (ANOVA) with Bonferroni post-hoc test or Tukey's multiple comparison post hoc tests in GraphPad Prism 6 (GraphPad Software). Statistical analyses involving IS were performed with the R software (r- project.org). Differences were considered statistically significant when *P* values < 0.05.

Acknowledgements

The authors thank Dr. D. Burton and Dr. A. Iftimia-Mander for their help. V. Bruscaggin, V. Fiorio for technical assistance. We also thanks Dr. Marcello Arsura for the English revision of the manuscript. A.F., M.Z., A.S., P.T. and J.B. have received funding from the European Union's Horizon 2020 research and innovation program under grant agreement HemAcure No. 667421. A.F was also supported in part by Telethon grant No. GGP19201 and by Horizon 2020, Vanguard grant No. 874700.

Authorship contributions

C.O., C.B., S.M., T.B., P.B., A.C., A.B.A., N.W., K.P. AC, FB, EU performed research and analyzed data. A.C., F.B. and E.M. performed integration analysis and analyzed data. A.B. and B.P. collected blood samples from hemophilic patients and performed analysis. A.F., J.B., A.S., D.M., P.T., M.Z. conceived the experiments generated funding, designed the research, and analyzed data. C.O., C.B., S.M. and A.F. wrote the manuscript that was revised by all authors.

Disclosure of Conflict of Interest

The authors have declared that no conflict of interest exists.

Supplemental Information

Supplemental Information includes Supplemental experimental procedures, two figures, and 1 table.

References

1. Bolton-Maggs, P.H.B., and Pasi, K.J. (2003). Haemophilias A and B. *Lancet*, pp. 1801–1809.
2. Roth, D.A., Tawa, N.E., O'Brien, J.M., Treco, D.A., and Selden, R.F. (2001). Nonviral transfer of the gene encoding coagulation factor viii in patients with severe hemophilia A. N Engl J Med *344*, 1735–1742.
3. Cormier, M., Batty, P., Tarrant, J., and Lillicrap, D. (2020). Advances in knowledge of inhibitor formation in severe haemophilia A. Br J Haematol *189*, 39–53.
4. Wion, K.L., Kelly, D., Summerfield, J.A., Tuddenham, E.G.D., and Lawn, R.M. (1985). Distribution of factor VIII MRNA and antigen in human liver and other tissues. Nature *317*, 726–729.
5. Jiang, H.C., Gao, Y., Dai, W.J., Sun, B., Xu, J., Qiao, H.Q., Meng, Q.H., and Wu, C.J. (2006). Ten-Year Experience With Living Related Donated Splenic Transplantation for the Treatment of Hemophilia A. Transplant Proc *38*, 1483–1490.
6. Hollestelle, M.J., Thinnes, T., Crain, K., Stiko, A., Kruijt, J.K., Van Berkel, T.J.C., Loskutoff, D.J., and Van Mourik, J.A. (2001). Tissue distribution of factor VIII gene expression in vivo - A closer look. Thromb Haemost *86*, 855–861.
7. Hollestelle, M.J., Poyck, P.P.C., Hollestelle, J.M., Marsman, H.A., Van Mourik, J.A., and Van Gulik, T.M. (2005). Extra-hepatic factor VIII expression in porcine fulminant hepatic failure. J Thromb Haemost *3*, 2274–2280.
8. Follenzi, A., Raut, S., Merlin, S., Sarkar, R., and Gupta, S. (2012). Role of bone marrow transplantation for correcting hemophilia A in mice. Blood *119*, 5532–5542.
9. Zanolini, D., Merlin, S., Feola, M., Ranaldo, G., Amoruso, A., Gaidano, G., Zaffaroni, M., Ferrero, A., Brunelleschi, S., Valente, G., et al. (2015). Extrahepatic sources of factor VIII potentially contribute to the coagulation cascade correcting the bleeding phenotype of mice with hemophilia A. Haematologica *100*, 881–92.
10. Kumaran, V., Benten, D., Follenzi, A., Joseph, B., Sarkar, R., and Gupta, S. (2005). Transplantation of endothelial cells corrects the phenotype in hemophilia A mice. J Thromb Haemost *3*, 2022–2031.
11. Fomin, M.E., Zhou, Y., Beyer, A.I., Publicover, J., Baron, J.L., and Muench, M.O. (2013). Production of Factor VIII by Human Liver Sinusoidal Endothelial Cells Transplanted in Immunodeficient uPA Mice. PLoS One *8*.
12. Follenzi, A., Benten, D., Novikoff, P., Faulkner, L., Raut, S., and Gupta, S. (2008). Transplanted endothelial cells repopulate the liver endothelium and correct the phenotype of hemophilia A mice. J Clin Invest *118*, 935–945.
13. Fomin, M.E., Zhou, Y.C., Beyer, A.I., Publicover, J., Baron, J.L., and Muench, M.O. (2013). Production of Factor VIII by Human Liver Sinusoidal Endothelial Cells Transplanted in Immunodeficient uPA Mice. PloS One *8*.
14. Filali, E. El, Hiralall, J.K., Van Veen, H.A., Stolz, D.B., and Seppen, J. (2013). Human Liver Endothelial Cells, But Not Macrovascular or Microvascular Endothelial Cells, Engraft in the Mouse Liver. Cell Transplant *22*, 1801–1811.
15. Gollomp, K.L., Doshi, B.S., and Arruda, V.R. (2019). Gene therapy for hemophilia: Progress to date and challenges moving forward. Transfus Apher Sci *58*, 602–612.
16. Peyvandi, F., and Garagiola, I. (2019). Clinical advances in gene therapy updates on clinical trials of gene therapy in haemophilia. Haemophilia *25*, 738–746.
17. Samelson-Jones, B.J., and Arruda, V.R. (2020). Translational Potential of Immune Tolerance Induction by AAV Liver-Directed Factor VIII Gene Therapy for Hemophilia A. Front Immunol *11*.
18. Merlin, S., Famà, R., Borroni, E., Zanolini, D., Bruscaggin, V., Zucchelli, S., and Follenzi, A. (2019). FVIII expression by its native promoter sustains long-term correction avoiding immune response in hemophilic mice. Blood Adv *3*, 825–838.
19. Olgasi, C., Talmon, M., Merlin, S., Cucci, A., Richaud-Patin, Y., Ranaldo, G., Colangelo, D., Di Scipio, F., Berta, G.N., Borsotti, C., et al. (2018). Patient-Specific iPSC-Derived Endothelial Cells Provide Long-Term Phenotypic Correction of Hemophilia A. Stem Cell Reports *11*.
20. Gao, K., Kumar, P., Cortez-Toledo, E., Hao, D., Reynaga, L., Rose, M., Wang, C., Farmer, D., Nolta, J., Zhou, J., et al. (2019). Potential long-term treatment of hemophilia A by neonatal co-transplantation of cord blood-derived endothelial colony-forming cells and placental mesenchymal stromal cells. Stem Cell Res Ther *10*.

21. Park, C.-Y., Kim, D.H., Son, J.S., Sung, J.J., Lee, J., Bae, S., Kim, J.-H., Kim, D.-W., and Kim, J.-S. (2015). Functional Correction of Large Factor VIII Gene Chromosomal Inversions in Hemophilia A Patient-Derived iPSCs Using CRISPR-Cas9. Cell Stem Cell *17*, 213–220.
22. Tatsumi, K., Sugimoto, M., Lillicrap, D., Shima, M., Ohashi, K., Okano, T., and Matsui, H. (2013). A novel cell-sheet technology that achieves durable factor VIII delivery in a mouse model of hemophilia a. PLoS One *8*.
23. Lin, Y., Weisdorf, D.J., Solovey, A., and Hebbel, R.P. (2000). Origins of circulating endothelial cells and endothelial outgrowth from blood. J Clin Invest *105*, 71–77.
24. Yoder, M.C., Mead, L.E., Prater, D., Krier, T.R., Mroueh, K.N., Li, F., Krasich, R., Temm, C.J., Prchal, J.T., and Ingram, D.A. (2007). Redefining endothelial progenitor cells via clonal analysis and hematopoietic stem/progenitor cell principals. Blood, 1801–1809.
25. Hoshi, R.A., Van Lith, R., Jen, M.C., Allen, J.B., Lapidos, K.A., and Ameer, G. (2013). The blood and vascular cell compatibility of heparin-modified ePTFE vascular grafts. Biomaterials *34*, 30–41.
26. Melero-Martin, J.M., Khan, Z.A., Picard, A., Wu, X., Paruchuri, S., and Bischoff, J. (2007). In vivo vasculogenic potential of human blood-derived endothelial progenitor cells. Blood *109*, 4761–4768.
27. Jantzen, A.E., Lane, W.O., Gage, S.M., Jamiolkowski, R.M., Haseltine, J.M., Galinat, L.J., Lin, F.H., Lawson, J.H., Truskey, G.A., and Achneck, H.E. (2011). Use of autologous blood-derived endothelial progenitor cells at point-of-care to protect against implant thrombosis in a large animal model. Biomaterials *32*, 8356–8363.
28. Sarlon, G., Zemani, F., David, L., Duong van Huyen, J.P., Dizier, B., Grelac, F., Colliec-Jouault, S., Galy-Fauroux, I., Bruneval, P., Fischer, A.M., et al. (2012). Therapeutic effect of fucoidan-stimulated endothelial colony-forming cells in peripheral ischemia. J Thromb Haemost *10*, 38–48.
29. Lin, Y., Chang, L., Solovey, A., Healey, J.F., Lollar, P., and Hebbel, R.P. (2002). Use of blood outgrowth endothelial cells for gene therapy for hemophilia A. Blood *99*, 457–462.
30. Medicines Agency, E. (2015). Reflection paper on classification of advanced therapy medicinal products. https://www.ema.europa.eu/en/documents/scientific-guideline/reflection-paper-classification-advanced-therapy-medicinal-products_en-0.pdf
31. Medicines Agency, E (2020). Guideline on quality, non-clinical and clinical aspects of medicinal products containing genetically modified cells. https://www.ema.europa.eu/en/documents/scientific-guideline/guideline-quality-non-clinical-clinical-aspects-medicinal-products-containing-genetically-modified_en-0.pdf
32. Medicines Agency, E. (2008). Guideline on the non-clinical studies required before first clinical use of gene therapy medicinal products. https://www.ema.europa.eu/en/documents/scientific-guideline/guideline-non-clinical-studies-required-first-clinical-use-gene-therapy-medicinal-products_en.pdf
33. Pepper, A.R., Pawlick, R., Gala-Lopez, B., MacGillivary, A., Mazzuca, D.M., White, D.J.G., Toleikis, P.M., and James Shapiro, A.M. (2015). Diabetes is reversed in a murine model by marginal mass syngeneic islet transplantation using a subcutaneous cell pouch device. Transplantation *99*, 2294–2300.
34. Charrier, S., Ferrand, M., Zerbato, M., Précigout, G., Viornery, A., Bucher-Laurent, S., Benkhelifa-Ziyyat, S., Merten, O.W., Perea, J., and Galy, A. (2011). Quantification of lentiviral vector copy numbers in individual hematopoietic colony-forming cells shows vector dose-dependent effects on the frequency and level of transduction. Gene Ther *18*, 479–487.
35. Zhao, Y., Stepto, H., and Schneider, C.K. (2017). Development of the First World Health Organization Lentiviral Vector Standard: Toward the Production Control and Standardization of Lentivirus-Based Gene Therapy Products. Hum Gene Ther Methods *28*, 205–214.
36. Furuhata, S., Ando, K., Oki, M., Aoki, K., Ohnishi, S., Aoyagi, K., Sasaki, H., Sakamoto, H., Yoshida, T., and Ohnami, S. (2007). Gene expression profiles of endothelial progenitor cells by oligonucleotide microarray analysis. Mol Cell Biochem *298*, 125–138.
37. Nelson, G.M., Padera, T.P., Garkavtsev, I., Shioda, T., and Jain, R.K. (2007). Differential gene expression of primary cultured lymphatic and blood vascular endothelial cells. Neoplasia *9*, 1038–1045.
38. Nielsen, J.S., and Mcnagny, K.M. (2008). Novel functions of the CD34 family. J Cell Sci *121*, 3683–3692.

39. Barr, S.D., Ciuffi, A., Leipzig, J., Shinn, P., Ecker, J.R., and Bushman, F.D. (2006). HIV Integration Site Selection: Targeting in Macrophages and the Effects of Different Routes of Viral Entry. Mol Ther *14*, 218–225.
40. Aiuti, A., Biasco, L., Scaramuzza, S., Ferrua, F., Cicalese, M.P., Baricordi, C., Dionisio, F., Calabria, A., Giannelli, S., Castiello, M.C., et al. (2013). Lentiviral hematopoietic stem cell gene therapy in patients with wiskott-aldrich syndrome. Science *341*.
41. Biffi, A., Montini, E., Lorioli, L., Cesani, M., Fumagalli, F., Plati, T., Baldoli, C., Martino, S., Calabria, A., Canale, S., et al. (2013). Lentiviral hematopoietic stem cell gene therapy benefits metachromatic leukodystrophy. Science *341*.
42. Kvaratskhelia, M., Sharma, A., Larue, R.C., Serrao, E., and Engelman, A. (2014). Molecular mechanisms of retroviral integration site selection. Nucleic Acids Res *42*, 10209–10225.
43. Dose-Ranging Study of Recombinant AAV2/6 Human Factor 8 Gene Therapy SB-525 in Subjects With Severe Hemophilia A ClinicalTrials.gov Identifier: NCT03061201.
44. Gene Therapy for Haemophilia A. ClinicalTrials.gov Identifier: NCT03001830.
45. A Gene Transfer Study for Hemophilia A ClinicalTrials.gov Identifier: NCT03003533.
46. A Safety, Tolerability, and Pharmacokinetics Study of a Single Intravenous Injection of Recombinant Coagulation Factor VIII Fc - Von Willebrand Factor - XTEN Fusion Protein (rFVIIIFc-VWF-XTEN) (BIVV001) in Previously Treated Adults With Severe Hemophilia A (EXTEN-A) ClinicalTrials.gov Identifier: NCT03205163.
47. Shahani, T., Covens, K., Lavend'homme, R., Jazouli, N., Sokal, E., Peerlinck, K., and Jacquemin, M. (2014). Human liver sinusoidal endothelial cells but not hepatocytes contain factor VIII. J Thromb Haemost *12*, 36–42.
48. Everett, L.A., Cleuren, A.C.A., Khoriaty, R.N., and Ginsburg, D. (2014). Murine coagulation factor VIII is synthesized in endothelial cells. Blood *123*, 3697–3705.
49. Fahs, S.A., Hille, M.T., Shi, Q., Weiler, H., and Montgomery, R.R. (2014). A conditional knockout mouse model reveals endothelial cells as the principal and possibly exclusive source of plasma factor VIII. Blood *123*, 3706–3713.
50. Terraube, V., O'Donnell, J.S., and Jenkins, P. V. (2010). Factor VIII and von Willebrand factor interaction: Biological, clinical and therapeutic importance. Haemophilia *16*, 3–13.
51. Ozelo, M.C., Vidal, B., Brown, C., Notley, C., Hegadorn, C., Webster, S., Harpell, L., Ahlin, J., Winterborn, A., Handforth, J., et al. (2014). Omental implantation of BOECs in hemophilia dogs results in circulating FVIII antigen and a complex immune response. Blood *123*, 4045–4053.
52. Ormiston, M.L., Toshner, M.R., Kiskin, F.N., Huang, C.J.Z., Groves, E., Morrell, N.W., and Rana, A.A. (2015). Generation and culture of blood outgrowth endothelial cells from human peripheral blood. J Vis Exp *2015*.
53. Hebbel, R.P. (2017). Blood endothelial cells: Utility from ambiguity. J Clin Invest *127*, 1613–1615.
54. Merlin, S., Cannizzo, E.S., Borroni, E., Bruscaggin, V., Schinco, P., Tulalamba, W., Chuah, M.K., Arruda, V.R., VandenDriessche, T., Prat, M., et al. (2017). A Novel Platform for Immune Tolerance Induction in Hemophilia A Mice. Mol Ther *25*, 1815–1830.
55. Kriz, J., Vilk, G., Mazzuca, D.M., Toleikis, P.M., Foster, P.J., and White, D.J.G. (2012). A novel technique for the transplantation of pancreatic islets within a vascularized device into the greater omentum to achieve insulin independence. Am J Surg *203*, 793–797.
56. A Safety, Tolerability and Efficacy Study of Sernova's Cell Pouch™ for Clinical Islet Transplantation ClinicalTrials.gov Identifier: NCT03513939.
57. Hur, J., Yoon, C.H., Kim, H.S., Choi, J.H., Kang, H.J., Hwang, K.K., Oh, B.H., Lee, M.M., and Park, Y.B. (2004). Characterization of Two Types of Endothelial Progenitor Cells and Their Different Contributions to Neovasculogenesis. Arterioscler Thromb Vasc Biol *24*, 288–293.
58. Zhang, X., Xu, Y., Thomas, V., Bellis, S.L., and Vohra, Y.K. (2011). Engineering an antiplatelet adhesion layer on an electrospun scaffold using porcine endothelial progenitor cells. J Biomed Mater Res *97 A*, 145–151.
59. Bittorf, P., Bergmann, T., Merlin, S., Olgasi, C., Pullig, O., Sanzenbacher, R., Zierau, M., Walles, H., Follenzi, A., and Braspenning, J. (2020). Regulatory-Compliant Validation of a Highly Sensitive qPCR for Biodistribution Assessment of Hemophilia A Patient Cells. Mol Ther Methods Clin Dev *18*, 176–188.

60. Kolbe, M., Dohle, E., Katerla, D., Kirkpatrick, C.J., and Fuchs, S. (2010). Enrichment of outgrowth endothelial cells in high and low colony-forming cultures from peripheral blood progenitors. Tissue Eng Part C Methods *16*, 877–886.
61. Gillet, N.A., Malani, N., Melamed, A., Gormley, N., Carter, R., Bentley, D., Berry, C., Bushman, F.D., Taylor, G.P., and Bangham, C.R.M. (2011). The host genomic environment of the provirus determines the abundance of HTLV-1-infected T-cell clones. Blood *117*, 3113–3122.
62. Firouzi, S., López, Y., Suzuki, Y., Nakai, K., Sugano, S., Yamochi, T., and Watanabe, T. (2014). Development and validation of a new high-throughput method to investigate the clonality of HTLV-1-infected cells based on provirus integration sites. Genome Med *6*, 46.
63. Sessa, M., Lorioli, L., Fumagalli, F., Acquati, S., Redaelli, D., Baldoli, C., Canale, S., Lopez, I.D., Morena, F., Calabria, A., et al. (2016). Lentiviral haemopoietic stem-cell gene therapy in early-onset metachromatic leukodystrophy: an ad-hoc analysis of a non-randomised, open-label, phase 1/2 trial. Lancet *388*, 476–487.

64. Spinozzi, G., Calabria, A., Brasca, S., Beretta, S., Merelli, I., Milanesi, L., and Montini, E. (2017). VISPA2: A scalable pipeline for high-throughput identification and annotation of vector integration sites. BMC Bioinformatics *18*.
65. Berry, C.C., Gillet, N.A., Melamed, A., Gormley, N., Bangham, C.R.M., and Bushman, F.D. (2012). Estimating abundances of retroviral insertion sites from DNA fragment length data. Bioinformatics *28*, 755–762.
66. Biffi, A., Bartholomae, C.C., Cesana, D., Cartier, N., Aubourg, P., Ranzani, M., Cesani, M., Benedicenti, F., Plati, T., Rubagotti, E., et al. (2011). Lentiviral vector common integration sites in preclinical models and a clinical trial reflect a benign integration bias and not oncogenic selection. Blood *117*, 5332–5339.
67. McLean, C.Y., Bristor, D., Hiller, M., Clarke, S.L., Schaar, B.T., Lowe, C.B., Wenger, A.M., and Bejerano, G. (2010). GREAT improves functional interpretation of cis-regulatory regions. Nat Biotechnol *28*, 495–501.
68. Kumaran, V., Benten, D., Follenzi, A., Joseph, B., Sarkar, R., and Gupta, S. (2005). Transplantation of endothelial cells corrects the phenotype in hemophilia A mice. J Thromb Haemost *3*, 2022–2031.
69. Liu, Y. (2012). Standardizing a simpler, more sensitive and accurate tail bleeding assay in mice. World J Exp Med *2*, 30.
70. Schuettrumpf, J., Herzog, R.W., Schlachterman, A., Kaufhold, A., Stafford, D.W., and Arruda, V.R. (2005). Factor IX variants improve gene therapy efficacy for hemophilia B. Blood *105*, 2316–2323.

Figure legends

Figure 1. Healthy and HA BOEC isolation, LV transduction, and *in vitro* FVIII detection. (**A**) Light microscope pictures of cultured healthy and HA BOECs at passage 3. (**B**) Representative RT-PCR analysis for the expression of endothelial markers. HUVECs and fibroblasts were used as positive and negative control, respectively. (**C**) RT-PCR for endothelial markers specific for blood endothelial cells (BECs). iPSC-derived ECs and fibroblasts were used as positive and negative control, respectively. (**D**) Representative histograms of healthy non-transduced (black line) and LV-VEC.hBDD-FVIII transduced healthy BOECs (red line), showing endothelial marker expression and absence of hematopoietic markers. The filled-up histograms represent unstained BOECs. (**E**) Representative histograms of HA non-transduced (black line) and LV-VEC.hBDD-FVIII transduced HA BOECs (red line) showing endothelial marker expression and absence of hematopoietic markers. The filled-up histograms represent unstained BOECs. (**F**) Matrigel assay confirming tubule formation of transduced BOECs. (**G)** RT-PCR, using primers specific for the exogenous *F8* in non-transduced and LV-VEC.hBDD-FVIII BOECs. Unrelated transduced cells and fibroblast were used as positive and negative control respectively. (**H**) FVIII intracytoplasmic staining on non-transduced (black line) or transduced healthy BOECs (red line). The filled-up histogram represents unstained BOECs. (**I**) FVIII intracytoplasmic staining on non-transduced (Black line) or transduced HA BOECs (Red line). The filled-up histogram represents unstained BOECs. (**J**) FVIII detection by immunofluorescence: blue: DAPI, red: anti-FVIII. Data are expressed as mean ± SD and are representative of four independent experiments.

Figure 2. Intraperitoneal implantation of BOECs with Cytodex micro-carrier beads. (A) Kinetics of the percentage of FVIII activity measured by aPTT assay in the plasma of transplanted NSG-HA mice. BOECs used were transduced with either LV-VEC.GFP or LV-VEC.hBDD-FVIII. Data are expressed as mean ± SD and are representative of two independent experiments using BOECs from two healthy donors (n = 7 mice), and four independent experiments using HA BOECs from four patients (n = 23 mice). (**B**) Blood loss evaluation on NSG-HA mice between week 7 and 10 (n = 4) after cell transplantation. (**C**) FVIII concentration in plasma of mice transplanted with transduced or non-transduced BOECs at week 16. Data are expressed as mean ± SD, ($P < 0.0001$ ***, $P < 0.001$ **) (**D**) Representative immunofluorescence on beads showing cells co-expressing GFP and CD31.

Figure 3. Large-scale expansion of HA patient derived BOECs. (**A**) Light microscope pictures of transduced HA BOECs pre- and post-expansion. (**B**) Cell size, cell density, culture time, and population doubling level during pre- and post- large-scale expansion. (**C**) Endothelial marker expression pre- and post- large-scale expansion expressed as stained cells *vs* cells with secondary isotype controls. (**D**) Tubulogenic assay to assess the functionality of transduced HA BOECs after pre- and post-large-scale expansion. (**E**) Kinetics of the percentage of FVIII activity measured by aPTT assay in plasma of transplanted NSG-HA mice. Data are expressed as mean ± SD and are representative of two independent experiments (n = 7).

Figure 4. Pathological assessment after transplantation of LV-VEC.hBDD-FVIII HA BOECs into the Cell Pouch™ device. (**A**) Sernova Cell Pouches™ were removed at 4, 8, or 12 weeks and stained by H&E and Masson's Trichrome for blinded histopathological analysis. Histology scores and representative images at 12 weeks post- transplant with

10×106 LV-VEC.hBDD-FVIII BOECs (animal groups n = 2-3). (B) Quantification of H&E and Masson's Trichrome for blinded histopathological analysis.

Figure 5. Bleeding phenotype and cell survival of LV-VEC.hBDD-FVIII HA BOECs after implantation in the Cell Pouch™ device. (**A**) Bleeding assay on mice transplanted with 10×10^6 or 20×10^6 HA and LV-VEC.hBDD-FVIII BOECs, or left untreated (n = 3-6, mean ± SEM, $^{**}P < 0.05$, ns: not significant). (**B**) The transplanted Cell Pouch™ devices were removed from the recipients NSG-HA mice, and immunofluorescence was performed to detect cell survival within the mouse tissue by human cell staining (HLA-ABC) and blood vessel formation through staining with cross-reacting human/mouse von Willebrand Factor (vWF) antibody. The images shown are representative of two transplant groups (10×10^6 n = 5; 20×10^6 n = 12). (**C**) Quantification of HLA-ABC and blood vessel formation from blinded histopathological assessment.

Figure 6. Genome wide distribution of lentiviral vector IS. (**A**) The pink track represents the density distribution of genes (RefSeq annotation, hg19 genome). The green tracks are the density distributions of all the IS retrieved in the HA transduced with LV-VEC.GFP and Healthy transduced with LV-VEC.GFP groups. The blue tracks are the density distributions of all the IS retrieved in the LV-VEC.hBDD-FVIII HA BOECs and LV-VEC.hBDD-FVIII Healthy BOECs groups. (**B)** Distribution of IS of the 4 groups along the whole human genome and with respect to gene transcription start site (TSS).

Figure 7. Box plot representation of clonal abundance. For each sample, the abundance values for each clone are represented as dots. Clones over 10% are presented as dots labeled with the closest gene symbol (RefSeq hg19).

Figure 8. Clonal diversity comparison. (**A**) Shannon diversity index for each transduced cell population according to cell passage and time point. (**B**) H Index comparison between different groups.

Figure 1

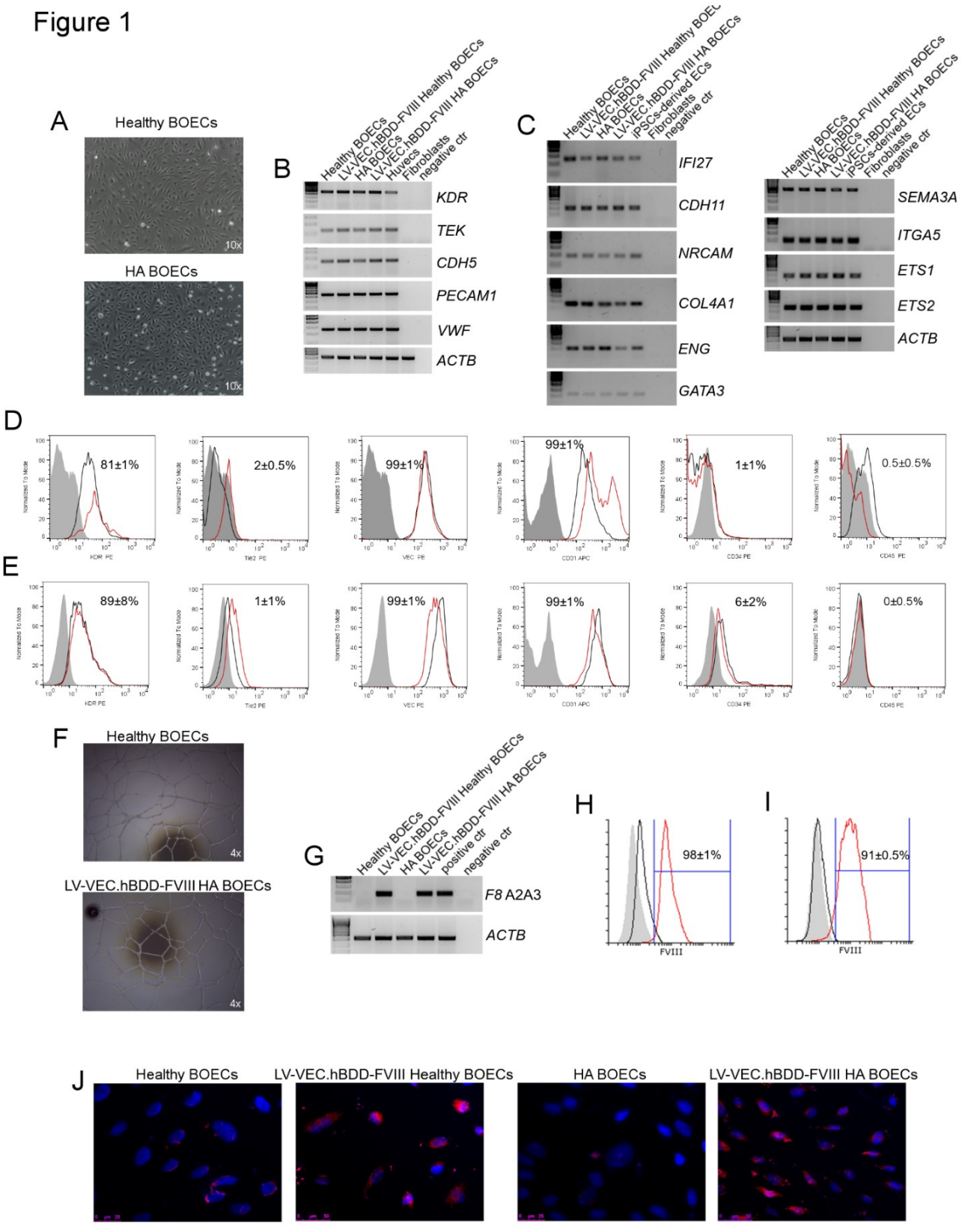
A
Healthy BOECs
10x
HA BOECs
10x
B
Healthy BOECs
LV-VEC.hBDD-FVIII Healthy BOECs
HA BOECs
LV-VEC.hBDD-FVIII HA BOECs
Huvecs
Fibroblasts
negative ctr
KDR
TEK
CDH5
PECAM1
VWF
ACTB
C
Healthy BOECs
LV-VEC.hBDD-FVIII Healthy BOECs
HA BOECs
LV-VEC.hBDD-FVIII HA BOECs
iPSCs-derived ECs
Fibroblasts
negative ctr
IFI27
CDH11
NRCAM
COL4A1
ENG
GATA3
SEMA3A
ITGA5
ETS1
ETS2
ACTB
D
81±1%
2±0.5%
99±1%
99±1%
1±1%
0.5±0.5%
E
89±8%
1±1%
99±1%
99±1%
6±2%
0±0.5%
F
Healthy BOECs
4x
LV-VEC.hBDD-FVIII HA BOECs
4x
G
Healthy BOECs
LV-VEC.hBDD-FVIII Healthy BOECs
HA BOECs
LV-VEC.hBDD-FVIII HA BOECs
positive ctr
negative ctr
F8 A2A3
ACTB
H
98±1%
FVIII
I
91±0.5%
FVIII
J
Healthy BOECs
LV-VEC.hBDD-FVIII Healthy BOECs
HA BOECs
LV-VEC.hBDD-FVIII HA BOECs

Figure 2

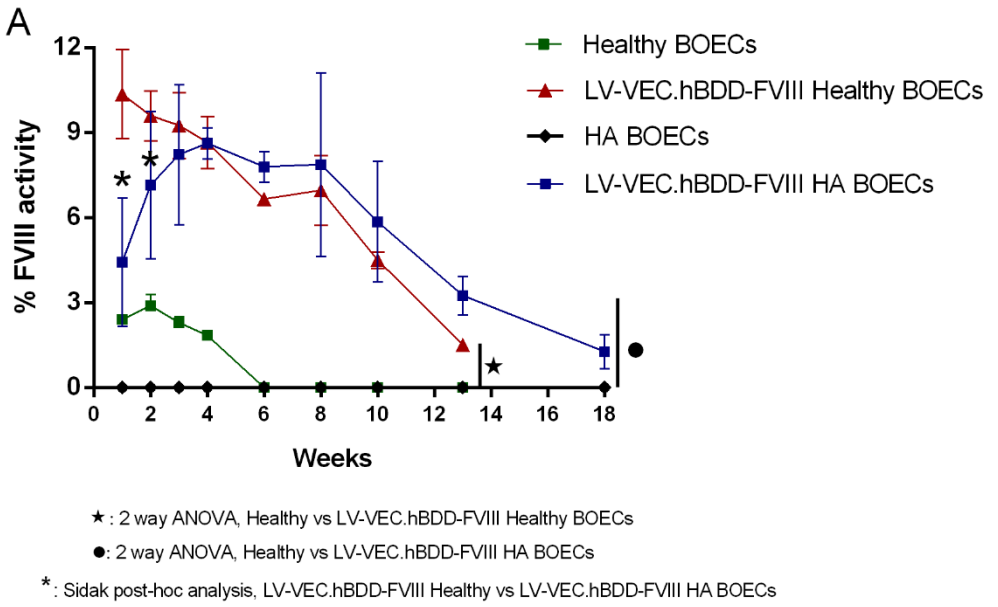

★: 2 way ANOVA, Healthy vs LV-VEC.hBDD-FVIII Healthy BOECs

●: 2 way ANOVA, Healthy vs LV-VEC.hBDD-FVIII HA BOECs

*: Sidak post-hoc analysis, LV-VEC.hBDD-FVIII Healthy vs LV-VEC.hBDD-FVIII HA BOECs

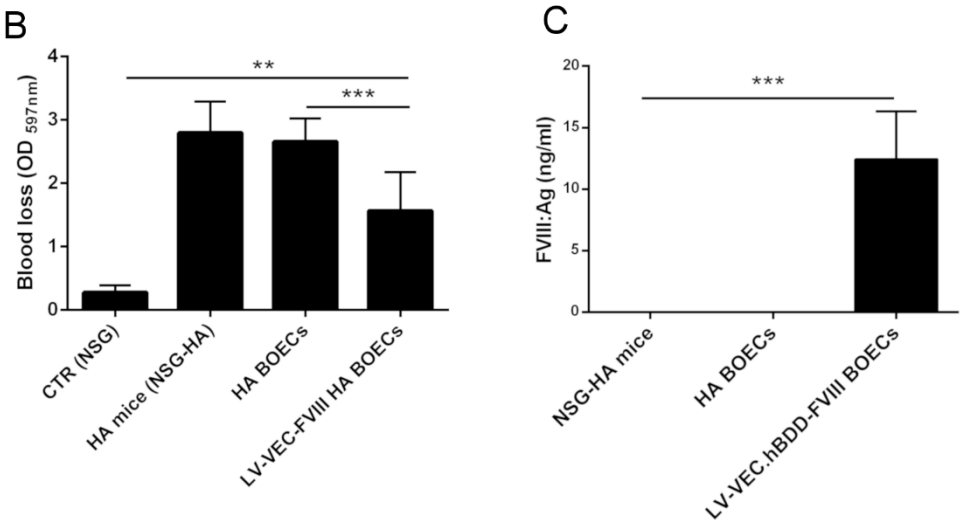

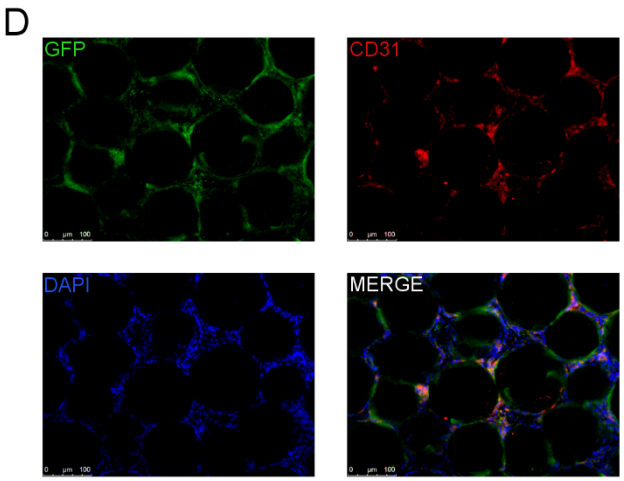

Figure 3

A

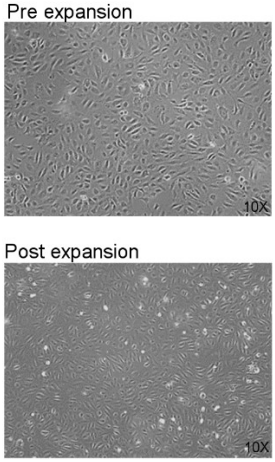

B

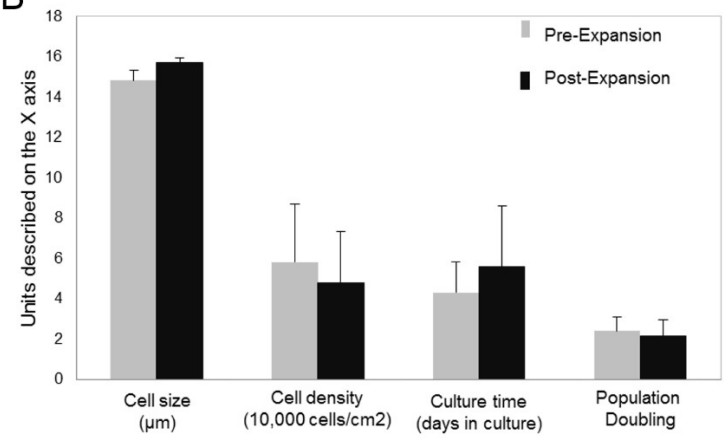

C

	Pre-expansion	Post-expansion
Surface markers	Expression (%)	Expression (%)
Tie2	3.9 ± 1.9	4.5 ± 1.0
KDR	20.9 ± 2.8	44.1 ± 3
CD45	2.9 ± 1.0	2.5 ± 2.4
CD34	3.5 ± 0.2	85.8 ± 0.9
CD31	99.1 ± 0.3	98.4 ± 1.0
VE-Cadherin	98.8 ± 0.4	96.1 ± 0.9

D

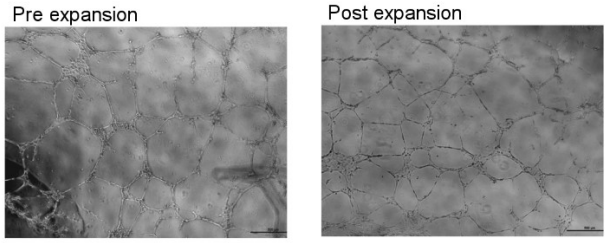

E

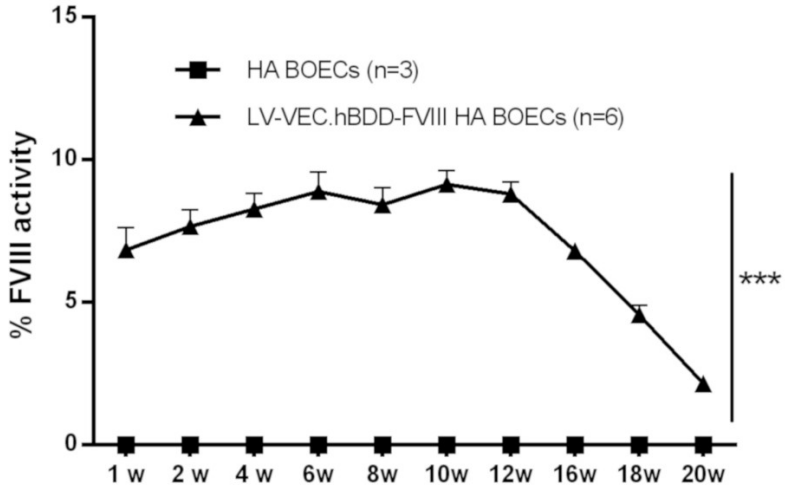

Figure 4

A

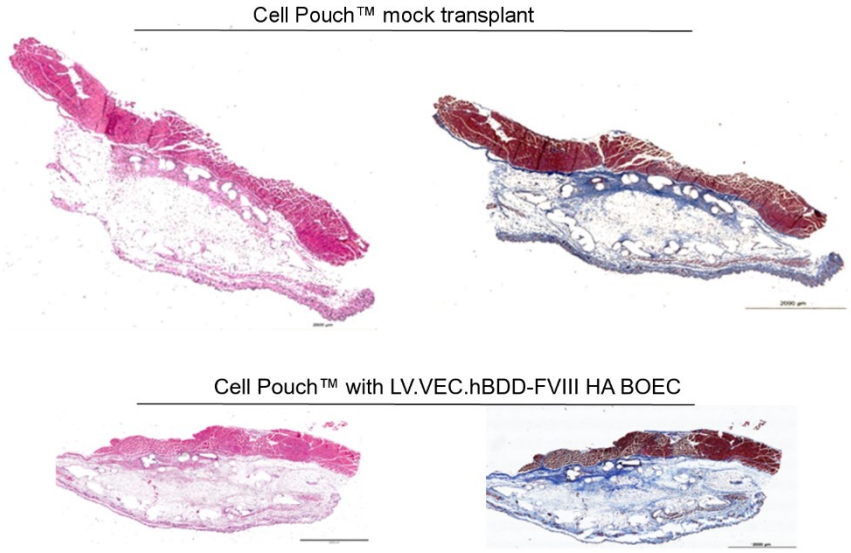
Cell Pouch™ mock transplant
Cell Pouch™ with LV.VEC.hBDD-FVIII HA BOEC

B

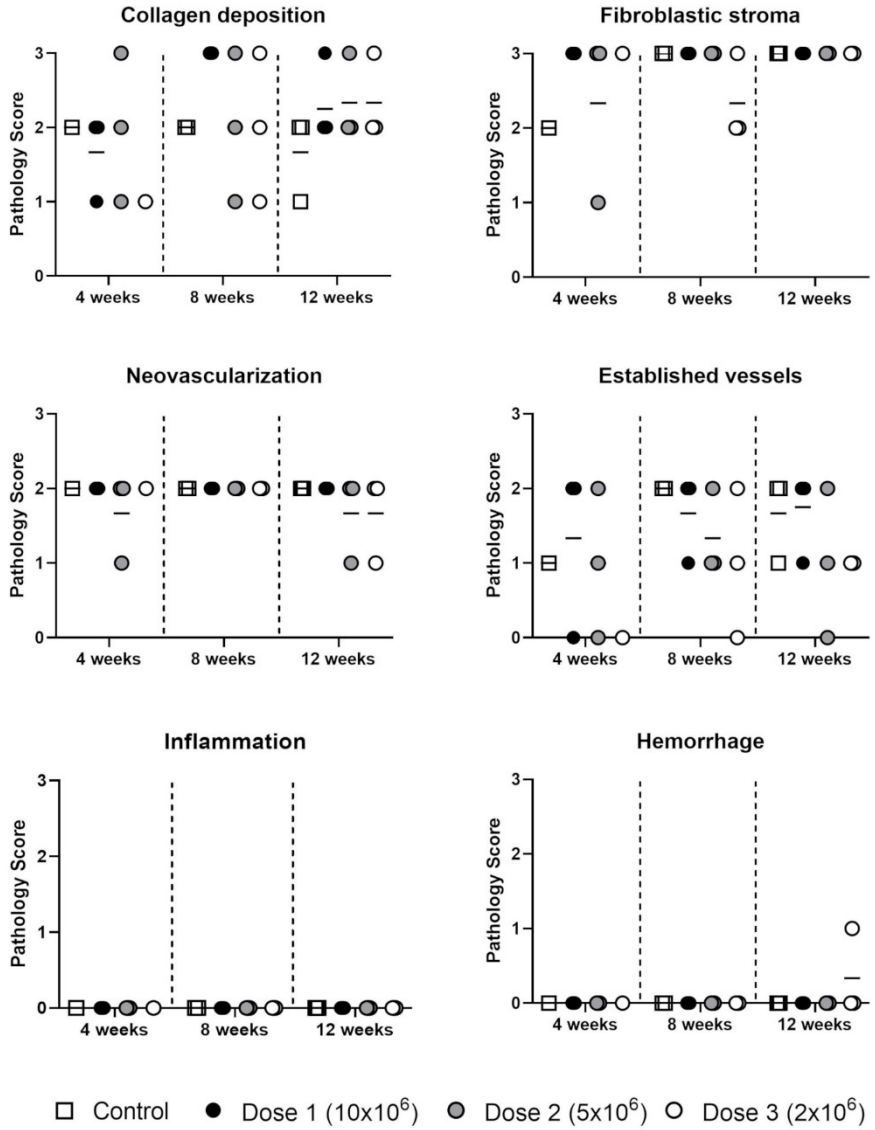
Collagen deposition
Fibroblastic stroma
Neovascularization
Established vessels
Inflammation
Hemorrhage
Pathology Score
0
1
2
3
4 weeks
8 weeks
12 weeks
Control
Dose 1 (10x10^6)
Dose 2 (5x10^6)
Dose 3 (2x10^6)

Figure 5

A

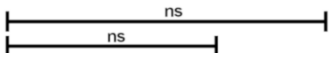

Figure 6

A

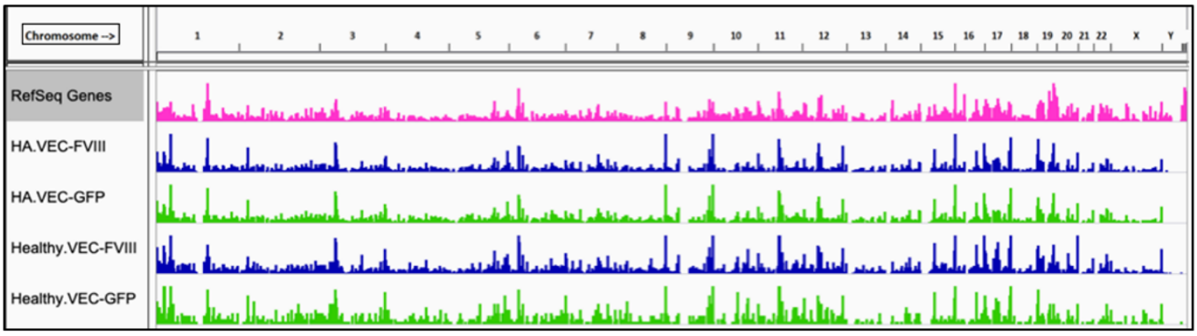

B

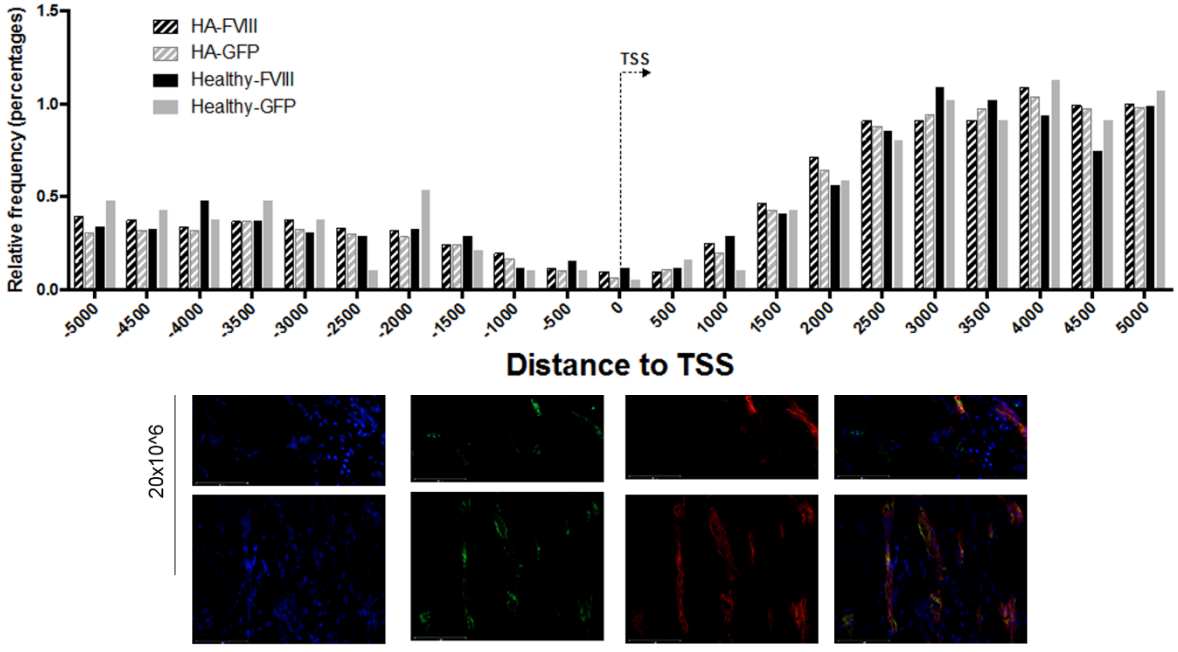

C

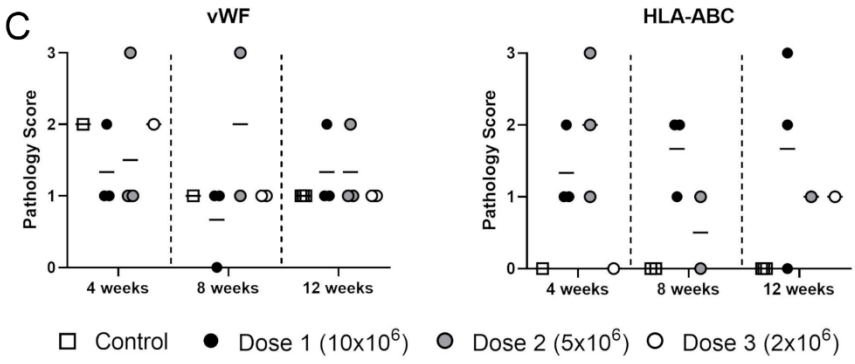

Figure 7

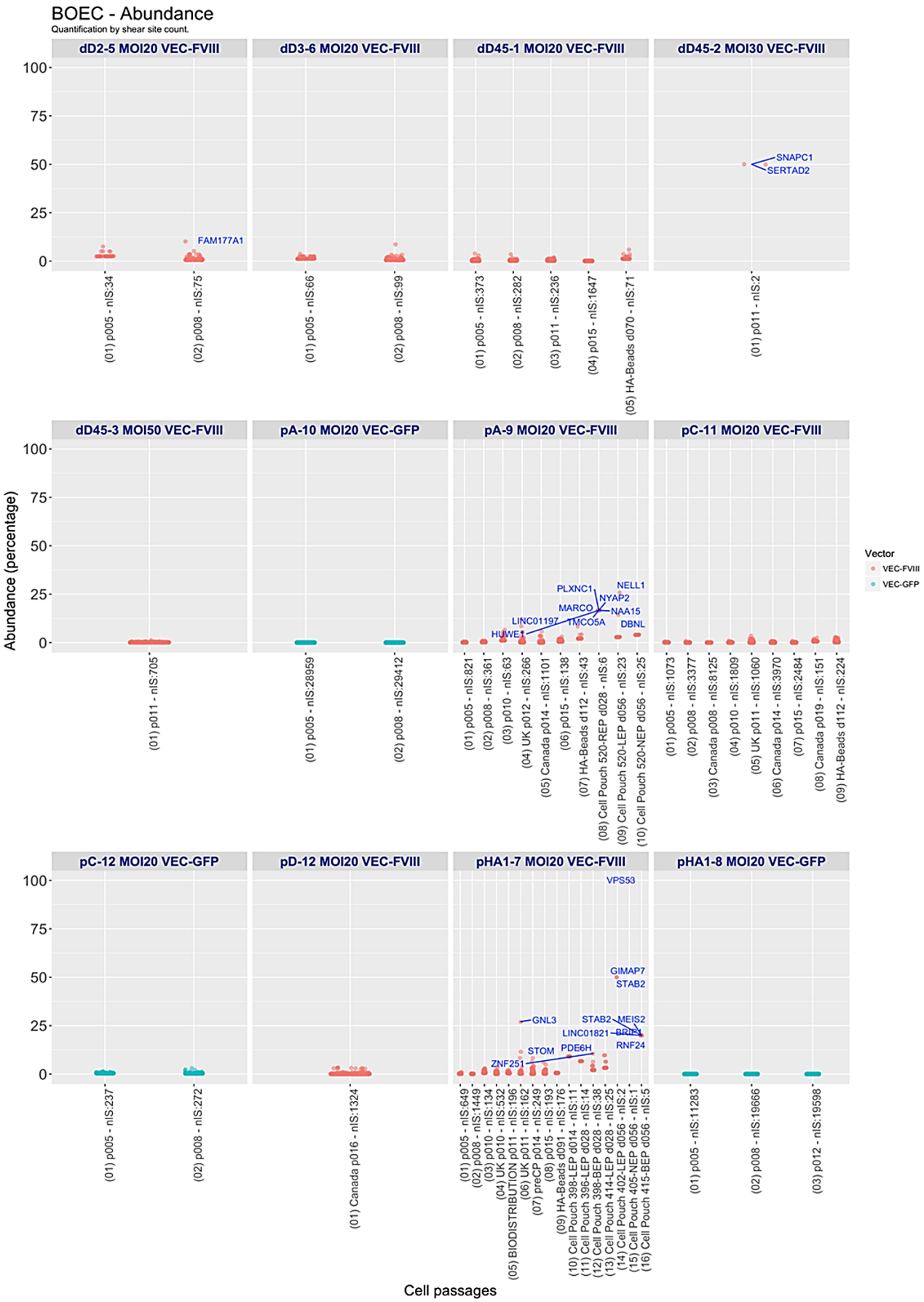
BOEC - Abundance
Quantification by shear site count.
dD2-5 MOI20 VEC-FVIII
dD3-6 MOI20 VEC-FVIII
dD45-1 MOI20 VEC-FVIII
dD45-2 MOI30 VEC-FVIII
dD45-3 MOI50 VEC-FVIII
pA-10 MOI20 VEC-GFP
pA-9 MOI20 VEC-FVIII
pC-11 MOI20 VEC-FVIII
pC-12 MOI20 VEC-GFP
pD-12 MOI20 VEC-FVIII
pHA1-7 MOI20 VEC-FVIII
pHA1-8 MOI20 VEC-GFP
Abundance (percentage)
Cell passages
Vector
VEC-FVIII
VEC-GFP
FAM177A1
SNAPC1
SERTAD2
PLXNC1
NELL1
NYAP2
MARCO
NAA15
LINC01197
TMCO5A
DBNL
HUWE1
VPS53
GIMAP7
STAB2
GNL3
MEIS2
LINC01821
BRD1
RNF24
STOM
PDE6H
ZNF251

Figure 8

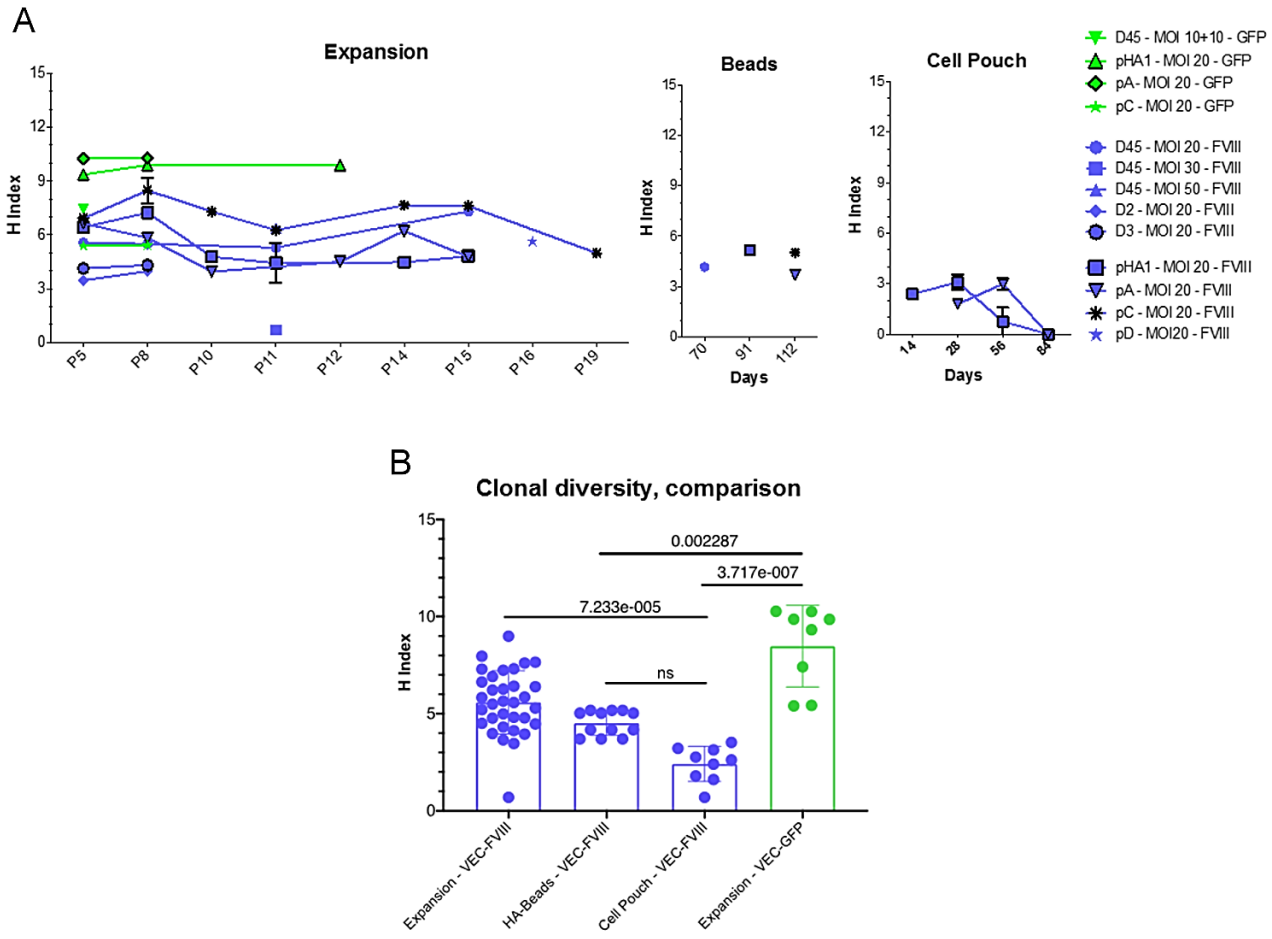
A
Expansion
Beads
Cell Pouch
H Index
Days
P5
P8
P10
P11
P12
P14
P15
P16
P19
70
91
112
14
28
56
84
D45 - MOI 10+10 - GFP
pHA1 - MOI 20 - GFP
pA- MOI 20 - GFP
pC - MOI 20 - GFP
D45 - MOI 20 - FVIII
D45 - MOI 30 - FVIII
D45 - MOI 50 - FVIII
D2 - MOI 20 - FVIII
D3 - MOI 20 - FVIII
pHA1 - MOI 20 - FVIII
pA - MOI 20 - FVIII
pC - MOI 20 - FVIII
pD - MOI20 - FVIII
B
Clonal diversity, comparison
H Index
0.002287
3.717e-007
7.233e-005
ns
Expansion - VEC-FVIII
HA-Beads - VEC-FVIII
Cell Pouch - VEC-FVIII
Expansion - VEC-GFP

Supplemental Material and Methods

Lentiviral vector generation. Third generation self-inactivating LVs were produced as previously published.[1] Briefly, 293T cells were expanded and transiently transfected by the calcium phosphate precipitation method with four plasmids encoding for two core packaging constructs (pMDLg/pol and pRSV-Rev), the envelope construct (pMD.VSV.G), and the transfer vector construct (pVEC.hBDD-FVIII.LV or pVEC.GFP.LV). The cell supernatant was harvested, and LV particles were concentrated by ultracentrifugation. For GMP-grade production of LV, the KR2i TFF System® (Spectrum Lab) was used according to the manufacturer's protocol. The product is ISO 9001:2008 certified. The system consists of a digital peristaltic pump, man/machine interface with a graphical LCD display, digital pressure monitor, KR2i Easy-Load Pump head, Automatic Backpressure Valve, filter module stand, and a real-time data collection software. The Tangential Flow Filtration (TFF) System uses a constant turbulent flow along a porous membrane to eliminate impurities from the sample. The tangential flow along the membrane prevents the accumulation of material on the membrane surface, as opposed to the classical "dead-end filtration", and allows the maximum recovery with high purity of the product.

Analysis of lentiviral vector copy number. Genomic DNA from LV-VEC.hBDD-FVIII and LV-VEC.GFP transduced BOECs was isolated using ReliaPrep gDNA Tissue Miniprep System (Promega). Real-time qPCR was used to evaluate the integrated LV copy numbers per cell in the DNA. Primers used for the qPCR recognize the Wpre sequence: Forward TTGCTTCCCGTATGGCTTTC, Reverse AGCTGACAGGTGGTGGCAAT. Finally, TU/ml was calculated with the following formula: TU/ml = (LV copies/cell × No. of transduced cells) / LV volume (expressed in ml).

Evaluation of HIV-1 p24 in culture medium of transduced BOECs. The presence of HIV-1 p24 was evaluated in culture medium of transduced cells after several time points and passages. Samples were analyzed using Liaison® XL (Diasorin) in the Virology Laboratory of the Hospital (Ospedale Maggiore della Carità di Novara, Italy).

RNA isolation and RT-PCR. Total RNA was isolated by Isol-RNA Lysis Reagent (Invitrogen). One µg of RNA was treated with DNase I (Thermo Scientific), and cDNAs were obtained using the RevertAid First Strand cDNA Synthesis Kit (Thermo Scientific). All PCRs were performed with GoTaq® Flexi DNA Polymerase (Promega). Primers, annealing temperatures, and product sizes are listed below in Supplemental Table 1. PCR products were resolved in 2% agarose gels.

In vitro tubulogenesis assay. Pure Matrigel (BD Bioscience) was added to each well of a 24-well tissue culture plate and allowed to solidify at 37°C for 1 h. A cell suspension containing 10^5 BOECs, resuspended in culture medium, was placed on top of the Matrigel. Plates were incubated at 37°C, 5% CO_2 and observed and imaged at 16 h to detect capillary-like structure formation using an inverted microscope Leica ICC50.

Flow cytometry analysis. BOECs were characterized by flow cytometric analysis using antibodies listed in Supplemental Table 2. For each sample, 1.5×10^5 live events were acquired either on the Attune NxT Acoustic Focusing Cytometer (ThermoFisher Scientific, Waltham, MA, USA) or on BD FACSCanto II. Data were analyzed by FCS Express 6 (DeNovo Software, Glendale, CA, USA) or using FlowJo Software V10.6 (FlowJo LLC).

Histopathological staining and analysis of samples from Cell Pouch™. Sernova Cell Pouches™ with transplanted FVIII-BOECs were explanted from the mice, dissected into segments, fixed in 10% neutral buffered formalin, and paraffin-embedded. Sections (5-6 µM-thick) were stained with hematoxylin and eosin (H&E) and Masson's Trichrome (Nucro-Technics, Scarborough, Ontario).

Immunostaining. For immunofluorescence (IF) staining, BOECs were cultured on plastic and fixed in PFA 4%, for nuclear staining permeabilized in 0,5% PBS-Triton X100 and then incubated with blocking buffer (BB, 5% goat serum, 1% BSA, 0.1% Triton X-100 in PBS) at room temperature (RT). Mouse tissues were fixed in 4% PFA, equilibrated in sucrose, and embedded in cryostat embedding medium (Bio-Optica). Cryostat sections of 4-µm thickness were blocked in BB, incubated with primary antibody at RT, and then incubated in the dark at RT with the secondary antibody. The Cell Pouch™ with transplanted FVIII-BOECs was explanted from each animal, dissected into segments, and immediately cryopreserved in Tissue-Tek® O.C.T. compound (VWR) using an isopentane (2-methylbutane)/dry ice slurry (-70°C), and stored at -80°C. Prior to staining, cryostat sections (5-6 µm) were air-dried and pre-treated by immersion in cold acetone (-20°C), followed by washes in tris-buffered saline (TBS). Sections were blocked in TBS containing 10% goat serum and 1% BSA. A list of the antibodies used in these experiments is provided in Supplemental Table 3.

Histology analysis and preservation techniques of tissues. Following explantation, gross observations of Cell Pouches™ were made and images taken just prior to further histological processing. The 1 Plug Cell Pouches™ were then dissected into 3 segments (a – c) (see Figure 1). Segments 'a' and 'c' were processed for fixation in 10% neutral buffered formalin (Sernova Histology SOP-H900). Cell Pouches™ were washed from 10% formalin in 1X phosphate buffered saline (PBS) to 70% ethanol and subsequently processed for paraffin embedding. Segment 'b' was flash frozen for cryopreservation at the time of dissection using an isopentane/dry ice slurry and embedded in optimal cutting temperature compound (O.C.T.) (Sernova Histology SOP-H936). Cryopreserved or paraffin-embedded segments were then serially sectioned with a cryostat or microtome, respectively.

Preparation of slides and high-resolution images with description of tissue stains. Prior to staining or immunohistochemistry (IHC) analysis, sections were deparaffinized and rehydrated. Sections were stained with H&E for either formalin-fixed paraffin embedded (FFPE) or cryopreserved tissues. Masson's trichrome staining was performed on FFPE (Nucro-Technics, Scarborough, Ontario). For IHC staining, cryopreserved O.C.T. embedded tissues were dried, pre-treated with fixation and permeabilization with cold acetone (-20 ºC, 10 min) and stained to detect microvessel formation with von Willebrand factor (vWF). For human cell detection, sections were stained with a human leukocyte antigen (HLA-ABC) antibody. High resolution images and full slide scanning of the sections were imaged with an EVOS™ FL Auto 2 Imaging System (Invitrogen™, ThermoFisher Scientific) for both light microscopy (H&E and Masson's Trichrome) and fluorescent IHC (vWF/HLA).

Analysis methodology. The following histological assessment was conducted on the serial sections of formalin-fixed paraffin embedded (FFPE) segments taken within the chambers of each of the Cell Pouches™ from the animals across the doses and explanation time points: 1) stromal development, including type, distribution, and maturity; 2) vascularity, including neovascularization, established vessels, and their respective relationship to the

chamber area; 3) inflammation, including type and relative abundance; and 4) hemorrhage. Masson's trichrome stains were assessed for collagen deposition as a marker of stromal maturity. Histological variables were assessed in a semi-quantitative fashion: - absent; + mild; ++ moderate; and +++ marked.

A histological assessment was conducted of the serial sections of frozen embedded segments taken within the chambers of each of the Cell Pouches™ from the animals across the doses and explanation time points: 1) cell transplant survival; 2) interactions and development post-transplant; 3) interactions of the surrounding pre-vascularized tissue of the Cell Pouch™; and 4) blood vessel formation relative to transplant cells. Histological variables were assessed in a semi-quantitative fashion: - negative (no staining); +/- equivocal staining; + mild positivity; ++ moderate positivity; +++ marked positivity; n/a image not available.

For histological assessment the slides and high-resolution images were sent to a certified pathologist for analysis. The assessment was conducted in a blinded-fashion, with no knowledge of the animal time points. The assessment was unblinded for writing the final report. Pathological definitions were as follows: Fibroblastic stroma – mesenchymal tissue consisting of fibroblastic cells and the extracellular matrix, including variable collagen produced by these cells; Collagen – usually a fibrillar protein within the extracellular matrix of connective tissue that provides mechanical strength to the tissues; Neovascularization – tiny, immature capillary-like vessels arising during new blood vessel formation and growth.

Supplemental figures and tables

Gene	Synthetic oligonucleotide	Expected band
ACTB	F: 5'-GAGAAAATCTGGCACCACACC-3'	412 bp
	R: 5'-CGACGTAGCACAGCTTCTC-3'	
KDR	F: 5'- TGCAAGGACCAAGGAGACTATGT -3'	459 bp
	R: 5'- TAGGATGATGACAAGAAGTAGCC -3'	
TEK	F: 5'-AGACCAGCACGTTGATGTGA-3'	127 bp
	R: 5'-TGGGTTGCTTGACCCTATGT-3'	
CDH5	F: 5'-CAGCCCAAAGTGTGTGAGAA-3'	162 bp
	R: 5'-TGTGATGTTGGCCGTGTTAT-3'	
PECAM1	F: 5'-AGGTCAGCAGCATCGTGGTCAACAT-3'	469 bp
	R: 5'-GTGGGGTTGTCTTTGAATACCGCAG-3'	
VWF	F: 5'- TGGAGTACCCCTTCAGCGAG -3'	263 bp
	R: 5'- GTTGGCATTAGGGCCCACTC -3'	
F8 A2-A3 domain	F: 5'- Tgccacaactcagactttcg-3'	184 bp
	R: 5'- gatggcgtttcaagactggt -3'	
IFI27	F: 5'- TCTGGCTCTGCCGTAGTTTT-3'	243 bp

	R: 5'- GAACTTGGTCAATCCGGAGA -3'	
CDH11	F: 5'- Tggcagcaagtatccaatgg-3'	200 bp
	R: 5'- tttggttacgtggtaggcac-3'	
NRCAM	F: 5'- TCCAGAAGGCAATGCAAGTA-3'	117 bp
	R: 5'- AGCATTCCATCTTCCTTTGC -3'	
COL4A1	F: 5'- GGCCTATGAGTCCTGGGTAC -3'	146 bp
	R: 5'- TGGATTTCAGGGGATGCCAG -3'	
ENG	F: 5'- CCACTGCACTTGGCCTACA -3'	107 bp
	R: 5'- GCCCACTCAAGGATCTGG -3'	
GATA3	F: 5'- gaaccggcccctcattaag-3'	216 bp
	R: 5'- CTTGCATATCTGACCTATTCTAGCGTG-3'	
ITGA5	F: 5'- TGCAGTGTGAGGCTGTGTACA -3'	88 bp
	R: 5'- GTGGCCACCTGACGCTCT -3'	
ETS-1	F: 5'- catatcaagttaatggagtc-3'	268 bp
	R: 5'- tgtttgatagcaaagtagtc -3'	
ETS-2	F: 5'- gtggagtgagcaacaggtat-3'	282 bp
	R: 5'- ccaaaacctaatgtattgctg -3'	
Wpre/ dNEF	F: 5'- TCTGGCTCTGCCGTAGTTTT-3'	200 bp
	R: 5'- GGCTAAGATCTACAGCTGCCTTG-3'	

Supplemental Table 1. Primers used in RT-PCR and Real Time.

Antibody	Reactivity	Manufacturer	Format
CD45	human	clone 32D12, Miltenyi Biotec	PE
CD34	human	clone 4H11[APG], Invitrogen	PE
Anti - mouse		Thermo Scientific	488
FVIII	Human	Clone GMA-8015, Green Mountain	Not conjugated
KDR	human	clone ES8-20E6, Miltenyi Biotec	PE
Tie-2	human	clone REA198, Miltenyi Biotec	PE
CD31	human	clone MEM-05; Invitrogen	APC
VE-cadherin	human	clone REA199, Miltenyi Biotec	PE

Supplemental Table 2. Antibodies used for FACS staining.

Primary antibodies	Host	Reactivity	Manufacturer	Dilution
FVIII	Mouse	Human	Clone GMA-8015, Green Mountain	1:100
CD31	Mouse	Human	BD Bioscience	1:100
HLA-ABC	Rat	Human	Novus Biologicals, clone YTH862.2	1:150
von Willebrand Factor	Rabbit	H, M, R	Millipore	1:100
GFP	Rabbit		Life Technologies	1:300
Secondary antibodies	**Fluorophores**		**Manufacturer**	**Dilution**
Goat anti-Rabbit	AlexaFluor 488 or 546		Life Technologies	1:500/1:1000
Goat anti-Rat	AlexaFluor 594			1:500
Goat anti-Mouse	AlexaFluor 488 or 546		Life Technologies	1:500

Supplemental Table 3. Antibodies used for immunofluorescence staining.

Name of donor	Donor	Mutation	ml of peripheral blood samples	No. of BOECs colonies
pHA1	Severe HA	c.6273G>A exon 21	25	30
pA	Severe HA	intron 22 inversion	22	60
pC	Severe HA	unknown	25	40
pD	Severe HA	intron 22 inversion	26	30

Supplemental Table 4. List of hemophilic patients from whom BOECs were isolated

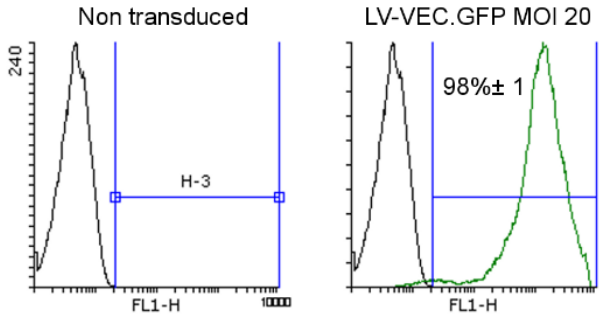

Supplemental Figure 1. Representative histograms for GFP evaluation by FACS analysis in healthy and HA BOECs transduced with an MOI of 20.

Sample	LV copy number/ cell
Healthy BOECs	0
LV-VEC.GFP Healthy BOECs	5.2± 0.6
LV-VEC.hBDD-FVIII Healthy BOECs	3.1± 0.5
HA BOECs	0
LV-VEC.GFP HA BOECs	6.2± 0.8
LV-VEC.hBDD-FVIII HA BOECs	3±0.2

Supplemental table 5. qPCR analysis of integrated LV copy number/cell

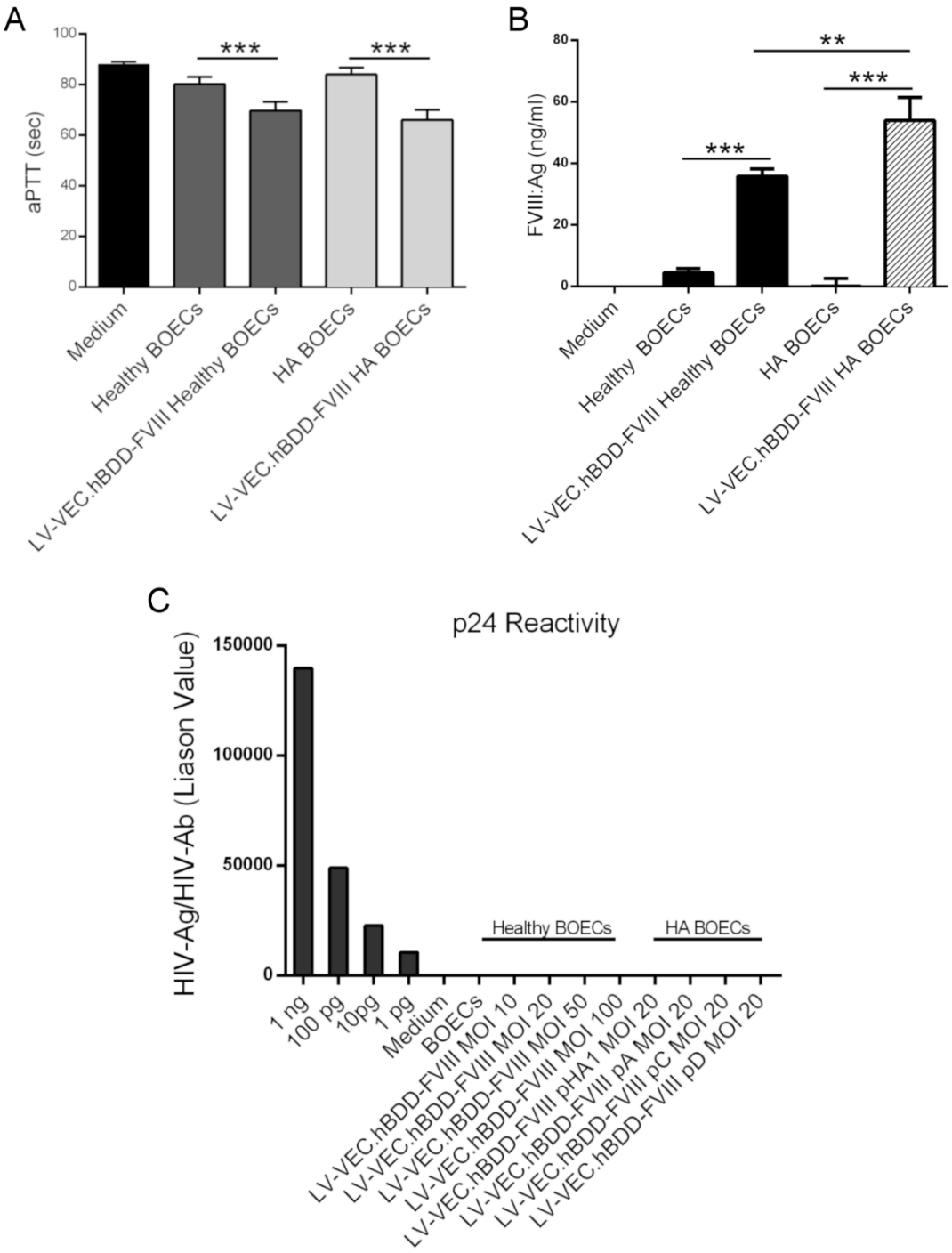

Supplemental Figure 2. (**A**) aPTT assay on supernatant of transduced and non-transduced healthy and HA BOECs (**B**) Antigen assay on supernatant of transduced and non-transduced healthy and HA BOECs. Data are expressed as mean ± SD and are representative of four independent experiments. (**F**) HIV-1 p24 analysis on medium of non-transduced and transduced and healthy and HA BOECs at different MOIs.

Animal ID	Inflammation	Fibroblastic stroma	Collagen deposition	Neovascularization	Established vessels	Hemorrhage
Cell Lot HA1, 4 weeks, 10×10^6 (Dose 1)						
396-LEP	-	+++	+	++	*	-
398-REP	-	+++	++	++	++	-
Cell Lot HA1, 4 weeks, 5×10^6 (Dose 2)						
397-LEP	-	+	+	+	*	-
397-BEP	-	+++	+++	++	++	-
Cell Lot HA1, 4 weeks, 2×10^6 (Dose 3)						
398-BEP	-	+++	+	++	*	-
Cell Lot HA1, 8 weeks, 10×10^6 (Dose 1)						
405-NEP	-	+++	+++	++	++	-
Cell Lot HA1, 8 weeks, 5×10^6 (Dose 2)						
414-NEP	-	+++	+	++	+	-
415-BEP	-	+++	+++	++	+	-
Cell Lot HA1, 8 weeks, 2×10^6 (Dose 3)						
402-LEP	-	+++	++	++	++	-
405-REP	-	++	+	++	+	-
413-LEP	-	++	+++	++	*	-
Cell Lot HA1, 12 weeks, 10×10^6 (Dose 1)						
399-NEP	-	+++	++	++	+	-
413-BEP	-	+++	+++	++	++	-
Cell Lot HA1, 12 weeks, 5×10^6 (Dose 2)						
406-REP	-	+++	++	++	*	-
406-NEP	-	+++	++	++	+	-
411-BEP	-	+++	+++	+	++	-
Cell Lot HA1, 12 weeks, 2×10^6 (Dose 3)						
396-REP	-	+++	+++	+	+	+
398-NEP	-	+++	++	++	+	-
399-BEP	-	+++	++	++	+	-
Cell Lot HAA, 4 weeks, 10×10^6 (Dose 1)						
520-RREP	-	+++	++	++	++	-
Cell Lot HAA, 4 weeks, 5×10^6 (Dose 2)						
523-LEP	-	+++	++	++	+	-

Cell Lot HAA, 8 weeks, 10×10^6 (Dose 1)						
520-NEP	-	+++	+++	++	+	-
524-LEP	-	+++	+++	++	++	-
Cell Lot HAA, 8 weeks, 5×10^6 (Dose 2)						
523-REP	-	+++	++	++	++	-
Cell Lot HAA, 12 weeks, 10×10^6 (Dose 1)						
522-RREP	-	+++	++	++	++	-
524-BEP	-	+++	++	++	++	-
Controls (no cell transplant)						
4 weeks						
525-REP	-	++	++	++	+	-
8 weeks						
521-RREP	-	+++	++	++	++	-
525-RREP	-	+++	+	++	++	-
12 weeks						
403-NEP	-	+++	+	++	+	-
521-BEP	-	+++	++	++	++	-
525-BEP	-	+++	++	++	++	-

*present immediately adjacent to Cell Pouch™

Supplemental Table 6. Histological features of NSG-HA Cell Pouches™ transplanted with FVIII-BOECs (H&E and Trichrome).

Animal ID	HLA-ABC (red)	vWF (green)
Cell Lot HA1, 4 weeks, 10×10^6 (Dose 1)		
396-LEP	+	+
398-REP	+	+
Cell Lot HA1, 4 weeks, 5×10^6 (Dose 2)		
397-REP	+	+
397-LEP	n/a	n/a
414-LEP	+/-	+
Cell Lot HA1, 4 weeks, 2×10^6 (Dose 3)		
398-BEP	-	++
Cell Lot HA1, 8 weeks, 10×10^6 (Dose 1)		
405-NEP	++	-
Cell Lot HA1, 8 weeks, 5×10^6 (Dose 2)		
414-NEP	+	n/a
415-BEP	+/-	+
Cell Lot HA1, 8 weeks, 2×10^6 (Dose 3)		
402-LEP	+/-	+
405-REP	+/-	+
413-LEP	n/a	n/a
Cell Lot HA1, 12 weeks, 10×10^6 (Dose 1)		
399-NEP	-	n/a
413-BEP	+/-	+
Cell Lot HA1, 12 weeks, 5×10^6 (Dose 2)		
406-REP	+	+
406-NEP	+/-	++
411-BEP	+/-	+
Cell Lot HA1, 12 weeks, 2×10^6 (Dose 3)		
396-REP	+/-	+
398-NEP	+	+
399-BEP	+/-	+
Cell Lot HAA, 4 weeks, 10×10^6 (Dose 1)		
520-RREP	++	++
Cell Lot HAA, 4 weeks, 5×10^6 (Dose 2)		

520-REP	++	+
523-LEP	+++	+++
Cell Lot HAA, 8 weeks, 10×10^6 (Dose 1)		
520-NEP	++	+
524-LEP	+	+
Cell Lot HAA, 8 weeks, 5×10^6 (Dose 2)		
523-REP	-	+++
Cell Lot HAA, 12 weeks, 10×10^6 (Dose 1)		
522-RREP	++	++
524-BEP	+++	+
Controls		
4 weeks		
525-REP	-	++
8 weeks		
521-RREP	-	N/A
525-RREP	-	+
12 weeks		
403-NEP	-	+
521-BEP	-	+
525-BEP	-	+

- negative (no staining); +/- equivocal staining; + mild positivity; ++ moderate positivity; +++ marked positivity; N/A image not available

Supplemental Table 7. Immunofluorescence of NSG-HA Mouse Cell Pouches™ transplanted with FVIII-BOECs.

Group	Donor	Transduction	Vector	MOI	Timepoint	Sample ID	N.IS
Healthy.GFP	D45	4	VEC-GFP	10+10	P5	BOEC-008	1,862
Healthy.FVIII	D45	1	VEC-FVIII	20	P5	BOEC-001	5,864
					P8	BOEC-002	
					P11	BOEC-003	
					P15	BOEC-004	
					70 days HA Beads	BOEC-010	
					70 days HA Beads	BOEC-011	
					70 days HA Beads	BOEC-013	
		2	VEC-FVIII	30	P11	BOEC-005	
		3		50	P11	BOEC-006	
	D2	5	VEC-FVIII	20	P5	BOEC-014	
					P8	BOEC-043A	
	D3	6	VEC-FVIII	20	P5	BOEC-043B	
					P8	BOEC-043C	
HA.GFP	pHA1	8	VEC-GFP	20	P5	BOEC-020	106,554
					P8	BOEC-021	
					P12	BOEC-022	
	pA	10	VEC-GFP	20	P5	BOEC-032	
					P8	BOEC-033	
	pC	12	VEC-GFP	20	P5	BOEC-040	
					P8	BOEC-041	
HA.FVIII	pHA1	7	VEC-FVIII	20	P5	BOEC-016	28,069
					P8	BOEC-017	
					P10	BOEC-018	
					P15	BOEC-019	
					P11	BOEC-024	
					P11	BOEC-025	
					P14	BOEC-026	
					P11	HA1-VEC-UNILO	
					91 days HA Beads	BOEC-044A	
					91 days HA Beads	BOEC-044B	
					91 days HA Beads	BOEC-044C	
					2 weeks Cell Pouch	397-LEP	
					2 weeks Cell Pouch	398-LEP	
					4 weeks Cell Pouch	398-BEP	
					4 weeks Cell Pouch	414-LEP	
					4 weeks Cell Pouch	396-LEP	
					8 weeks Cell Pouch	402-LEP	
					8 weeks Cell Pouch	415-BEP	
					8 weeks Cell Pouch	405-NEP	
					12 weeks Cell Pouch	398-NEP	
					12 weeks Cell Pouch	406-REP	
					12 weeks Cell Pouch	399-NEP	
	pA	9	VEC-FVIII	20	P5	BOEC-027	
					P8	BOEC-028	
					P10	BOEC-029	
					P14	HA-A-p14	
					P15	BOEC-030	
					P12	BOEC-031	
					112 days HA Beads	BOEC-045A	
					112 days HA Beads	BOEC-045B	
					112 days HA Beads	BOEC-045C	
					4 weeks Cell Pouch	520-REP	
					4 weeks Cell Pouch	520-RREP	
					8 weeks Cell Pouch	520-LEP	
					8 weeks Cell Pouch	520-NEP	
					12 weeks Cell Pouch	522-RREP	
	pC	11	VEC-FVIII	20	P5	BOEC-035	
					P8	BOEC-036	
					P8	HA-C-p8	
					P10	BOEC-037	
					P11	BOEC-039	
					P14	HA-C-p14	
					P15	BOEC-038	
					P19	HA-C-p19	
					112 days HA Beads	BOEC-046A	
					112 days HA Beads	BOEC-046B	
					112 days HA Beads	BOEC-046C	
	pD	13	VEC-FVIII	20	P16	HA-D-p16	
	TOTAL						142,349

Supplemental Table 8. Summary of sequencing reads and IS retrieved by group. Non redundant IS (column N.IS) retrieved from Healthy or HA Donors and transduced with VEC-FVIII or VEC-GFP were grouped. IS shared between different time points of the same transduction are counted once.

	HA-FVIII		HA-GFP		Healthy-FVIII		Healthy-GFP	
GO Biological Process	DNA repair	323.92	DNA repair	300.00	DNA repair	27.77	cellular response to DNA damage stimulus	16.37
	nuclear division	60.43	Golgi vesicle transport	291.50	Golgi vesicle transport	19.74	DNA repair	15.95
	RNA splicing, via transesterification reactions	60.17	mRNA transport	238.91	DNA replication	15.58	DNA metabolic process	15.85
	DNA-templated transcription, termination	55.84	DNA replication	219.12	RNA 3'-end processing	15.55	chromosome organization	10.20
	regulation of defense response to virus	55.05	DNA-templated transcription, termination	213.72	mRNA splicing, via spliceosome	14.37	DNA replication	8.56
	ribonucleoprotein complex export from nucleus	54.65	termination of RNA polymerase II transcription	211.29	ER to Golgi vesicle-mediated transport	14.37	Golgi organization	4.87
	mRNA export from nucleus	53.65	ribonucleoprotein complex export from nucleu	210.38	RNA splicing, via transesterification reactions	14.28	double-strand break repair via homologous recombinatio	4.74
	ribonucleoprotein complex localization	51.97	mRNA export from nucleus	203.64	RNA localization	13.80	negative regulation of DNA metabolic process	4.12
	termination of RNA polymerase II transcription	51.74	RNA localization	202.37	mRNA 3'-end processing	13.54	hyaluronan catabolic process	3.60
	mRNA transport	51.13	ribonucleoprotein complex localization	201.37	Golgi organization	12.75		
	DNA replication	50.97	nuclear export	193.91	mRNA transport	12.21		
	DNA-templated transcription, elongation	48.37	cytoskeleton-dependent intracellular transport	190.61	establishment of RNA localization	11.45		
	spindle organization	47.80	RNA 3'-end processing	187.27	RNA transport	10.99		
	nuclear export	47.23	mRNA 3'-end processing	184.44	nucleobase-containing compound transport	10.97		
	double-strand break repair	46.42	establishment of RNA localization	178.64	DNA biosynthetic process	10.80		
	RNA localization	45.32	double-strand break repair	175.33	nuclear export	10.29		
	transcription elongation from RNA polymerase II promoter	44.66	RNA transport	170.65	retrograde vesicle-mediated transport, Golgi to ER	7.97		
	mRNA 3'-end processing	44.20	transport along microtubule	170.00	DNA integrity checkpoint	7.15		
	RNA 3'-end processing	43.29	mRNA catabolic process	169.27	regulation of nucleobase-containing compound transpo	6.99		
	cytoskeleton-dependent intracellular transport	38.25	ER to Golgi vesicle-mediated transport	168.66	DNA-dependent DNA replication	6.96		
GO Cellular Component	spliceosomal complex	43.19	chromosomal region	300.00	spliceosomal complex	12.88	ribonucleoprotein complex	13.38
	ribonucleoprotein granule	39.97	condensed chromosome	196.55	protein kinase complex	7.74	intracellular ribonucleoprotein complex	13.07
	mRNA cleavage and polyadenylation specificity factor comple	33.67	chromosome, centromeric region	194.72	mitotic spindle	6.89	protein kinase complex	5.85
	mitotic spindle	32.31	ribonucleoprotein granule	194.28	actomyosin	6.80	mitotic spindle pole	4.99
	catalytic step 2 spliceosome	31.21	spliceosomal complex	161.94	cyclin-dependent protein kinase holoenzyme complex	6.18	serine/threonine protein kinase complex	4.77
	mRNA cleavage factor complex	29.88	kinetochore	156.85	serine/threonine protein kinase complex	5.82	actomyosin	4.74
	P-body	27.62	cytoplasmic ribonucleoprotein granule	138.99	cis-Golgi network	5.69	checkpoint clamp complex	4.38
	transcription elongation factor complex	21.05	mitotic spindle	135.00	tethering complex	5.26		
	cytoplasmic stress granule	20.50	condensed chromosome, centromeric region	127.89	clathrin adaptor complex	4.65		
	SWI/SNF superfamily-type complex	20.37	protein kinase complex	125.56	nuclear replisome	3.49		
	AP-type membrane coat adaptor complex	18.46	spindle pole	124.99	replisome	3.43		
	cis-Golgi network	18.41	serine/threonine protein kinase complex	122.27	microtubule end	2.70		
	DNA repair complex	18.13	condensed chromosome kinetochore	114.17				
	Cul4-RING E3 ubiquitin ligase complex	16.56	catalytic step 2 spliceosome	110.88				
	microtubule end	15.00	small nuclear ribonucleoprotein complex	108.79				
	vesicle coat	13.52	spliceosomal snRNP complex	108.03				
	mitochondrial nucleoid	11.34	Golgi-associated vesicle	98.22				
	exon-exon junction complex	10.66	exon-exon junction complex	97.58				
	clathrin coat of endocytic vesicle	9.73	P-body	95.98				
	integrator complex	8.17	AP-type membrane coat adaptor complex	94.31				
GO Molecular Function	cadherin binding	58.73	cadherin binding	300.00	cadherin binding	20.74	cadherin binding	9.82
	helicase activity	39.49	ribonucleoprotein complex binding	149.66	ribonucleoprotein complex binding	10.06	helicase activity	5.55
	DNA helicase activity	31.92	protein transporter activity	140.04	helicase activity	9.76	damaged DNA binding	5.42
	ubiquitin-like protein binding	30.11	helicase activity	138.01	protein N-terminus binding	9.48	ATP-dependent DNA helicase activity	4.26
	protein N-terminus binding	30.09	ubiquitin-like protein binding	135.33	DNA polymerase activity	7.03	SH3/SH2 adaptor activity	2.95
	ubiquitin binding	27.16	ubiquitin binding	112.11	DNA-directed DNA polymerase activity	5.27		
	ATP-dependent helicase activity	23.92	DNA helicase activity	101.51	4 iron, 4 sulfur cluster binding	4.41		
	translation factor activity, RNA binding	22.80	protein N-terminus binding	99.30				
	lysine N-methyltransferase activity	18.89	ATP-dependent helicase activity	94.64				
	damaged DNA binding	15.69	unfolded protein binding	90.68				
	histone deacetylase activity	15.66	polyubiquitin binding	88.30				
	protein deacetylase activity	15.31	translation initiation factor activity	86.09				
	tRNA binding	13.03	deoxyribonuclease activity	85.32				
	transforming growth factor beta binding	11.43	ATP-dependent DNA helicase activity	73.66				
	thioesterase binding	11.19	translation factor activity, RNA binding	72.80				
	type I transforming growth factor beta receptor binding	9.71	DNA polymerase activity	65.44				
	3'-5' DNA helicase activity	9.24	cysteine-type endopeptidase activity	59.23				
	cyclin-dependent protein serine/threonine kinase activity	8.50	endodeoxyribonuclease activity	58.38				
	cyclin-dependent protein kinase activity	8.33	histone deacetylase activity	52.98				
	RNA polymerase II carboxy-terminal domain kinase activity	5.52	protein deacetylase activity	51.70				

Supplemental Figure 3. Gene Ontology (GO) enrichment for Molecular Function and Biological Process. IS coordinates from IS retrieved from HA.VEC-FVIII, HA.VEC-GFP, Healthy.VEC-FVIII, and Healthy.VEC-GFP were analyzed by G.R.E.A.T. enrichment discovery algorithms. GO Biological Process, Molecular Function and Cellular Component databases highlighted significantly overrepresented gene classes. The gene classes found in at least two groups are highlighted in pink.

Subject ID	Transduction	Vector	MOI	Gene Name	Chr.	Integration locus	N IS per Gene	average transcript length	integration frequency with tolerance	tdist fdr
dD3	6	VEC-FVIII	20	SPG7	16	89,585,048	5	39,358	0.036	0.078
dD45	1	VEC-FVIII	20	SZT2	1	43,952,080	13	64,363	0.079	0.006
				MROH1	8	145,269,797	10	89,530	0.053	0.054
				TRAF2	9	139,825,912	6	40,103	0.043	0.114
				CPSF1	8	145,629,805	5	16,288	0.043	0.114
dD45	4	VEC-GFP	10+10	NPLOC4	17	79,591,992	10	36,856	0.073	0.005
				TRAF2	9	139,825,791	8	40,103	0.057	0.020
pA	10	VEC-GFP	20	SZT2	1	43,955,802	117	64,363	0.712	0.510
				NPLOC4	17	79,602,479	106	36,856	0.775	0.510
pA	9	VEC-FVIII	20	NPLOC4	17	79,600,522	7	36,856	0.051	0.067
				PMPCA	9	139,315,510	5	13,189	0.044	0.108
pC	11	VEC-FVIII	20	SZT2	1	43,955,797	49	64,363	0.298	0.039
				MROH1	8	145,299,016	46	89,530	0.243	0.097
				NPLOC4	17	79,600,496	45	36,856	0.329	0.032
pD	13	VEC-FVIII	20	NSD1	5	176,707,259	10	166,759	0.037	0.100
				ZGPAT	20	62,354,996	6	28,232	0.047	0.047
				NONO	X	70,517,315	5	17,977	0.042	0.074
				MAN1B1	9	139,997,714	4	22,261	0.033	0.139
				PTBP1	19	808,672	4	14,936	0.035	0.122
pHA1	7	VEC-FVIII	20	PHRF1	11	599,765	8	35,777	0.059	0.077
				ZNF251	8	145,983,504	8	34,677	0.059	0.077
pHA1	8	VEC-GFP	20	MROH1	8	145,292,887	121	89,530	0.638	0.337
				SZT2	1	43,954,990	112	64,363	0.681	0.337
				NPLOC4	17	79,599,815	94	36,856	0.687	0.337
				ZNF251	8	145,987,938	77	34,677	0.572	0.361

Supplemental Figure 4. Common Insertion site (CIS) analysis in 2 healthy BOECs, and 4 HA BOECs.

References

1. Follenzi, A., and Naldini, L. (2002). Generation of HIV- 1 derived lentiviral vectors. Methods Enzymol *346*, 454–465.

Acknowledgements

During my doctoral program, I was not alone. The path has been hard, and not that linear, but again, I was not alone. Here I would like to thank all the people that have been taking part in my life during this peculiar journey.

I would first like to thank my supervisor and mentor, Professor Antonia Follenzi, whose expertise was invaluable in formulating the research questions and methodology. Your insightful feedback pushed me to sharpen my thinking and brought my work to a higher level. She deserves the sincerest sense of gratitude for being a priceless guide during all my academic career that began with my bachelor's degree in her lab.

In the process of preparing this dissertation, many people supported my efforts. First, I ought to thank Cristina that has been a precious colleague and a brilliant scientist that always supported me and helped me gain the self-consciousness as a young scientist as I am now.

All the lab members of histology lab of Novara should be thanked as I considered them as a second family. I would like to express my genuine thank you to Professor Prat, Simone M, Chiara B, Ester, Anna, Gillian, Annarita, Charan, Valentina, Silvietta and all the others.

A special thank is intended for my colleagues with whom I share my working day (and so most of my day): my darling Francesca (that unfortunately comes and go from Granada), Simone A. and Chiara S. that altogether with Cristina we make a great team!

Throughout the past few years, I received a great support from my friends. They have been patient enough to listen to my fears and my worries, and they never backed down when something nice was worth to be celebrated. Thank you, guys!

In addition, I would like to thank my parents for their wise counsel and for being supportive from day 1 of my life. You are always there for me. And what about my dear sister? Thank you for taking care of me, for the longest talks and for all the support received.

Finally, I could not have completed this journey without the support of my beloved Yonatan. Without his understanding and encouragement, it would have been very challenging to reach all my goals. When I am down, he always offers stimulating discussions or happy distractions to rest my mind outside my research. Thank you for being here with me in our journey together.

The end M.F.